AD_____

Award Number: DAMD17-99-1-9483

TITLE: Neuroprotection by Progesterone Through Simulation of Mitochondrial Gene Expression

PRINCIPAL INVESTIGATOR: Gary Fiskum, Ph.D.

CONTRACTING ORGANIZATION: University of Maryland, Baltimore
Baltimore, Maryland 21201

REPORT DATE: August 2002

TYPE OF REPORT: Annual

PREPARED FOR: U.S. Army Medical Research and Materiel Command
Fort Detrick, Maryland 21702-5012

DISTRIBUTION STATEMENT: Approved for Public Release;
Distribution Unlimited

The views, opinions and/or findings contained in this report are those of the author(s) and should not be construed as an official Department of the Army position, policy or decision unless so designated by other documentation.

20030731 168

BEST AVAILABLE COPY

REPORT DOCUMENTATION PAGE

Form Approved
OMB No. 074-0188

Public reporting burden for this collection of information is estimated to average 1 hour per response, including the time for reviewing instructions, searching existing data sources, gathering and maintaining the data needed, and completing and reviewing this collection of information. Send comments regarding this burden estimate or any other aspect of this collection of information, including suggestions for reducing this burden to Washington Headquarters Services, Directorate for Information Operations and Reports, 1215 Jefferson Davis Highway, Suite 1204, Arlington, VA 22202-4302, and to the Office of Management and Budget, Paperwork Reduction Project (0704-0188), Washington, DC 20503

1. AGENCY USE ONLY (Leave blank)	2. REPORT DATE	3. REPORT TYPE AND DATES COVERED
	August 2002	Annual (1 Aug 01 -31 Jul 02)

4. TITLE AND SUBTITLE
Neuroprotection by Progesterone Through Simulation of Mitochondrial Gene Expression

5. FUNDING NUMBERS
DAMD17-99-1-9483

6. AUTHOR(S)
Gary Fiskum, Ph.D.

7. PERFORMING ORGANIZATION NAME(S) AND ADDRESS(ES)
University of Maryland, Baltimore
Baltimore, Maryland 21201

E-MAIL:
Gfisk001@umaryland.edu

8. PERFORMING ORGANIZATION REPORT NUMBER

9. SPONSORING / MONITORING AGENCY NAME(S) AND ADDRESS(ES)
U.S. Army Medical Research and Materiel Command
Fort Detrick, Maryland 21702-5012

10. SPONSORING / MONITORING AGENCY REPORT NUMBER

11. SUPPLEMENTARY NOTES

12a. DISTRIBUTION / AVAILABILITY STATEMENT
Approved for Public Release; Distribution Unlimited

12b. DISTRIBUTION CODE

13. ABSTRACT *(Maximum 200 Words)*

In year 3 of this grant, we made more progress toward meeting our original objectives and have made progress on the additional objectives in our revised statements of work. The most important experimental results were as follows: 1. Determined that low, physiological levels of plasma progesterone inhibited seizures produced by kainic acid while high levels of progesterone had no effect. 2. Protection against hippocampal neuronal death by progesterone is directly linked to inhibition of seizure activity. 3. Progesterone inhibition of kainate-induced seizures does not appear to be mediated via binding to its traditional nuclear receptor. 4. Low and high levels of plasma estrogen do not inhibit seizures produced by kainic acid. 5. Low and high levels of plasma estrogen inhibit hippocampal cell death caused by seizures induced by kainic acid. 6. Estrogen pretreatment, at supraphysiological levels, does not interfere with P's seizure suppressive effects. 7. At low doses, estrogen attenuates seizure suppression by progesterone. 8. Mitochondrial gene expression is dependent upon mitochondrial mRNA stability, apparently controlled by a mitochondrial form of RNase L. 9. Mitochondrial Ca^{2+} accumulation either inhibits or stimulates mitochondrial H_2O_2 production, depending on the respiratory substrate and the effect of Ca^{2+} on the mitochondrial membrane potential. 10. Bax plus a BH3 domain peptide stimulate H_2O_2 production by brain mitochondria due to release of cytochrome c and this stimulation is insensitive to changes in membrane potential.

14. SUBJECT TERMS
steroid, hormones, neuronal death, seizures, mitochondria, excitotoxicity, cytochrome oxidase, mRNA

15. NUMBER OF PAGES
115

16. PRICE CODE

17. SECURITY CLASSIFICATION OF REPORT	18. SECURITY CLASSIFICATION OF THIS PAGE	19. SECURITY CLASSIFICATION OF ABSTRACT	20. LIMITATION OF ABSTRACT
Unclassified	Unclassified	Unclassified	Unlimited

NSN 7540-01-280-5500

Standard Form 298 (Rev. 2-89)
Prescribed by ANSI Std. Z39-18
298-102

BEST AVAILABLE COPY

Table of Contents

BEST AVAILABLE COPY

(4) INTRODUCTION:

Organization of Report

Progress related to the statement of work for the original grant award is described under the subheading **Neuroprotection by Progesterone.** The scope of the original project has expanded due to two different altered statements of work that were approved and supported by supplement awards. The first altered statement of work (supplement award active August 9, 2001) is for pilot tests of progesterone neuroprotection using a rat traumatic brain injury model. Progress on this subproject is described under the subheading of **Neuroprotection by Gonadal Hormones in Traumatic Brain Injury**. The second statement of work (supplement award active February 13, 2002) is for projects described under the subheadings **Mitochondrial Free Radical Generation in Parkinson's Disease** and **Calcium-Neurotrophin Interactions in Neurodegenerative Disorders.**

(5) BODY:

A. Neuroprotection by Progesterone

The **specific hypotheses** to be tested are as follows:

1. **Progesterone protects against neuronal death caused by kainic acid-induced status epilepticus *in vivo* and excitotoxicity-induced neuronal death *in vitro.***
2. **Excitotoxic levels of glutamate down-regulate the expression of mitochondrial genes, e.g., cytochrome oxidase, both *in vitro* and *in vivo.***

BEST AVAILABLE COPY

3. A mechanism of neuroprotection by progesterone is the up-regulation of mitochondrial gene expression, thereby increasing the resistance of neurons to excitotoxicity.

APPROVED STATEMENT OF WORK

Years 1-3

Objective 1: Dose-response for progesterone and estrogen alone and in combination. Effects of 5α reductase inhibition (Finasteride) and progesterone receptor blockade (RU486) on neuroprotection by progesterone.

Our studies (see Appendix manuscript Hoffman et al.) established that progesterone administration attenuates seizure severity induced by kainic acid (KA) in a dose-dependent fashion. In particular, we found that administration of progesterone (P) at doses that produce plasma P levels between 10-36 ng/ml resulted in a significant attenuation of seizure severity; administration of P resulting in plasma P levels greater that 40 ng/ml produced no attenuation in seizure severity. By contrast, administration of estrogen, at either high or low physiological levels had no effect on KA-induced seizures. Indeed, no significant difference was observed in seizure severity scores for E treated animals in comparison to animals receiving no hormone replacement.

The results of these studies clearly demonstrated that P administration *at physiological levels* significantly reduces KA-induced seizures. However, in naturally cycling women, or women receiving either hormone replacement therapy or taking birth control, both estrogen and progesterone are present. Therefore, in our next series of experiments, we examined the effect of estrogen and progesterone co-administration on KA-induced seizures.

Estrogen and Progesterone Co-Administration

Adult female Sprague-Dawley rats (200-225 g) were used for these experiments. Seven days following ovariectomy, animals were implanted with estrogen pellets (Estradiol-17ß) manufactured to produce either high E (0.5 mg/21 days) or low E (0.1mg/21 days), progesterone filled silastic capsules designed to achieve plasma progesterone levels of 20-4 ng/ml, or a combination of the two. Seven days later, the animals were injected with KA (8.5 mg/kg; i.p.) and their behavior monitored for seizure activity for 6 hrs post-injection by a person blind to animal treatment. Following the 6 hr observation period, animals were given a seizure severity composite score that ranged from 0 (no seizures) to 5 (death) based on a modification of the Lothman scale. Ninety-six hours after KA administration, animals were perfused transcardially with saline followed by fixative and their brains removed and allowed to sink in sucrose. Brain sections were cut at 25 µm using a freezing microtome and stored in a cryoprotectant-antifreeze solution until immunocytochemical staining was initiated. Experiments using immunocytochemical localization of neuronal nuclear antigen in E, P and E+P treated animals are currently underway.

The effect of E, P or E+P administration on KA-induced seizures are shown in **Figure 1**. In agreement with our previous studies, P administration (plasma P levels ranging from 20-40 ng/ml) significantly reduced seizure severity in comparison to control animals receiving no hormone ($U=27$, $p<0.01$). E administration, at either the high or low dose, had no significant effect on KA-induced seizures (Low E, $U=94$, $p>0.05$; High E, U81.5, $p>0.05$ in comparison to control KA treated animals).

The effect of E+P co-administration on seizure severity was dependent on the dose of Estrogen. For the P + low Estrogen condition (mean plasma E level 42.4 + 6 ng/ml), seizure severity scores increased from 1.46 + .21 for P alone, to 2.11 + .64 for low E+P (U=40.0, p>0,05), and were not significantly different from the low E alone condition: mean seizure score, 2.47 + .38 (U=32.0, p>0,05). For the high E condition (mean plasma E level 242.4 + 32.6), co-administration of P significantly reduced seizure severity: mean seizure score for high E alone, 3.03 + .30 versus 1.70 + .20 for P+E high, U=6.0, p<0.05).

The results of these studies indicate that E+P co-administration produces a dose dependent effect on KA-induced seizure severity. Low physiological levels of E, along with P, produced a slight increase in seizure severity in comparison to animals receiving P alone. By contrast, animals receiving supraphysiological levels of E in conjunction with P, had seizure severity scores that were comparable to animals receiving P alone (i.e., were significantly suppressed). In our previous studies, we reported that while animals receiving E treatment alone displayed very high seizure activity following KA, these animals had very little neuronal loss within the hippocampus. By contrast, animals receiving P alone at doses that suppressed seizures had little damage to the hippocampus, but animals that received high doses of P displayed high levels of seizure behavior following KA and sustained a high degree of hippocampal neuronal loss. We are currently examining the brain sections from the high E+P treated animals. Based on our previous data, we predict that co-administration of high E+P will result in a significant attenuation of hippocampal neuronal loss in comparison to P alone, and that low E+P while unable to significantly reduce seizures, will attenuate damage from the seizures. These results may have profound implications on the future design of pharmacological intervention for the alleviation of epileptic seizures.

Mechanisms Underlying Progesterone Modulation of Seizure Severity

The results of our previous studies have clearly established that progesterone administration significantly attenuates KA-induced seizure behavior. There are two primary mechanisms by which P may be acting: (1) P may bind to its classical nuclear receptor, PR, and influence subsequent target gene transcription; or (2) progesterone may be acting through its 5α3α reduced metabolite, allopregnanolone, which acts as a positive allosteric modulator at the $GABA_A$ receptor.

Our first series of experiments were designed to test the hypothesis that progesterone is binding to its classical nuclear receptor by pretreating the animals with a progesterone receptor blocker. Two different PR antagonists were tested: RU486 (Sigma Chemical Co.) and CDB2914 (BioQual). The basic experimental protocol for these studies was similar to that used above. Ovariectomized female rats were implanted with progesterone filled silastic implants designed to produce plasma P levels of 20-40 ng/ml. Twelve hours prior to KA injection, animals received a priming dose of PR antagonist: RU486, 7 mg/kg; CDB2914, 6, 8, 10 or 12 mg/kg). All animals received a second dose of PR antagonist 5 hrs prior to KA. Following KA injection (8.5 mg/kg), animals were monitored for seizure behavior for 6 hours and a composite seizure severity score was derived for each animal by a person blinded to animal treatment. Ninety-six hours after KA, animals were perfused transcardially as described above, and their brains removed and sectioned for immunocytochemical localization of NeuN.

The results of these experiments are shown in **Figure 2**. Pretreatment with the PR antagonist RU486 significantly blocked P induced suppression of seizure behavior ($U=58$, $p<0.01$). Indeed, there was no significant difference in seizure scores for P+RU486 treated

animals in comparison to hormone-free control animals: mean seizure score for P+RU486, 3.08 $\pm$ .42 versus 3.50 + .31 for control animals; U=71, $p>0.05$. By contrast, pretreatment with CDB2914, at any dose, failed to block the effects of P (mean seizure score for P+CDB2914, 1.63 $\pm$ .33 versus 1.46 + .21 for P alone treated animals; U=222, $p>0.05$).

The CDB compound and RU486 are both antagonists of the progesterone receptor. CDB has greater specificity for PR than the other antagonist. Thus the results of these studies indicate that P suppresses KA induced behavioral seizures via an action independent of the progesterone receptor. RU486 can bind to glucocorticoid receptors in addition to PR. Thus it will be important in the upcoming year to test whether the RU486 effects are due to genomic alterations. We are currently examining several mitochondrial gene products that may be influenced by genomic effects of P binding, including COXI and COXIII.

Experiments are also currently underway to examine the contribution of the progesterone metabolite, allopregnanolone, to P mediated suppression of seizure behavior. These studies will compare the effect of allopregnanolone administration to P in our model of KA induced seizures and will determine if the two PR antagonists interfere or mimic allopregnanolone's activity. In addition, we are actively searching for a compound that will block the metabolism of P, either at the 5α reductase step, or the 3α-hydroxysteroid oxidoreductase stage. Unfortunately, to date, these compounds are not commercially available.

In summary, our studies have demonstrated that P administration significantly reduces KA induced seizures. Estrogen pretreatment, at supraphysiological levels, does not interfere with P's seizure suppressive effects. At low doses, E appears to attenuate seizure suppression. Analyses are underway to determine if E in the presence of P confers neuroprotection to the hippocampus by reducing the degree of hippocampal loss associated with KA induced seizures.

The results of our experiments using PR blockers suggest that P is not producing its effect via binding to its traditional nuclear receptor.

Objectives 2 and 3:

- **Determination of effects of kainate, progesterone and estrogen on brain mitochondrial gene expression**
- **Demonstration of progesterone protection against neuronal cell death in vitro and determination of mechanisms of regulating mitochondrial gene expression**

Hippocampal Cytochrome Oxidase Subunit III mRNA

One proposed mechanism by which hormones may afford neuroprotection is the up-regulation of mitochondrial gene expression. Our studies have shown that P does not protect against seizure-induced damage per se, but only reduces seizure intensity, while E protects against hippocampal damage associated with each level of seizure. Therefore, only E may increase mitochondrial cytochrome oxidase III mRNA and protein levels, as well as cytochrome oxidase enzyme activity.

The animals used for these studies were processed as described above. Briefly, ovariectomized female rats were given hormone implants (designed to give plasma levels of low E, high E, or P) or empty (blank) capsules, injected with KA seven days later and observed for 6 hours. 24 or 48 hours following KA injection, animals were sacrificed by decapitation; their brains removed and allowed to sink in sucrose. Brain sections were cut at 12 μm using a cryostat, thaw-mounted onto slides and stored in a -70°C freezer until experiments were initiated. COX subunit III mRNA levels were measured by in situ hybridization. The sections were hybridized with the COX III probe and processed as previously described (1, 2) counter-stained

with cresyl violet (a Nissl stain). Regional changes in levels of subunit mRNA were analyzed with IP Sectrum software operating on a Power Computing Macintosh computer. COX III mRNA was quantified only in areas containing cells, as determined by the Nissl stain; *therefore, decreases in mRNA can not be attributed simply to a lower number of cells present in the KA-treated groups*. Additionally, CA1 measurements were normalized using the dentate gyrus, which is known to be unaffected by KA treatment, to adjust for varying levels of background. At 24 hours post-KA injection, there was no effect of any hormone treatment on COX III mRNA in the CA1 area of the hippocampus (data not shown). *However at 48 hours post-KA, COX III mRNA was reduced in animals given KA and either no hormone or P, as compared to control saline animals; this deficit was ameliorated by either dose of E* (**Figure 3**). Experiments testing the levels of COX enzyme activity and COX subunit protein levels are underway using adjacent sections. Additionally, experiments are underway to examine the effects of the hormones (without KA) on COX enzyme activity, as well as COX subunit mRNA and protein levels, in the hippocampus.

Protection by Progesterone against Glutamate Excitotoxicity, and Possible Involvement of RNase L in Regulating Mitochondrial Gene Expression

Experiments were performed to test the protective effect of progesterone and estrogen against glutamate-induced neuronal death in cellular models of excitotoxicity. We used rat cerebellar granule neurons and rat cortical neurons as models of excitotoxicity. Neuronal death was measured by propidium iodide (PI) staining. Posttranscriptional mechanism of regulation of mitochondrial gene expression was examined in mammalian cells that are devoid of stress-related interferon-associated mitochondrial RNase, RNase-L.

MATERIALS AND METHODS

Procedures involving animals and their care were conducted in conformity with institutional guidelines that are in compliance with national and international laws and policies (NIH guide for the Care and Use of Laboratory Animals, NIH publication no. 85-23,1985).

Primary neuronal cultures:

Cerebellar granule cell cultures were prepared from 7-day old Sprague-Dawley rat pups. Cortical neurons were prepared from embryonic day 17 (E17) fetuses. Neurons were seeded at a density of 2 $x10^5$ cells/cm^2 in 6-well tissue culture chambers coated with poly-L-lysine (MW 30 000 - 700 000) and cultured in Eagle's Basal Medium supplemented with Earle's salts, 10% inactivated fetal bovine serum or 10% inactivated gelded horse serum, 25 mM KCl and gentamycin (50 ng/ml). To prevent growth of glial cells, cytosine arabinoside (10 μM) was added to the cultures 24h after seeding.

Excitotoxicity:

Cultures were exposed to glutamate (50 - 250 μM) in a Locke solution (134-mM NaCl, 25 mM KCl, 4 mM $NaHCO_3$, 5 mM HEPES, 2.3 mM $CaCl_2$ and 5 mM glucose) for 30 min in the presence of 10 μM glycine (3). After exposure to glutamate, the cells were washed and kept in the old culture medium without glutamate for up to 24 hr. Control cultures were treated with the vehicle for the same time period as that of glutamate treated cells.

Drugs:

In experiments with cell cultures, progesterone and estrogen (17 β-estradiol) were dissolved in 60% alcohol and the final alcohol concentration was less than 0.01%. Cultures were treated with the vehicle alone were used as controls. Progesterone was used at a final concentration from 1 to 10 μM. Estrogen was used at a final concentration from 0. 1 to 10 μM.

Cell viability:

Cell viability was determined using a two-color fluorescence assay based on the simultaneous determination of live and dead cells with two probes that measure two recognized parameters of cell viability – intracellular esterase activity and plasma membrane integrity. Viable granule cell neurons were quantified after staining of cells with cell-permeant calcein AM (2 μM). Nonviable neurons were quantified with cell-impermeant propidium iodide (10 μg/ml). The number of PI positive (nonviable) cells to the total number of cells in a field was determined.

RNA analysis

Rat cerebellar granule neurons were exposed to glutamate (100 μM) for 30 min in the presence or absence of progesterone (10 μM) as described. After exposure to glutamate, the cells were washed and kept in the old culture medium without glutamate for up to 24 hr. At various periods of time up to 24h, cells were washed with Dulbecco's Phosphate Buffered Saline (DPBS) without calcium and magnesium and total RNA was isolated using the Qiagen RNeasy kit. Total RNA was subjected to northern blot analysis.

Two μg of total RNA was separated on 1.2% formaldehyde-agarose gel and transferred to GeneScreen Plus (NEN Life Sciences) using controlled vacuum (The Hybaid vacu-aid). Prehybridization and hybridization were done with Hybridizol reagent (Hybridizol I and II mixed 4 to 1 ratios, Oncor, MD, USA). The blots was prehybridized at 42°C for 16 h, then hybridized for 48 h at 42°C with [^{32}P]-labeled probe (4). The blots were washed with increasing stringency and the final wash was performed at 65°C with 0.2 X SSC (1 X SSC = 150 mM sodium chloride and 15 mM sodium citrate) and 1% SDS (sodium dodecylsulfate). The blots were exposed to X-ray film (Bio-max MS, Kodak, NY, USA) with an intensifying screen for 45 min to 2 days at -

70°C. The level of hybridized RNA was quantified using an image analysis program (NIH image 1.57 program, Wayne Rasband). The probe for evaluation of mtDNA transcripts was created by PCR amplification of mtDNA using specific primers (nt 8861-14549 of mtDNA). This probe hybridizes to COX III, ND3, ND4L, ND4, ND5 and ND6 mRNAs (5). To control for equal loading and transfer of RNA, the blots was reprobed with β-actin or 18S rRNA.

Statistical analysis

Results are expressed as the mean ± S.E.M. Differences between controls and test samples were evaluated by ANOVA: Fischer's F-test was first used to compare between-groups and within-groups variance; if the former was significantly ($P<0.05$) higher than the latter, individual groups were compared by Tukey's test for multiple comparisons.

RESULTS

Effect of glutamate on cell death in cerebellar granule and cortical neurons:

We reported previously that for cerebellar granule neurons maintained in culture medium containing 10% inactivated fetal bovine serum, the neurotoxicity produced by a 30min exposure to glutamate increased with increasing concentrations of glutamate (60 to ± 7% with 100 μM glutamate and 90 ± 5% with 250 μM glutamate (measured on sister cultures in 5 different preparations). In rat cortical neurons maintained in culture medium with 10% fetal bovine serum, the neurotoxicity produced by a 30min exposure to glutamate increased with increasing concentrations of glutamate (58 to ± 6% with 100 μM glutamate and 92 ± 8% with 250 μM glutamate). The glutamate-induced neurotoxicity in both cultures was blocked by the selective NMDA-receptor antagonist MK-801 (10 μM) and by the glycine antagonist 7-chlorokynurenic acid (10 μM). The results established that transient (30 min) exposure to glutamate (100 and 250

μM) produced reliable and consistent neuronal death after 24h in both cerebellar and cortical neuronal cultures.

Progesterone and estrogen-mediated protection against glutamate-induced excitotoxic cell death in neuronal cultures:

Using the protocol of 30min exposure to glutamate, we evaluated the protective effect of addition of progesterone against neuronal death. In the previous report we showed that addition of progesterone at physiological concentrations (up to 1 μM) failed to provide significant protection against death in rat cerebellar granule neuronal cultures, whereas higher non-physiological concentrations of progesterone (5 - 10 μM) protected neurons against glutamate-induced excitotoxicity. Progesterone receptors are maximal in rat cerebral cortex and lowest in the cerebellum (6-8). Therefore, in this study we tested the effect of progesterone using rat cortical neurons. We maintained the cortical neurons in the cell culture medium containing 10% gelded horse serum. The rationale for using gelded horse serum (devoid of sex hormones) is to eliminate the contribution of contaminating progesterone present in the serum. However, we found that under these conditions cortical neurons could not be maintained in culture beyond a period of 1 week. The viability of the cortical neurons decreased from 80 ± 7% at day 5 in vitro (DIV) to 10 ± 1% at 10 DIV. Therefore, the protective effect of progesterone against glutamate-induced neuronal death could not be tested. We could not use cortical neurons at 5DIV because neuronal cultures at 5DIV are resistant to glutamate-induced excitotoxicity (9).

Progesterone-mediated protection against glutamate-induced neuronal death in hippocampal neurons maintained in Neurobasal medium with B27 supplements has been observed (10). However, the B27 supplement contains 5 ng/ml progesterone, suggesting that

progesterone is required for neuronal survival. Therefore, to study the role of progesterone in neuronal survival and protection against excitotoxicity, we propose the following approaches:

1. We will determine the effect of addition of progesterone to gelded horse serum on survival of cortical neurons in culture. 2. We will maintain neuronal cultures in presence of gelded horse serum and progesterone or in presence of neurobasal medium with B27 supplement. We will then evaluate whether progesterone mediated protection is due to genomic or non-genomic effect by exposing cortical neurons at 10 DIV in Locke solution in presence or absence of added progesterone. 3. We will determine the synergistic effect of added progesterone and estrogen on neuronal survival and on glutamate-induced neuronal death in cortical neurons at 10 DIV.

Glutamate decreases mitochondrial gene expression and regulation of mitochondrial gene expression.

We presented results demonstrating that addition of glutamate to cerebellar granule neurons rapidly reduces the expression of mtDNA-encoded mRNA (mt-mRNA) in the absence of changes in mtDNA. Reprobing of the blots with β-actin showed no specific reduction, suggesting that the decrease is not due to loss of RNA or due to differences in RNA loading. These results suggested that the glutamate-induced decrease in mt-mRNA could be due to a decrease in transcription of mtDNA or increased degradation of mt-mRNA. Based on the results obtained with PC12 cells, we postulated the existence of a mechanism of posttranscriptional regulation of mitochondrial gene expression that is independent of the energetic status of the cell and that may operate under pathological conditions such as glutamate-induced excitotoxicity (11). However, the molecular components of this mechanism were unknown. Recently, an RNase called RNase L that is regulated by stress and interferon was also shown to mediate the

degradation of a number of mitochondrial mRNAs in response to interferon. (12). RNase L was also found to be present in mitochondria (12). In this study, we evaluated whether RNase L is involved in regulating the stability of mt-mRNA under normal conditions and under conditions of ionic stress. In cells devoid of interferon-regulated RNase, RNase-L, the half-life of mt-mRNAs was stabilized. In RNase-L $^{+/+}$ cells the average half-life of mt-mRNA, determined after termination of transcription with actinomycin D, was 3h, whereas in RNase-L $^{-/-}$ cells the half-life of mt-mRNA was >6h (**Figure 4**). In contrast, the stability of nuclear DNA-encoded β-actin mRNA and mtDNA-encoded 12S rRNA were unaffected. Steady state levels of 12S rRNA and β-actin mRNA remained constant, whereas there was an increase in mt-mRNA levels in RNase-L $^{-/-}$ cells compared to RNase-L $^{+/+}$ cells (**Figure 5**). Induction of expression of RNase-L in mouse fibroblasts also reduced the half-life of mt-mRNA from 3h to 1.5h (**Figure 6**). We previously reported that chronic exposure to the sodium ionophore monensin to cultured mammalian cells reduced the half-life of mt-mRNA from 3h to 1.5h (11). We subsequently found that the half-life of mt-mRNA in monensin-induced RNase-L $^{+/+}$ cells was 1.5h, whereas in RNase-L $^{-/-}$ cells the half-life of mt-mRNA was >4h (**Figure 7**). We conclude that RNase-L causes (i) a decrease in the steady-state levels of mt-mRNA, (ii) a selective decrease in the half-life of mt-mRNA, and (iii) accelerates degradation of mt-mRNA in cells exposed to sodium ionophore. *Our results demonstrate a role for RNase-L in regulating the stability of mitochondrial DNA-encoded mRNAs.* A manuscript describing these results is present in the Appendix (Chandrasekaran et al). We are extending these studies to investigate whether RNase L is responsible for glutamate-induced reduction in mitochondrial gene expression. We are also testing the effect of progesterone and estrogen on mitochondrial gene expression. The rationale for this is that estradiol has been shown to increase levels of several mtDNA-encoded mRNA in

hepG2 cells (13) and stimulate expression of adenine nucleotide translocator ANT1 messenger RNA in female rat hearts (14).

B. Neuroprotection by Gonadal Hormones in Traumatic Brain Injury

The **specific hypotheses** to be tested are as follows:

1. **Progesterone protects against early, prelethal alterations to brain mitochondria that influence brain energy metabolism, oxidative stress, and apoptotic neural cell death.**
2. **Progesterone stimulates expression of mitochondrial and (or) nuclear genes, e.g., cytochrome oxidase and Bcl-2, that increase resistance to necrotic or apoptotic cell death.**

APPROVED STATEMENT OF WORK

Year 1 of Supplement

Objective: Obtain preliminary results that will provide the rationale for conducting a complete study assessing the neuroprotective effects and mechanisms of action of different doses and combinations of progesterone and estrogen.

Experimental Protocol

Female rats (Sprague Dawley, Zivic Miller) were ovariectomized and then implanted with blank pellets designed to deliver 20 or 60 pg/ml of progesterone. Seven days after ovariectomy and implantation, rats underwent TBI using controlled cortical impact (CCI) injury with a pneumatic impactor device as previously described (15, 16). For this injury, a left-sided craniotomy was performed, and trauma was produced on the exposed brain using the CCI device. The injury was delivered at an impact velocity of 4 m/sec, 2.5 mm depth of penetration and 50

msec duration of brain deformation. This delivers a moderate level of TBI severity with minimal mortality (< 10%). Following CCI, the craniotomy was sealed and the scalp was closed.

Isolation of forebrain mitochondria for analysis was performed at 24h after CCI. Histologic and immunohistochemical analysis was performed at 24h, 48h, 72h and 7 days after CCI.

Results

Mitochondrial effects of progesterone on uninjured brain

In order to evaluate any baseline effects that progesterone may have on mitochondrial respiration, an initial set of studies was performed on uninjured rats. Female rats underwent ovariectomy, followed by implantation with either blank or progesterone pellets. Seven days later, mitochondria were isolated from rat forebrain and analyzed. Mitochondrial rates of respiration in the two groups were compared.

Progesterone administration did not change the ability of isolated mitochondria to consume oxygen in either State 3 (oxidative phosphorylation) or State 4 (resting) respiration. **Figure 8A** demonstrates the relative rates of State 3 respiration of the progesterone and blank-implanted rats using the oxidizable substrates glutamate and malate. State 3 rates were also similar between groups in the presence of succinate and rotenone (**Figure 8B**). Furthermore, the acceptor control ratio (defined as the ratio of State 3 to State 4 respiration) was not different between groups (**Figure 9**). This ratio reflects the degree to which mitochondrial oxidative phosphorylation is coupled to ATP production, and can be altered after acute brain injury. These results suggest that in the uninjured state, progesterone does not significantly alter mitochondrial

respiratory function, and provides important baseline information for the study of progesterone after TBI.

Basic histologic assessment of lesion volume

Rats underwent CCI for assessment of tissue loss early after TBI. These rats were perfusion fixed at 24h after CCI and neurons were labeled with the neuronal nuclear marker NeuN. A representative photomicrograph of tissue loss is seen in **Figure 10**. Note the significant loss of cortical tissue with relative sparing of the underlying, ipsilateral hippocampus.

Time course of Bcl-2 upregulation after CCI

Previous studies of experimental TBI have demonstrated alterations in both pro- and anti-apoptotic proteins. Specifically, the anti-apoptotic protein bcl-2 is increased following TBI in the ipsilateral cortex and hippocampus (17). In order to establish a baseline, we evaluated the pattern and time course of bcl-2 expression following CCI in ovariectomized female rats without progesterone implants. Bcl-2 expression was evident at 24h in neurons of the cortex and hippocampus ipsilateral to the side of injury (**Figure 11A**). The greatest expression was seen nearest to the injury, with less bcl-2 staining more distally. The contralateral hemisphere did not demonstrate any bcl-2 staining (**Figure 11B**).

Time course assessment revealed that bcl-2 staining was more pronounced at 48h compared to 24h after CCI, with bcl-2 positive neurons appearing much denser (**Figure 12 A&B**). At 48 h, a similar pattern of distribution was seen, with the greatest bcl-2 expression in the injury penumbra and none seen in the contralateral hemisphere. By 72h, there was noticeably fewer bcl-2 positive cells. Those cells that were seen were much more faintly stained

(**Figure 12C**). Throughout all timepoints, the contralateral hemisphere did not show any evident bcl-2 staining.

Limitations

Upon assessment of total tissue loss at 7 days, it was evident that there was a moderate amount of variability between rats. In addition, the degree of injury inflicted appeared to be more severe than originally planned. We are attributing both of these experimental limitations to the use of an older CCI device that was currently in use in our laboratory. We have recently purchased a newer device that will significantly increase the reliability and reproducibility of this model. It is likely that that more severe TBI produced by the older device would not be amenable to manipulation. Specifically, it would be difficult to detect any possible neuroprotective effects of progesterone in this severe of an injury. Future studies will utilize a reduced degree of injury severity using the new CCI device.

Conclusions

Mechanisms of neuroprotection of estrogen and progesterone remain unclear, despite studies demonstrating gender differences after acute brain injury. Given the important role of mitochondria in neuronal cell death and survival, it is possible that the gonadal hormones influence cell survival via mitochondrial interaction. From our preliminary studies, we have demonstrated the lack of effect of progesterone on basic, uninjured brain mitochondrial respiration. We have also demonstrated the ability to study mechanisms of gonadal hormone neuroprotection after TBI through the use of sophisticated mitochondrial analyses, including *in vitro* analysis of mitochondrial metabolism and *in vivo* analysis of anti-apoptotic protein

expression (bcl-2). Future studies will continue to apply these techniques to assess outcome measures of cellular apoptotic protein alterations and mitochondrial activity, in correlation with neurologic function. Studies will include further assessment of the role of progesterone and estrogen in mitochondrial function after TBI.

C. Mitochondrial Free Radical Generation in Parkinson's Disease

Hypothesis/Objective for Year 1 of Supplement

Mitochondrial reactive oxygen species production is modulated by neurotoxins, Ca^{2+}, and pro-apoptotic proteins

Abnormal accumulation of Ca^{2+} and exposure to pro-apoptotic proteins, e.g., Bax, is believed to stimulate mitochondrial generation of reactive oxygen species and contribute to neural cell death during acute ischemic and traumatic brain injury and in neurodegenerative diseases, e.g., Parkinson's disease. However the mechanism by which Ca^{2+} or apoptotic proteins stimulate mitochondrial ROS production is unclear. We used a sensitive fluorescent probe to compare the effects of Ca^{2+} on H_2O_2 emission by isolated rat brain mitochondria in the presence of physiological concentrations of ATP and Mg^{2+} and different respiratory substrates. In the absence of respiratory chain inhibitors, Ca^{2+} suppressed H_2O_2 generation and reduced the membrane potential of mitochondria oxidizing succinate, or glutamate plus malate. In the presence of the respiratory chain Complex I inhibitor rotenone, accumulation of Ca^{2+} stimulated H_2O_2 production by mitochondria oxidizing succinate, and this stimulation was associated with release of mitochondrial cytochrome c. In the presence or glutamate plus malate, or succinate, cytochrome c release and H_2O_2 formation were stimulated by human recombinant full-length Bax in the presence of a BH3 cell death domain peptide. These results indicate that in the

presence of ATP and Mg^{2+}, Ca^{2+} accumulation either inhibits or stimulates mitochondrial H_2O_2 production, depending on the respiratory substrate and the effect of Ca^{2+} on the mitochondrial membrane potential. Bax plus a BH3 domain peptide stimulate H_2O_2 production by brain mitochondria due to release of cytochrome c and this stimulation is insensitive to changes in membrane potential. These findings will soon be published in the Journal of Neurochemistry. A copy of the accepted manuscript is included in the Appendix (Starkov et al., 2002).

Mitochondrial production of reactive oxygen species (ROS) at Complex I of the electron transport chain is implicated in the etiology of neural cell death in acute and chronic neurodegenerative disorders. This study used Amplex Red fluorescence measurements of H_2O_2 to test the hypothesis that ROS production by isolated brain mitochondria is regulated by membrane potential ($\Delta\Psi$) and NAD(P)H redox state and varies with the presence of different NAD^+-linked respiratory substrates. $\Delta\Psi$ was monitored by following the medium concentration of TPP^+ with a selective electrode. NAD(P)H redox state was estimated by autofluorescence. While the rate of H_2O_2 production was closely related to $\Delta\Psi$ and the level of NAD(P)H reduction at high values of $\Delta\Psi$, 30% of the maximal rate of H_2O_2 formation was still observed in the presence of uncoupler (FCCP) concentrations that provided for maximum depolarization of $\Delta\Psi$ and oxidation of NAD(P)H. Rates of H_2O_2 production varied with the type of respiratory substrate that was used with α-ketoglutarate >> pyruvate > malate ≥glutamate, but were not related to relative rates of respiration. Our findings indicate that ROS production by mitochondria oxidizing NAD^+-dependent substrates is regulated by $\Delta\Psi_m$ and by the NAD(P)H redox state but is also dependent on the presence of specific NAD^+-linked respiratory substrates. These manuscript describing these results is in preparation and will be submitted to the journal Free Radical Biology and Medicine (Starkov and Fiskum).

D. Calcium-Neurotrophin Interactions in Neurodegenerative Disorders

Hypothesis/Objective for Year 1 of Supplement

We have been testing the hypothesis that elevated neuronal [Ca^{2+}] causes abnormal synthesis or processing of the BDNF receptor, trkB.

Mouse cortical neurons were transfected with trkB promoter constructs containing a luciferase reporter and the cells were depolarized in the absence and presence of extracellular Ca^{2+}. Of the two promoters in the trkB gene, the downstream promoter, P2, is stimulated by depolarization and this stimulation requires extracellular Ca^{2+}. In contrast, P1 is inhibited by Ca^{2+}. We have identified several regulatory elements in the DNA sequence of P2 including two, tandem CRE sites, which interact with the phosphorylated form of the transcription factor, CREB. We have also found a novel Ca^{2+} enhancer element upstream of the CREs. We are presently identifying the sequence of this enhancer and its cognate transcription factor. The results to date demonstrate that trkB expression is under the control of cytoplasmic [Ca^{2+}] via Ca^{2+}-dependent regulatory elements in the trkB promoter. Our results are consistent with the hypothesis that Ca^{2+}-dependent regulation of trkB transcription can regulate the neuron's response to BDNF and, consequently, its survival. Dysregulation of this process may underlie accelerated neuron death in neurodegenerative disorders such as Parkinson's disease.

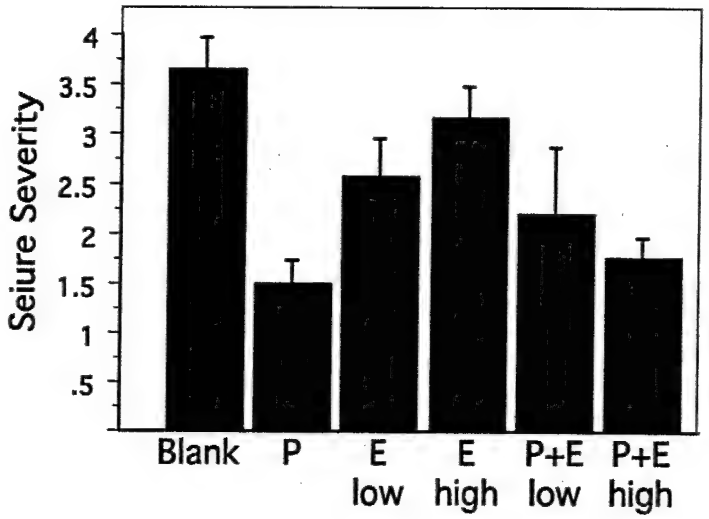

Figure 1. Effects of progesterone and estrogen on kainate-induced seizures

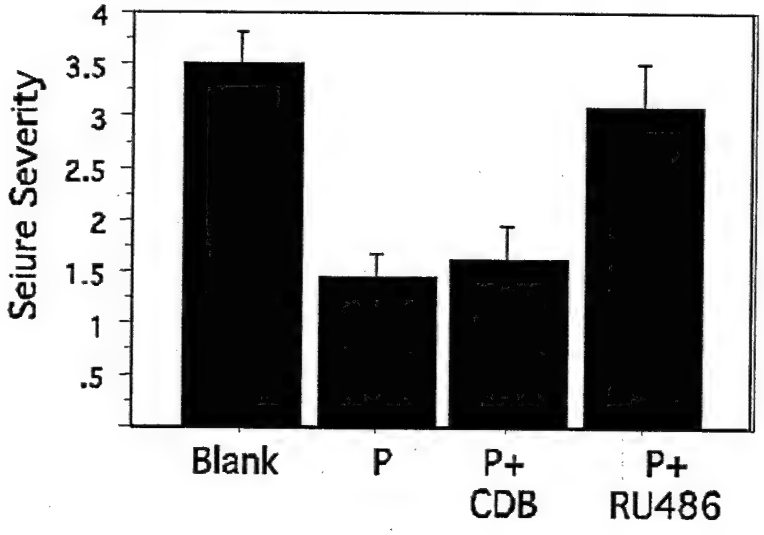

Figure 2. Effects of progesterone receptor antagonists on inhibition of seizure activity by progesterone.

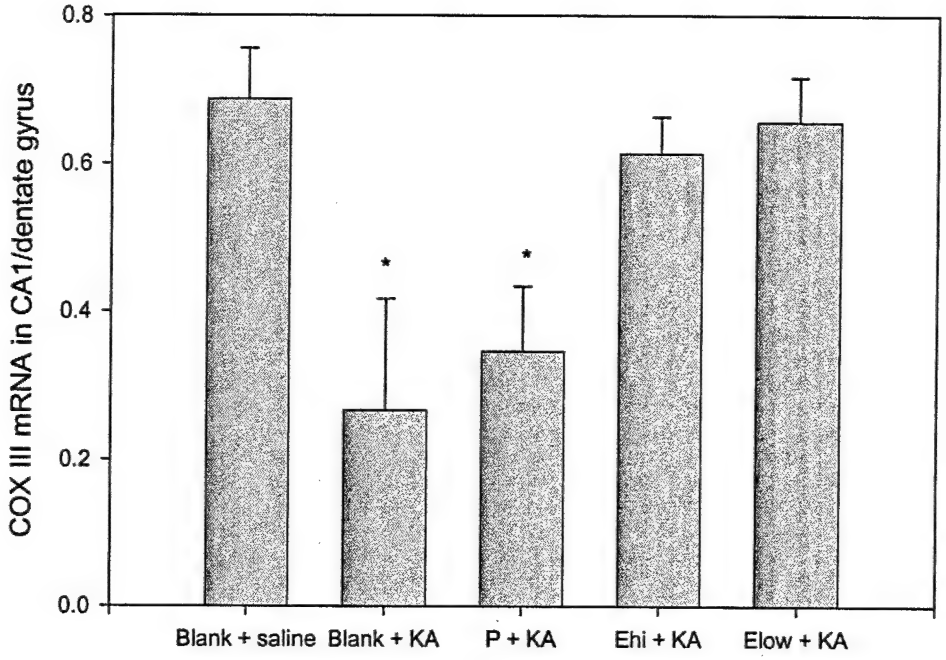

Figure 3. Estradiol, but not progesterone, protects against KA-induced decrease of COX III mRNA in the CA1 region of the hippocampus

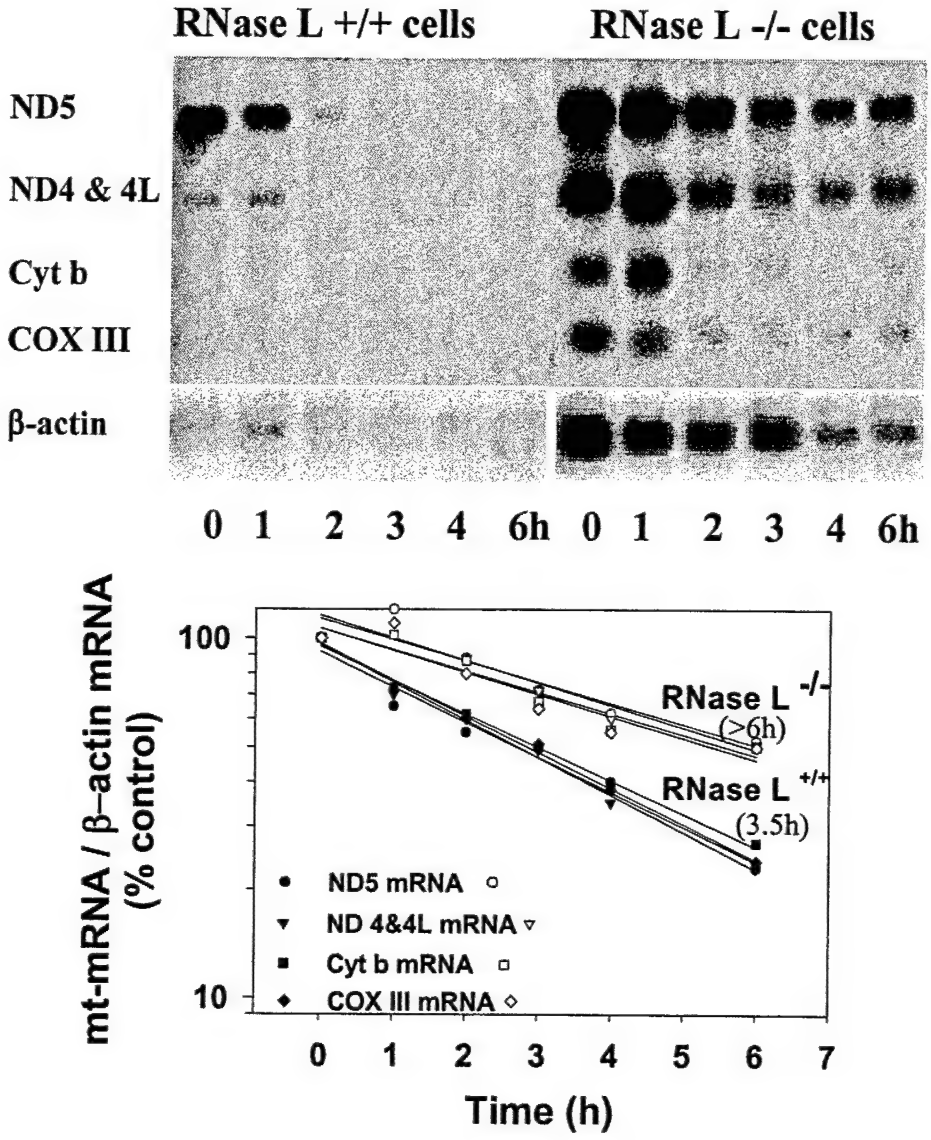

Figure 4. Mitochondrial transcripts are stabilized in RNase L $^{-/-}$ cells. Total cytosolic RNA was isolated from RNase L $^{+/+}$ and RNase L $^{-/-}$ mouse embryo fibroblasts at indicated time points after termination of transcription by actinomycin D, and 2 μg aliquots were subjected to Northern blot analysis as described under "Materials and Methods". Hybridization was quantified by image analysis of autoradiograms. Semi-log plots of transcript remaining *versus* time is depicted in case of β-actin mRNA.

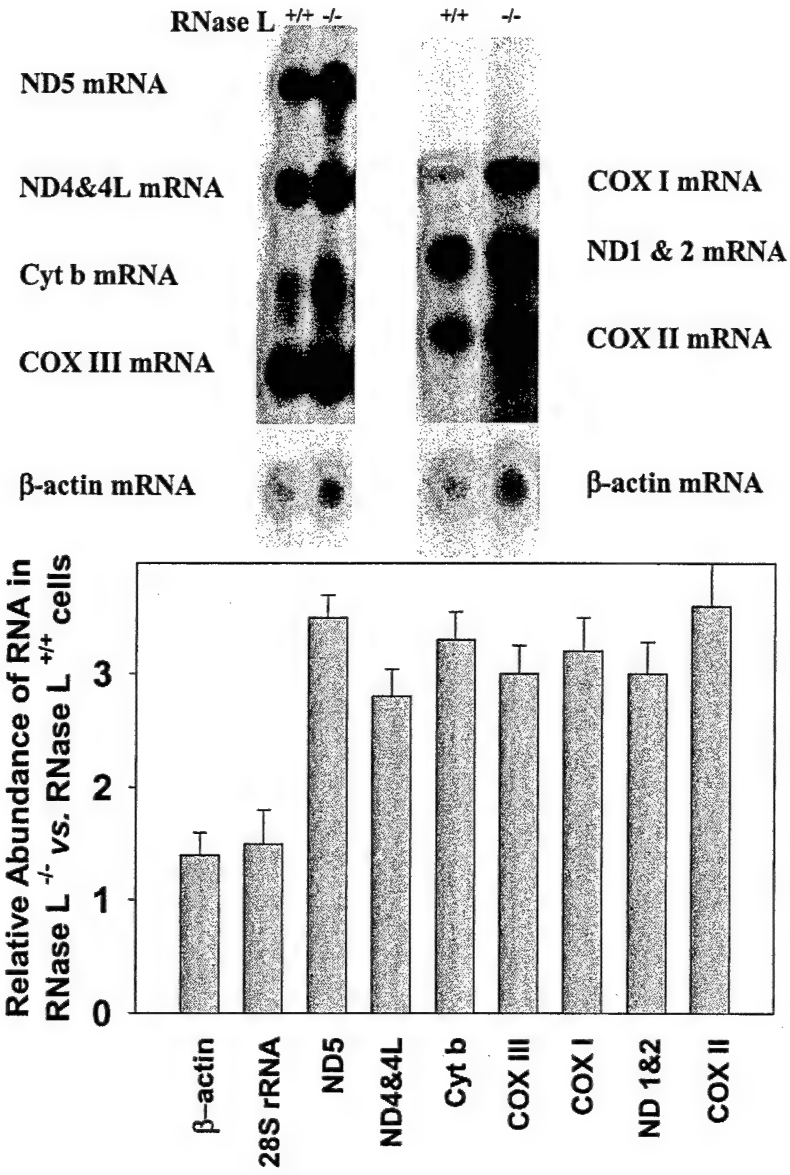

Figure 5. Comparison of the steady state levels of mRNAs mitochondrial proteins in RNase L $^{+/+}$ and RNase L $^{-/-}$ mouse embryo fibroblasts. Total RNA was isolated from 3 x 10^6 RNase L $^{+/+}$ and RNase L $^{-/-}$ mouse embryo fibroblasts and 2 μg aliquots were subjected to Northern blot analysis as described under 'Materials and Methods'. Hybridization was quantified using image analysis of autoradiograms. The amount in RNase L $^{-/-}$ cells relative to RNase L $^{+/+}$ cells is shown.

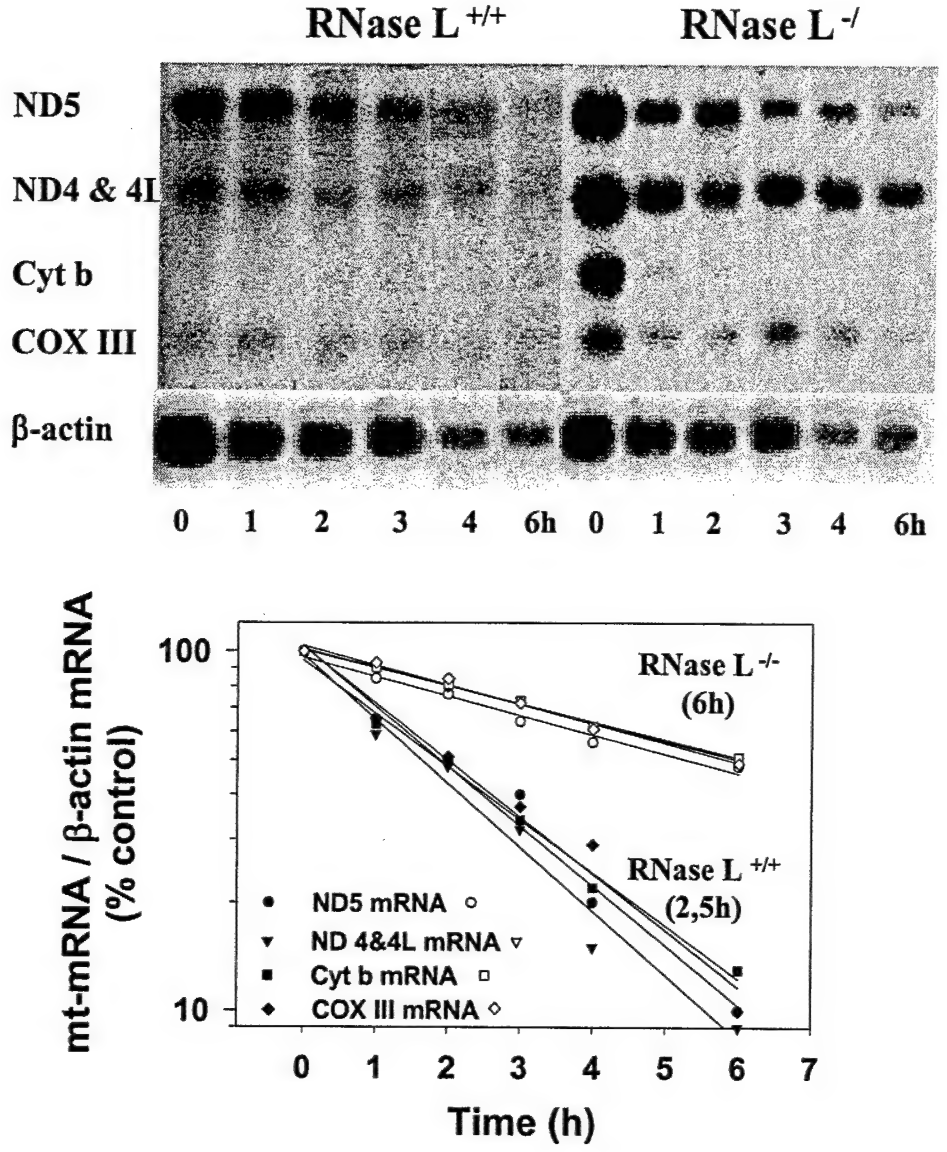

Figure 6. Mitochondrial transcripts are stabilized in monensin-treated RNase L $^{-/-}$ cells. Total cytosolic RNA was isolated from RNase L $^{+/+}$ and RNase L $^{-/-}$ mouse embryo fibroblasts at indicated time points after addition of the sodium ionophore, monensin (250 nM) and termination of transcription by actinomycin D. Two 2 μg RNA aliquots were subjected to Northern blot analysis as described under "Materials and Methods". Hybridization was quantified by image analysis of autoradiograms. Semi-log plots of transcript remaining *versus* time is depicted in case of β-actin mRNA.

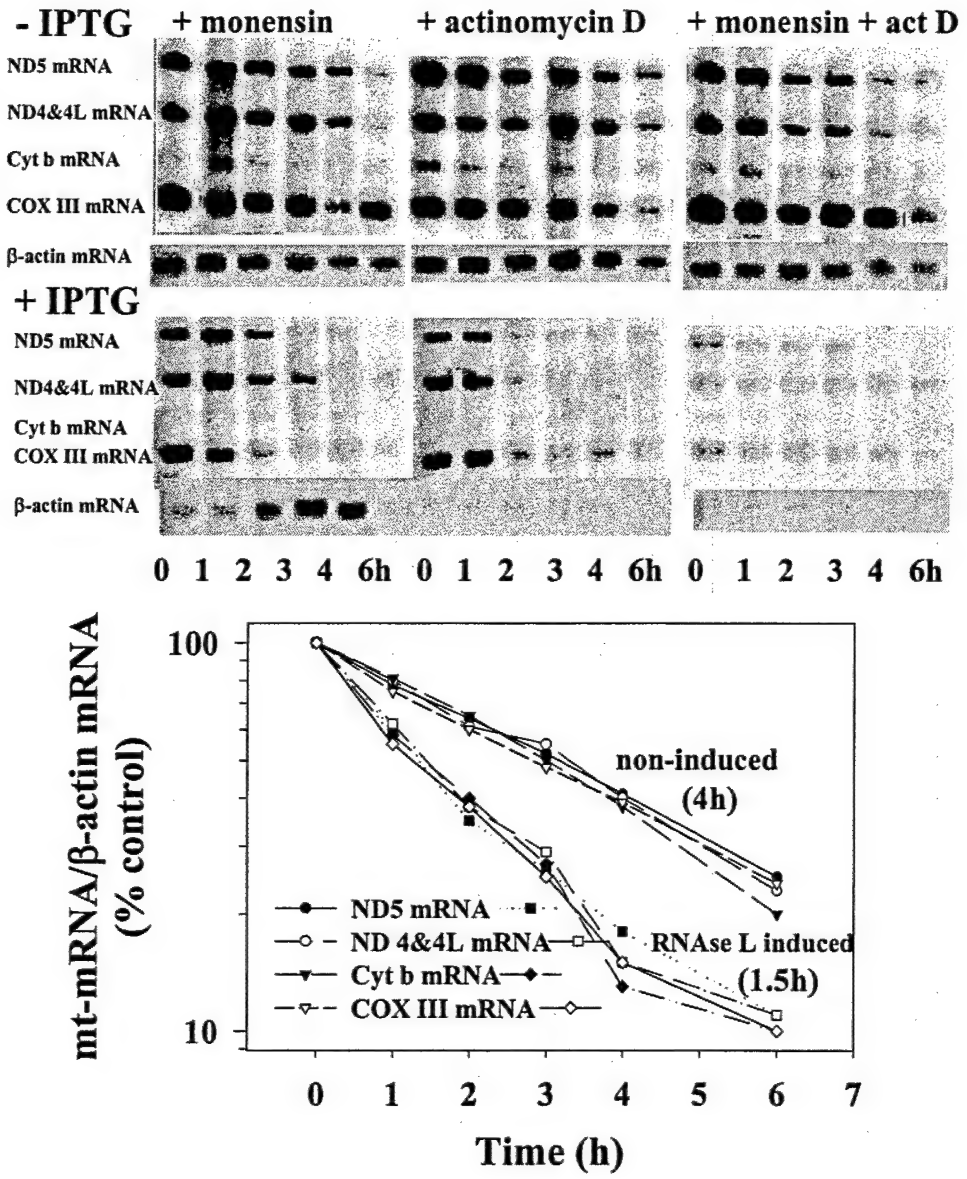

Figure 7. Mitochondrial transcripts are de-stabilized in monensin-treated RNase L induced mouse embryo fibroblasts. Total cytosolic RNA was isolated from un-induced and RNase L-induced mouse embryo fibroblasts at indicated time points after addition of actinomycin D or the sodium ionophore, monensin (250 nM) or after addition of monensin and actinomycin D. Two 2 μg RNA aliquots were subjected to Northern blot analysis as described under "Materials and Methods". Hybridization was quantified by image analysis of autoradiograms. Semi-log plots of transcript remaining *versus* time in monensin plus actinomycin D-treated cells are depicted in case of β-actin mRNA.

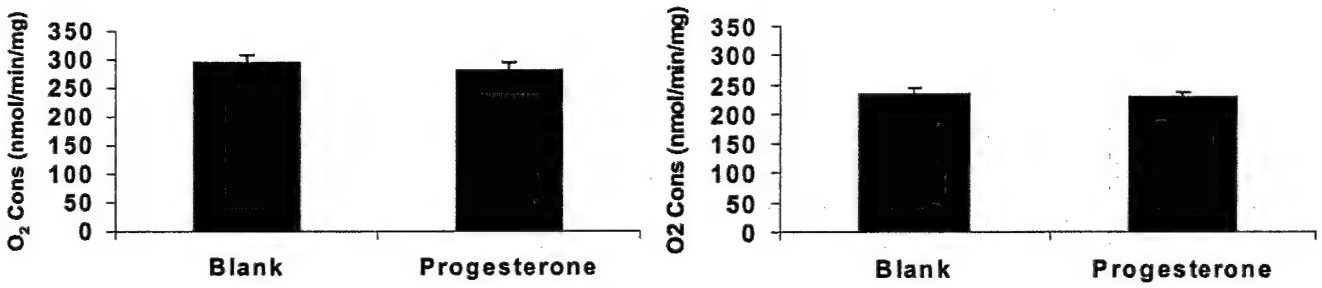

Figure 8. State 3 rates of oxygen consumption (nmol/min/mg mitochondrial protein) of isolated forebrain mitochondria (0.5 mg/ml) in the presence of 40 mM ADP and 1 mM $MgCl_2$ in a KCl media (n=3 rats/group). Figure 1A rates were obtained in the presence of 5 mM glutamate and 5 mM malate. Figure 1B rates were obtained in the presence of 5 mM glutamate and 5 mM malate.

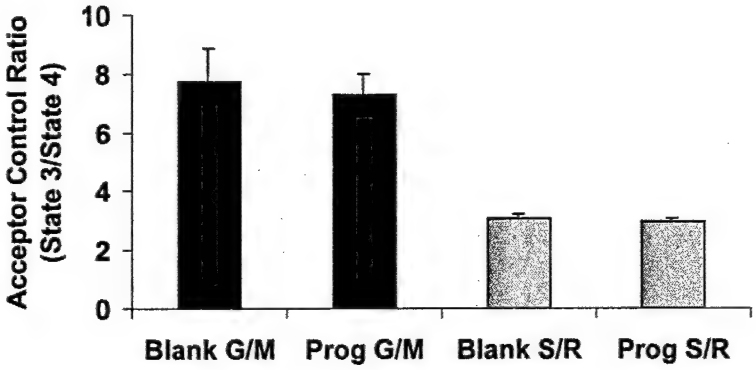

Figure 9. Acceptor control ratio of isolated forebrain mitochondria (0.5 mg/ml) defined as the ratio of ADP-stimulated (State 3) to resting (State 4) rates of oxygen consumption in the presence of 5 mM glutamate and 5 mM malate (G/M,black bars) or 5 mM succinate and 2 μM rotenone (S/R, gray bars). Mitochonria were isolated from ovariectomized female rats implanted with either blank or progesterone (Prog) pellets.

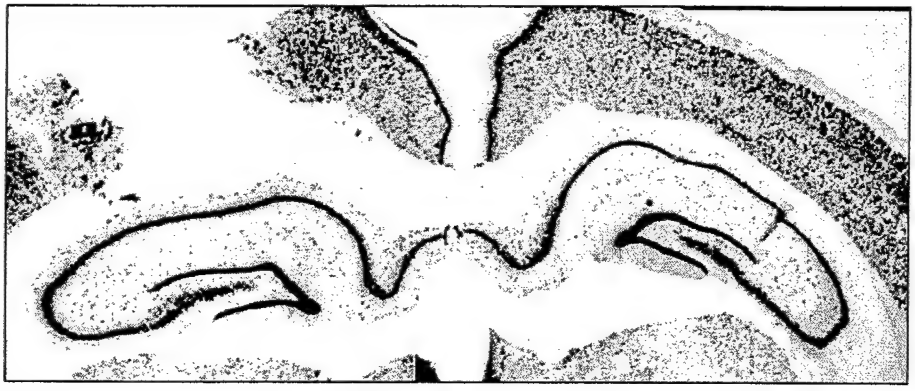

Figure 10. Representative photomicrograph of coronal section of ovariectomized female rat 24h after CCI. Neurons are labeled with neuronal nuclear marker (NeuN) and stain black. Cortical tissue loss is seen ipsilateral (left) to the side of injury through the full thickness of the cortical layers. Note the relative sparing of the underlying hippocampus and the contralateral structures.

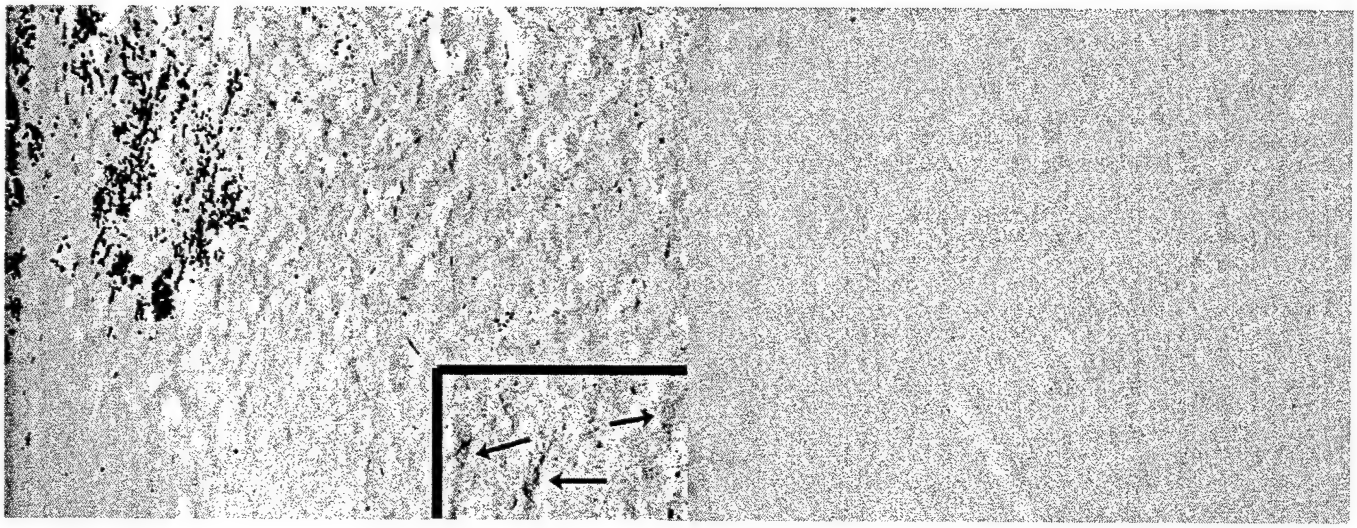

Figure 11. Photomicrograph of the ipsilateral (A) and contralateral (B) cortex 24h after CCI. Tissue has been incubated with antibodies to the anti-apoptotic protein bcl-2. Note numerous positive neurons in the ipsilateral cortex. Area shown is in the injury penumbra (high-powered view in inset). The contralateral hemisphere (B) did not demonstrate any bcl-2 staining.

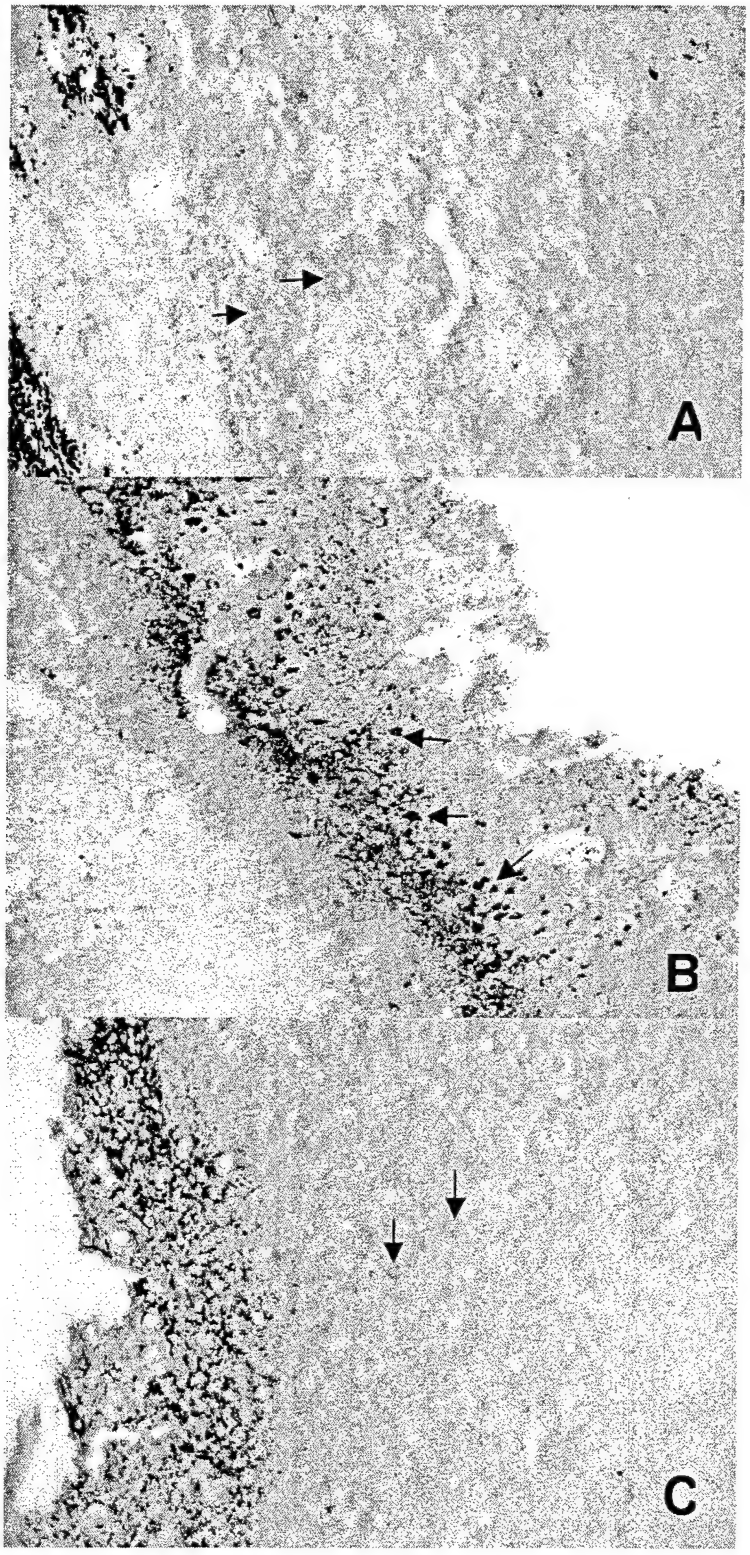

Figure 12. Photomicrographs of ipsilateral cortex at 24 h (A), 48 h (B) and 72 h (C) after CCI in ovariectomized rats (blank pellets), with tissue incubated with bcl-2 antibodies. At 24 h, numerous cells with neuronal morphology demonstrate bcl-2 staining near the area of injury. By 48 h, neuronal staining is much denser within cells. However, by 72 h the bcl-2 labeling has decreased throughout the injured hemisphere, with only scattered neurons with faint bcl-2 detection.

(6) Key Research Accomplishments

A. Neuroprotection by Progesterone

- Determined that low, physiological levels of plasma progesterone inhibited seizures produced by kainic acid while high levels of progesterone had no effect.
- Protection against hippocampal neuronal death by progesterone is directly linked to inhibition of seizure activity.
- Progesterone inhibition of kainate-induced seizures does not appear to be mediated via binding to its traditional nuclear receptor.
- Low and high levels of plasma estrogen do not inhibit seizures produced by kainic acid.
- Low and high levels of plasma estrogen inhibit hippocampal cell death caused by seizures induced by kainic acid.
- Estrogen pretreatment, at supraphysiological levels, does not interfere with P's seizure suppressive effects.
- At low doses, estrogen attenuates seizure suppression by progesterone.
- Mitochondrial gene expression is dependent upon mitochondrial mRNA stability, apparently controlled by a mitochondrial form of RNase L.

B. Mitochondrial Free Radical Generation in Parkinson's Disease

- Mitochondrial Ca^{2+} accumulation either inhibits or stimulates mitochondrial H_2O_2 production, depending on the respiratory substrate and the effect of Ca^{2+} on the mitochondrial membrane potential.
- Bax plus a BH3 domain peptide stimulate H_2O_2 production by brain mitochondria due to release of cytochrome c and this stimulation is insensitive to changes in membrane potential.

- Reactive oxygen species production by mitochondria oxidizing NAD^+-dependent substrates is regulated by mitochondrial membrane potential and by the NAD(P)H redox state but is also dependent on the presence of specific NAD^+-linked respiratory substrates.

(7) Reportable Outcomes

- **Manuscripts**

Chronic exposure of neural cells to elevated intracellular sodium decreases mitochondrial mRNA expression. Chandrasekaran K, Liu LI, Hatanpaa K, Shetty U, Mehrabyan Z, Murray PD, Fiskum G and Rapoport SI. ***Mitochondrion*** 1(2), 141-150 (2001).

Starkov, A.A., Polster, B.M., and Fiskum, G., Regulation of mitochondrial reactive oxygen species generation by calcium and Bax, ***J. Neurochem.*** (2002 in press)

Hoffman, G.E., Moore, N., Fiskum, G., and Murphy, A.Z., Ovarian steroid modulation of seizure severity and hippocampal neuronal cell death after kainic acid treatment, ***Exp. Neurol.*** (submitted)

Chandrasekaran, K., Mehrabyan, Z., Li, X-L., and Hassel, B., RNase-L regulates the stability of mitochondrial DNA-encoded mRNAs, ***J. Biol. Chem.*** (submitted)

Starkov, A.A. and Fiskum, G., H_2O_2 production by brain mitochondria is regulated by membrane potential and by NADH-dependent respiratory substrates, ***Free Rad. Biol. Med.*** (in preparation)

(8) Conclusions

- Physiological plasma levels of progesterone and estrogen are neuroprotective in a rat kainic acid model of status epilepticus. The mechanism of neuroprotection is different for these two gonadal hormones.
- As there is an interaction between progesterone and estrogen, their combined effects at different doses should be studied in different animal models of brain injury, including the kainate model and the controlled cortical impact model of traumatic brain injury.
- The mechanisms and regulation of mitochondrial gene expression and reactive oxygen species production are highly complex but also highly relevant to brain injury due to acute insults and to chronic neurodegenerative diseases. The relationships that exist between mitochondrial cytochrome c release caused by Ca^{2+} and Bax and mitochondrial free radical generation may be particularly important in understanding the molecular pathophysiology of Parkinson's disease and of related brain injury caused by mitochondrial neurotoxins.

(9) References

1. Chandrasekaran K, Stoll J, Brady DR, Rapoport SI. Localization of cytochrome oxidase (COX) activity and COX mRNA in the hippocampus and entorhinal cortex of the monkey brain: correlation with specific neuronal pathways. Brain Res 1992; 579(2):333-336.

2. Chandrasekaran K, Mehrabian Z, Spinnewyn B, Drieu K, Fiskum G. Neuroprotective effects of bilobalide, a component of the Ginkgo biloba extract (EGb 761), in gerbil global brain ischemia. Brain Res 2001; 922(2):282-292

3. Ankarcrona M, Dypbukt JM, Bonfoco E, Zhivotovsky B, Orrenius S, Lipton SA et al. Glutamate-induced neuronal death: a succession of necrosis or apoptosis depending on mitochondrial function. Neuron 1995; 15(4):961-973.

4. Chandrasekaran K, Giordano T, Brady DR, Stoll J, Martin LJ, Rapoport SI. Impairment in mitochondrial cytochrome oxidase gene expression in Alzheimer disease. Brain Res Mol Brain Res 1994; 24(1-4):336-340.

5. Murdock DG, Boone BE, Esposito LA, Wallace DC. Up-regulation of nuclear and mitochondrial genes in the skeletal muscle of mice lacking the heart/muscle isoform of the adenine nucleotide translocator. J Biol Chem 1999; 274(20):14429-14433.

6. Maggi A, Zucchi I, Perez J. Progesterone in rat brain: modulation of beta-adrenergic receptor activity. Pharmacol Res Commun 1985; 17(3):283-291.

7. Hagihara K, Hirata S, Osada T, Hirai M, Kato J. Expression of progesterone receptor in the neonatal rat brain cortex: detection of its mRNA using reverse transcription-polymerase chain reaction. J Steroid Biochem Mol Biol 1992; 41(3-8):637-640.

8. Kato J, Hirata S, Nozawa A, Yamada-Mouri N. Gene expression of progesterone receptor isoforms in the rat brain. Horm Behav 1994; 28(4):454-463.

9. Cheng C, Fass DM, Reynolds IJ. Emergence of excitotoxicity in cultured forebrain neurons coincides with larger glutamate-stimulated [Ca(2+)](i) increases and NMDA receptor mRNA levels. Brain Res 1999; 849(1-2):97-108.

10. Nilsen J, Brinton RD. Impact of progestins on estrogen-induced neuroprotection: synergy by progesterone and 19-norprogesterone and antagonism by medroxyprogesterone acetate. Endocrinology 2002; 143(1):205-212.

11. Chandrasekaran K, Liu LI, Hatanpaa K, Shetty U, Mehrabian Z, Murray PD et al. Chronic exposure of neural cells to elevated intracellular sodium decreases mitochondrial mRNA expression. Mitochondrion 1, 141-150. 2001.

12. Le Roy F, Bisbal C, Silhol M, Martinand C, Lebleu B, Salehzada T. The 2-5A/RNase L/RNase L inhibitor (RNI) pathway regulates mitochondrial mRNAs stability in interferon alpha-treated H9 cells. J Biol Chem 2001; 276(51):48473-48482.

13. Chen J, Gokhale M, Li Y, Trush MA, Yager JD. Enhanced levels of several mitochondrial mRNA transcripts and mitochondrial superoxide production during ethinyl estradiol-induced hepatocarcinogenesis and after estrogen treatment of HepG2 cells. Carcinogenesis 1998; 19(12):2187-2193.

14. Too CK, Giles A, Wilkinson M. Estrogen stimulates expression of adenine nucleotide translocator ANT1 messenger RNA in female rat hearts. Mol Cell Endocrinol 1999; 150(1-2):161-167.

15. Lighthall J. Controlled cortical impact: a new experimental brain injury model. J Neurotrauma 5:1-5, 1988.

16. Dixon C, Clifton G, Lighthall J, Yaghmai A and Hayes R. A controlled cortical impact model of traumatic brain injury in the rat. J Neurosci Meth 39: 253-262, 1991.

17. Clark RSB, Chen J, Watkins SC, Kochanek PM, Chen M, Stetler RA, Loeffert JE and Graham SH. Apoptosis-suppressor gene bcl-2 expression after traumatic brain injury in rats. J Neurosci 17: 9172-82, 1997.

(10) Appendices:

4 manuscripts

ELSEVIER

Mitochondrion 1 (2001) 141–150

Mitochondrion

www.elsevier.com/locate/mito

Chronic exposure of neural cells to elevated intracellular sodium decreases mitochondrial mRNA expression

Krish Chandrasekaran[a,*], Li-Ing Liu[b], Kimmo Hatanpää[b], Umesha Shetty[b], Zara Mehrabian[a], Peter D. Murray[a], Gary Fiskum[a], Stanley I. Rapoport[b]

[a]*Department of Anesthesiology, University of Maryland School of Medicine, MSTF 5-34, 685 West Baltimore Street, Baltimore, MD 21201, USA*

[b]*Section on Brain Physiology and Metabolism, National Institute on Aging, NIH, Bethesda, MD 20892, USA*

Received 14 December 2000; received in revised form 21 March 2001; accepted 29 March 2001

bstract

Regulation of expression of mitochondrial DNA- (mtDNA-) encoded genes of oxidative phosphorylation can occur rapidly in :ural cells subjected to a variety of physiological and pathological conditions. However, the intracellular signal(s) involved in gulating these processes remain unknown. Using mtDNA-encoded cytochrome oxidase subunit III (COX III), we show that ; mRNA expression in a differentiated rat pheochromocytoma cell line PC12S is decreased by chronic exposure to agents that crease intracellular sodium. Treatment of differentiated PC12S cells either with ouabain, an inhibitor of Na/K-ATPase, or ith monensin, a sodium ionophore, decreased the steady-state levels of COX III mRNA by 50%, 3–4 h after addition of the ugs. No significant reduction in mtDNA-encoded 12S rRNA or nuclear DNA-encoded β-actin mRNA were observed. :moval of the drugs restored the normal levels of COX III mRNA. Determination of half-lives of COX III mRNA, 12S .NA, and β-actin mRNA revealed a selective decrease in the half-life of COX III mRNA from 3.3 h in control cells to 1.6 h in abain-treated cells, and to 1 h in monensin-treated cells. These results suggest the existence of a mechanism of posttranriptional regulation of mitochondrial gene expression that is independent of the energetic status of the cell and may operate der pathological conditions. © 2001 Elsevier Science B.V. and Mitochondria Research Society. All rights reserved.

ywords: Neural cells; Mitochondrial mRNA; Intracellular sodium

Introduction

Neurons depend on a high rate of mitochondrial idative metabolism to produce ATP (Erecinska d Silver, 1989). ATP is needed for ion pumping restore the cellular membrane potential after depoization. The mitochondrial respiratory chain consists of five multisubunit oxidative phosphorylation (OXPHOS) enzyme complexes. Four of these OXPHOS complexes, including Complex IV (cytochrome oxidase (COX)), are bipartite in nature, consisting of subunits derived from both mitochondrial DNA (mtDNA) and nuclear DNA (nDNA). Mitochondrial DNA encodes 13 polypeptides, all of which are necessary for electron transport and OXPHOS. The large number of remaining subunits is specified by the nuclear genome. To form active enzyme complexes, both mtDNA- and nDNA-

Corresponding author. Tel.: +1-410-706-3418; fax: +1-410-2550.

E-mail address: kchandra@anesthlab.ummc.umaryland.edu . Chandrasekaran).

7-7249/01/$20.00 © 2001 Elsevier Science B.V. and Mitochondria Research Society. All rights reserved.
S1567-7249(01)00010-1

BEST AVAILABLE COPY

encoded subunits are required (Attardi and Schatz, 1988).

Neuronal activity and energy demand influence the expression of mitochondrial DNA-encoded genes. For example, under conditions of decreased neuronal activity induced by afferent impulse blockade, neuronal mitochondrial gene expression and COX enzyme activity are decreased (Wong-Riley, 1989; Wong-Riley et al., 1997). Removal of the afferent impulse blockade restores basal mitochondrial gene expression and COX activity (Wong-Riley, 1989; Wong-Riley et al., 1997). Such regulation occurs mainly at the transcriptional level (Wong-Riley et al., 1997; Zhang and Wong-Riley, 2000a,b). Using the in organello method, it was shown that high intramitochondrial ATP levels suppress transcription of mtDNA, explaining how energy demand can regulate mtDNA transcription (Gaines and Attardi, 1984; Enriquez et al., 1996a,b). Apart from transcriptional control, the primary regulation of mitochondrial gene expression is based on differences in RNA stability. Thus, although mitochondrial gene expression is a major component in the regulation of energy metabolism of the cell, the contribution of transcriptional and posttranscriptional mechanisms to the overall regulation of mitochondrial gene expression is not known (Kagawa and Ohta, 1990).

The goal of our present study was to probe the mechanism of regulation of mitochondrial gene expression under conditions of chronic exposure to two drugs that increase intracellular sodium ($[Na]_i$) but by two different independent mechanisms. Ouabain reduces cellular Na^+ efflux by inhibiting the Na/K-ATPase and would be expected to reduce cellular energy demand. Monensin is a Na^+ ionophore, which in contrast to ouabain, would increase the cellular energy demand through futile cycling of Na^+ across the plasma membrane. These expected effects on energy metabolism were confirmed by measurements of cellular ATP/ADP ratios and compared to the levels of mtDNA-encoded cytochrome oxidase subunit (COX III) mRNA in cultures of nerve growth factor-(NGF-) induced differentiated PC12 neural cells. Both the levels and half-lives of COX III mRNA, mtDNA-encoded 12S rRNA, and nDNA-encoded β-actin mRNA were quantified. Our results indicate a selective decrease in mtDNA-encoded mRNA stability in both ouabain- and monensin-treated cells, suggesting a Na^+-mediated mechanism of posttranscriptional regulation that is independent of the energetic status of the cell in neuronal cultures. A part of this work has been published as abstract (Liu et al., 1999).

2. Methods and materials

2.1. Cell culture

A morphological variant of rat pheochromocytoma PC12 cells (PC12S) that has the ability to grow in tissue culture dishes without polylysine treatment was used in experiments (Fukuyama et al., 1993). PC12S cells were maintained in Dulbecco's modified Eagle's medium (DMEM) containing 2 mM glutamine, 7.5% heat inactivated fetal calf serum, 7.5% heat inactivated horse serum, and penicillin–streptomycin. Differentiation was induced by the addition of NGF (Life Technologies, MD, USA) at 50 μg/ml to the cell culture medium. We showed previously that the morphology of PC12S cells resembles that of sympathetic neurons after addition of NGF for 5 days (Fukuyama et al., 1993). Differentiated PC12S maintained in NGF for 10 days was used throughout the experiments.

2.2. Chemicals

All reagents and chemicals used were of the highest grade available from Sigma Chemical Co. (St. Louis, MO, USA). Stock solutions of actinomycin D and ouabain were prepared in water, whereas monensin was dissolved in 95% ethanol. When ethanol was used as a solvent, appropriate control experiments were conducted using the vehicle alone. Ethanol concentrations were always <0.1%.

2.3. Experimental procedure

Cells grown in 60 × 15 mm dishes were treated either with ouabain, at a final concentration of 1 mM, or with monensin, at a final concentration of 100 nM. At timed points over a 6-h period, cells were washed with Dulbecco's phosphate buffered saline (DPBS) without calcium and magnesium and total RNA was isolated using the TRIzol reagent as recommended by the manufacturer (Life Technologies, MD,

USA). Total RNA was subjected to Northern blot analysis as described below.

The reversibility of the effect of ouabain and monensin on mitochondrial gene expression was evaluated by exposing the differentiated PC12S cells to the drugs for a period of 6 h. The cells were then washed three times with DPBS without calcium and magnesium, fresh DMEM growth medium with NGF was added, and total RNA was isolated at various times over a 24-h period and processed for Northern blot analysis.

The effect of ouabain or monensin on the stability of mtDNA- and nDNA-encoded transcripts was determined by adding the transcriptional inhibitor actinomycin D to the cultures at a final concentration of 5 μg/ml. After 1 h, either vehicle or ouabain or monensin was added. Total RNA was isolated at various times over an 8-h period and processed for Northern blot analysis.

2.4. RNA analysis

Ten μg of total RNA was run on a 1.2% formaldehyde agarose gel and transferred on to a GeneScreen Plus membrane as described by the manufacturer (Dupont, New England Nuclear, MA, USA). Prehybridization and hybridization were done with Hybridizol reagent (Hybridizol I and II mixed in the ratio of 4:1, Oncor, MD, USA). The blots were prehybridized at 42°C for 16 h, then [^{32}P]-labeled cytochrome oxidase subunit III (COX III) probe was added and hybridized for 48 h at 42°C (Chandrasekaran et al., 1994). The blots were washed with increasing stringency and the final wash was performed at 65°C with 0.2 × SSC (1 × SSC = 150 mM sodium chloride and 15 mM sodium citrate) and 1% sodium dodecylsulfate (SDS). The blots were exposed to X-ray film (Biomax MS, Kodak, NY, USA) with an intensifying screen for 45 min to 2 days at −70°C. Probe was removed from the blots by placing them in boiling DEPC-treated water for 10 min. The blots were then rehybridized with a [^{32}P]-labeled control β-actin probe as described above. Finally, the blots were hybridized with 12S rRNA probe. The level of RNA hybridized was quantified using an image analysis program (NIH image 1.57 program written by Wayne Rasband, NIH). To maintain measured intensities within the linear range, the blots hybridized with different probes were exposed for different periods. The level of RNA was quantified from autoradiograms of lower exposure than was used for photography. Ratios of COX III mRNA to β-actin mRNA and 12S rRNA to β-actin mRNA were calculated (Chandrasekaran et al., 1994).

2.5. Probe preparation and labeling

Cytochrome oxidase subunit III, 12S rRNA and β-actin probes were prepared by isolating the cDNA insert from the plasmid clones (American Type Culture Collection, VA, USA). The cDNA fragments were gel purified and labeled with [^{32}P] dCTP using a random primed labeling kit (Pharmacia, NJ, USA). The labeled probes were purified using probe purification columns (Pharmacia, NJ, USA). Northern blots hybridized with either probe showed a single band of expected size, verifying the specificity of the probes.

2.6. Estimation of half-lives of COX III mRNA, 12S rRNA, and β-actin mRNA

Ten μg of total RNA from cells treated with either vehicle or ouabain or monensin in the presence of actinomycin D was subjected to Northern blot analysis. The blots were hybridized with COX III, 12S rRNA, and β-actin probes and the levels of the respective RNA species were quantified. Levels of β-actin mRNA are expressed as the percentage of β-actin mRNA remaining at each experimental time compared to zero time. Levels of COX III mRNA and 12S rRNA were calculated as the ratio of the respective species to the level of β-actin mRNA. At each experimental time, the RNA ratios are expressed as a percentage of the ratio at time zero. The half-lives were determined from the equation $t_{1/2} = 0.301/\text{slope}$ of the best-fit line ($\log_{10}$ remaining RNA versus time).

2.7. Measurement of ATP/ADP ratio

Differentiated PC12S cells were treated with vehicle or ouabain or monensin for various periods as described. Nucleotides were extracted using hot methanol (Shryock et al., 1986). Briefly, the cells were scraped in 5 ml of hot (75°C) 80% methanol containing 0.5 mM EDTA. The extract was centrifuged at 8000 × *g* for 10 min at 4°C. The supernatant was transferred to a fresh glass tube and evaporated to

BEST AVAILABLE COPY

dryness. The residue was dissolved in 1 ml distilled water, 0.5 ml chloroform was added, vortexed, and the samples were centrifuged at 2000 × *g* for 4 min at 10°C. Fifty μl of the aqueous solution was injected on HPLC columns. The adsorbosphere nucleotide–nucleoside column (7 μm, 250 × 4.6 mm, Allteck) with two-solvent system was used for separation of ATP and ADP. Solvent A contained 60 mM $NH_4H_2PO_4$, 5 mM tetrabutyl-ammonium phosphate, pH 5.0 and solvent B contained methanol with 5 mM tetrabutyl-ammonium phosphate. The gradient of HPLC was from 90 to 64% of solvent A during a period of 20 min, then maintained for 10 min, then returned to 90% of solvent A for 10 min. The flow rate was 1 ml/min and the nucleotides were detected at 259 nM. The resolution of ADP and ATP were determined using external ATP and ADP standards. The peak areas were used to calculate the ratio of ATP to ADP.

2.8. Measurement of intracellular sodium

PC12 cells were differentiated with NGF (50 ng/ml) for 5 days. In order to measure the intracellular sodium concentration rather than the influx, the culture medium was replaced with a medium containing NGF and ^{22}Na (5 μCi or 185 KBq per ml) for another 5 days. Measurement of intracellular ^{22}Na showed that an equilibration between added radioactive label with the cold sodium in the medium was achieved within 24 h. The cells were then treated for various time periods with either the vehicle or monensin (final concentration: 100 nM). The reaction was terminated by aspiration of the medium, and the cells were quickly washed twice with ice-cold DPBS and digested for 1 h in 0.2 ml of 1 M NaOH at room temperature. Cell digests were assayed for ^{22}Na contents by scintillation counter.

2.9. Statistical analysis and replication of results

The results presented are representative of at least three to five independent experiments. Where indicated, statistical analysis was carried out using a one-way analysis of variance (ANOVA) followed by Tukey's test for multiple comparisons. The differences were considered significant when $P < 0.05$.

3. Results

3.1. Treatment of differentiated PC12S cells with ouabain or monensin alters the ratio of ATP/ADP

Ouabain, an inhibitor of the plasma membrane Na/K-ATPase, and monensin, an Na^+ ionophore, are useful tools for elevating $[Na]_i$ (Pressman and Fahim, 1982). This effect of monensin on differentiated PC12S cells was confirmed by incubating cell cultures in the presence of ^{22}Na. Exposure of cell cultures for 3 h to 100 nM monensin resulted in a 500% increase in ^{22}Na, from 30 ± 5 to 150 ± 12 pmol/μg protein. Exposure of cell cultures to ouabain (1 mM) for 3 h resulted in a 300% increase in ^{22}Na, from 30 ± 5 to 85 ± 9 pmol/μg protein (Pressman and Fahim, 1982).

The effect of ouabain and monensin on cellular ATP/ADP ratios was tested. Addition of ouabain caused a rapid and nearly 100% increase in the ATP/ADP ratio followed by a return to a ratio that was still significantly higher (≈ 50%) than that of vehicle-treated cells (Fig. 1). Addition of 100 nM monensin resulted in a sustained, approximately 40% decrease in ATP/ADP ratio. These results suggested that in differentiated PC12S cells, the Na/K-ATPase is one of the major consumers of ATP.

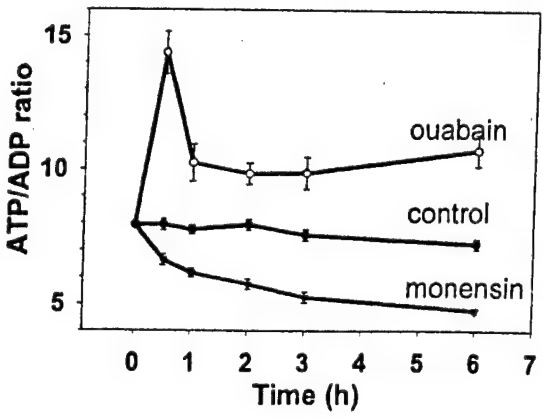

Fig. 1. Time course and extent of ouabain- and monensin-induced ATP/ADP ratio changes in differentiated PC12S cells. Extracts were prepared with hot methanol from cells that were treated with the drugs for various time periods. The nucleotide phosphates were resolved using HPLC and the ratio of ATP to ADP was determined from their peak areas. Each point is the mean ± SEM of four separate experiments.

Inhibition of the sodium pump by ouabain reduces the consumption of ATP and thereby increases the ATP/ADP ratio. In contrast, influx of sodium ions by the ionophore, monensin, activates the pump, causing an increased consumption of ATP and a decreased ATP/ADP ratio. However, measurements of cell viability using trypan blue exclusion indicated no decrease in viability (>95% trypan blue exclusion) following at least 6 h exposure to either ouabain or monensin. Microscopic examination of the cells indicated that within 1 h after the addition of ouabain or monensin there was cell swelling. This was likely due to increased intracellular sodium ion [$(Na^+)_i$], caused either by an inhibition of Na/K-ATPase (ouabain) or by an influx of sodium ions (monensin), accompanied by a passive influx of Cl^- and shifts in water content.

3.2. Chronic treatment of differentiated PC12S cells with ouabain decreases mtDNA-encoded COX III mRNA levels

To examine the effects of ouabain and monensin on mtDNA-encoded COX subunit III gene expression, it was first necessary to ascertain the steady-state level of COX III mRNA in PC12S cells treated with vehicle. PC12S cells were differentiated with NGF for 10 days. The cells were treated with the vehicle (water or ethyl alcohol (0.01%)) for various periods of time, total cellular RNA was isolated, and 10 μg aliquots were subjected to Northern analysis as described in Section 2. Blots of RNA were probed with mtDNA-derived cDNAs encoding COX III and 12S rRNA as well as nDNA-derived cDNA encoding β-actin. Levels of β-actin mRNA were determined to ensure that equivalent amounts of RNA were loaded and transferred into each lane in Northern blot analyses. The results showed that there was no evidence of any significant modulation of steady-state transcript levels of COX III, 12S rRNA, and β-actin genes in vehicle-treated PC12S cells (not shown).

Treatment of differentiated PC12S cells with the Na/K-ATPase inhibitor ouabain decreased the steady-state levels of mtDNA-encoded COX III mRNA (Fig. 2a,c). Mitochondrial DNA-encoded 12S rRNA, however, was unaffected by ouabain treatment (Fig. 2a,b). To ensure that the quantity of 12S-specific radiolabeled probes were not limiting in this experiment, serial dilutions of RNA from these cells were subjected to dot-blot analysis with specific probes, and analysis confirmed that the steady-state quantity of 12S rRNA was indeed unaffected (data not shown). There was also no evidence of any significant ouabain-induced modulation of steady-state nDNA-encoded β-actin mRNA levels (Fig. 2a).

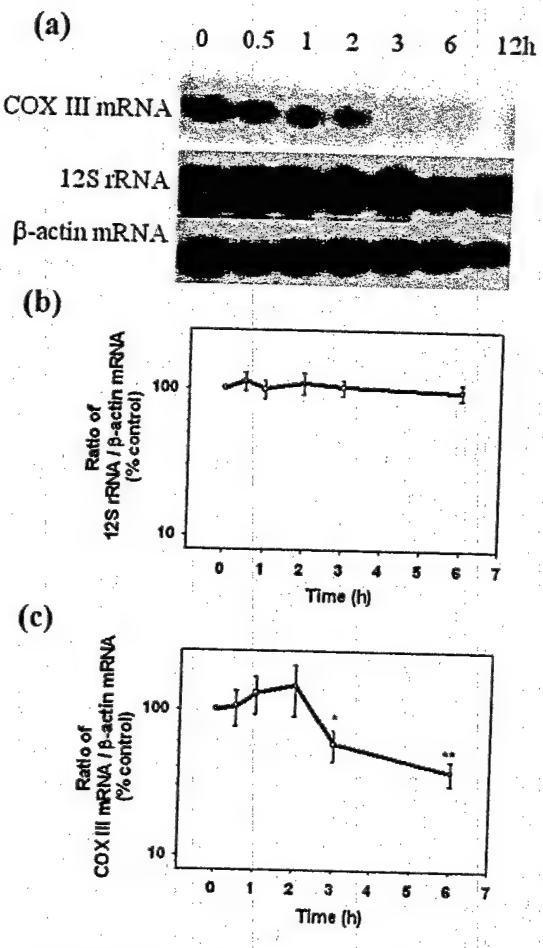

Fig. 2. The time course of changes in β-actin mRNA, 12S rRNA, and COX III mRNA levels in ouabain-treated cells. The β-actin mRNA, 12S rRNA, and COX III mRNA levels of differentiated PC12S cells exposed to ouabain (final concentration 1 mM) for the indicated periods were determined by Northern blot analysis and quantified by image analysis of autoradiograms. The relative changes in β-actin mRNA was related to zero time samples. The ratio of COX III mRNA to β-actin mRNA and 12S rRNA to β-actin mRNA ratio was calculated at each time point and was then related to the ratio of zero time samples. Each point is the mean ± SEM of three to five separate experiments. The asterisk indicates the significant difference from zero time samples ($P < 0.05$).

BEST AVAILABLE COPY

These results taken together with the elevation of the ATP/ADP ratio by ouabain shown in Fig. 1 suggested that inhibition of the sodium pump by ouabain decreased the consumption of ATP (energy demand) and consequently decreased the levels of mtDNA-encoded COX III mRNA.

3.3. Chronic treatment of differentiated PC12S cells with monensin decreases mtDNA-encoded COX III mRNA levels

If ouabain decreased mitochondrial gene expression by decreasing cellular energy demand, it follows that exposure of cells to a condition that increases energy demand should increase gene expression. Thus, cells were exposed to the Na^+ ionophore monensin, anticipating that the levels of COX III mRNA would increase due to the decrease in the ATP/ADP ratio (see Fig. 1) caused by cycling of Na^+ across the plasma membrane. Although there was a trend toward an increase in COX III mRNA following 1 h exposure to monensin, the net effect was a significant decrease 3 and 6 h after addition of monensin. Mitochondrial DNA-encoded 12S rRNA, however, was unaffected by monensin treatment (Fig. 3a,b). There was also no significant monensin-induced modulation of steady-state nDNA-encoded β-actin mRNA levels (Fig. 3a).

3.4. Removal of ouabain and monensin restores normal levels of mtDNA-encoded COX III mRNA

Differentiated PC12S cells were treated with ouabain or monensin for a period of 6 h. The cells were washed free of drugs and replaced with fresh medium. As shown in Fig. 4, removal of drugs restored the normal levels of COX III mRNA within 12 h, suggesting that the decrease in COX III mRNA was not due to the toxicity of ouabain and monensin. Moreover, cell viability as measured by trypan blue dye exclusion showed that the cells remained viable after addition of ouabain or monensin up to a period of 6 h. Estimation of mtDNA by dot-blot analysis showed no significant reduction in both ouabain- and monensin-treated cells compared to vehicle-treated cells, suggesting that the observed decrease in COX III mRNA was not due to loss of mitochondria (not shown).

3.5. Treatment of differentiated PC12S cells with ouabain or monensin decreases the stability of mtDNA-encoded COX III mRNA

To test whether the decrease in mtDNA-encoded

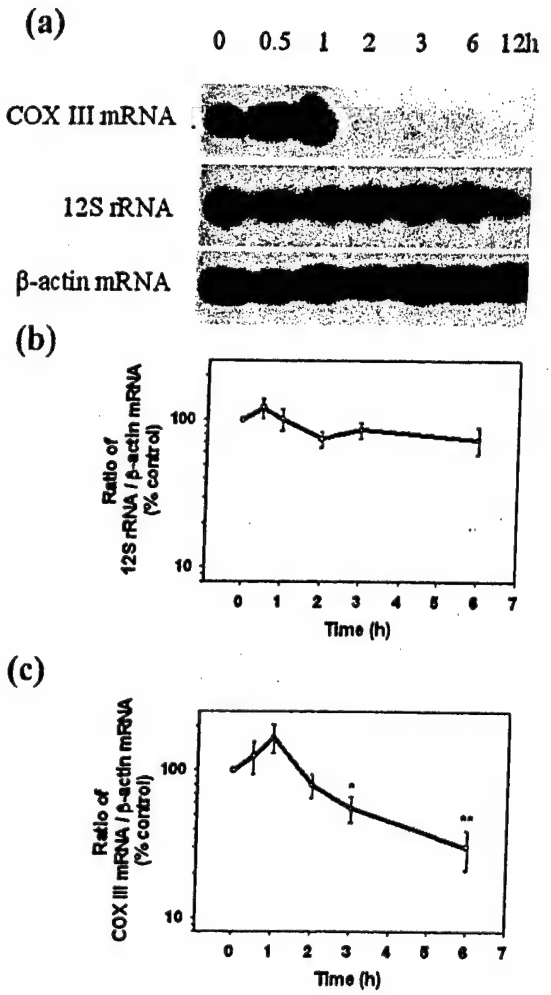

Fig. 3. The time course of changes in β-actin mRNA, 12S rRNA, and COX III mRNA levels in monensin-treated cells. The β-actin mRNA, 12S rRNA, and COX III mRNA levels of differentiated PC12S cells exposed to the vehicle for the indicated periods were determined by Northern blot analysis and quantified by image analysis of autoradiograms. The relative changes in β-actin mRNA were related to zero time samples. The ratios of COX III mRNA to β-actin mRNA and of 12S rRNA to β-actin mRNA were calculated at each time point and were then related to the ratio of zero time samples. Each point is the mean ± SEM of five separate experiments. The asterisks denote a significant difference of the sample from the zero time samples ($P < 0.05$).

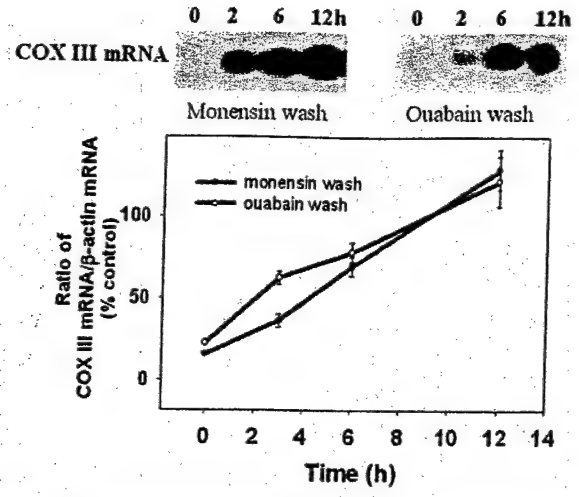

Fig. 4. Effect of the removal of ouabain and monensin on the ratio of COX III mRNA to β-actin mRNA. Differentiated PC12S cells exposed to ouabain and monensin for a period of 6 h. The cells were then washed free of drugs and were maintained in normal culture medium. The COX III mRNA and β-actin mRNA levels for the indicated periods were determined by Northern blot analysis and quantified by image analysis of autoradiograms. The relative change in COX III mRNA/and β-actin mRNA ratio was related to COX III mRNA/and β-actin mRNA ratio of zero time samples. Each point is the mean ± SEM of three separate experiments.

COX III mRNA in ouabain- or monensin-treated cells is due to increased degradation or decreased synthesis, we determined the half-life of COX III mRNA, 12S rRNA, and β-actin mRNA in control, ouabain-, and monensin-treated differentiated PC12S cells. Actinomycin D has been previously shown to inhibit total cellular transcription in PC12 cells by more than 90%. To estimate half-lives, actinomycin D was added to differentiated PC12S cells and after 1 h, vehicle, ouabain, or monensin was added. Total cellular RNA was isolated at various times over an 8-h period. Throughout this period, cell viability was not compromised and there was no substantial reduction in total RNA yield in the presence of actinomycin D. Fig. 5a shows autoradiograms of RNA isolated and probed with COX III and β-actin. Clearly, mRNA encoding COX III was significantly affected, decreasing the estimated $t_{1/2}$ from 3.3 h in control cells to 1.6 h in ouabain-treated cells and to 1 h in monensin-treated cells (Fig. 4c), respectively. No such decrease in half-lives were observed with mtDNA-encoded 12S rRNA (Fig. 4b) and nDNA-encoded β-actin mRNA (Fig. 4a) in both ouabain- and monensin-treated cells. Also, the estimated $t_{1/2}$ of COX III mRNA in control cells was much shorter (3.3 h) when compared to the $t_{1/2}$ of 12S rRNA (17 h) and β-actin mRNA (>17 h).

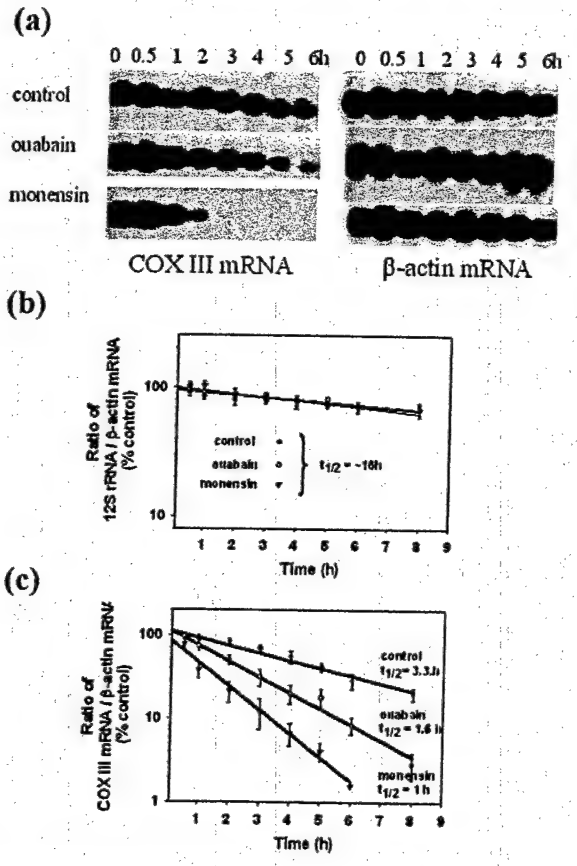

Fig. 5. Estimation of half-lives for β-actin mRNA, 12S rRNA, and COX III mRNA in control, ouabain-, and monensin-treated differentiated PC12S cells. Total cytosolic RNA was isolated from control, ouabain-, and monensin-treated cells at indicated time points after termination of transcription by actinomycin D, and 10 μg aliquots were subjected to Northern blot analysis as described in Section 2. Hybridization was quantified by image analysis of autoradiograms. Semi-log plots of transcript remaining versus time is depicted in the case of β-actin mRNA. In the cases of 12S rRNA and COX III mRNA, the ratios of 12S rRNA to β-actin mRNA and COX III mRNA to β-actin mRNA were calculated. The relative change in the ratio was related to the ratio of zero time samples. Each point is the mean ± SEM of three separate experiments.

BEST AVAILABLE COPY

4. Discussion

The results of the present study demonstrate that chronic treatment with both ouabain and monensin induced a selective decrease in mtDNA-encoded COX III mRNA expression in differentiated PC12S cells. No significant decreases were observed with mtDNA-encoded 12S rRNA and with nDNA-encoded β-actin mRNA in both ouabain- and monensin-treated cells. Moreover, estimation of mtDNA by dot-blot analysis showed no significant reduction in both ouabain- and monensin-treated cells compared to vehicle-treated cells. The observed decrease in COX III mRNA levels in both ouabain- and monensin-treated cells is, therefore, not due to either loss of mitochondria or a general breakdown of RNA. On the other hand, a similar reduction in both ouabain- and monensin-treated cells was observed with mtDNA-encoded COX subunit-I mRNA and -II mRNA (data not shown). Thus, the effect of ouabain and monensin appears to be specific for mtDNA-encoded mRNA and not for rRNA. This may relate to differences in the synthesis and stability between mtDNA-encoded mRNA and rRNA. A similar decrease in COX III mRNA with ouabain and monensin was observed also in undifferentiated and differentiated PC12 cells (T. Tom, personal communication), in a human neuroblastoma cell line SHSY5Y and in monensin-treated rat primary cerebellar granule neurons. Thus, it is unlikely that the choice of the cell culture could account for the ouabain- and monensin-induced response.

Addition of ouabain to differentiated PC12S cells led to a rapid and prolonged rise in the ATP/ADP ratio. In neural tissues, a major portion of the energy derived from metabolism is used to restore ionic gradients to resting levels and the Na/K-ATPase is one of the major consumers of ATP (Mata et al., 1980; Sokoloff, 1981; Erecinska and Silver, 1989). Consistent with these observations, our results show that an inhibition of Na/K-ATPase by ouabain decreases ATP consumption and increases the ATP/ADP ratio in differentiated PC12S cells.

We originally hypothesized that ouabain would reduce mitochondrial gene expression as a direct consequence of an elevated ATP/ADP ratio. In organello transcription experiments using isolated mitochondria show that mitochondrial RNA synthesis can be regulated in response to changes in intramitochondrial ATP levels (Gaines et al., 1987; Enriquez et al., 1996b). High levels of intramitochondrial ATP suppress mtDNA transcription possibly by inhibiting mitochondrial RNA polymerase, presenting a mechanism by which energy demand could regulate mtDNA transcription (Enriquez et al., 1996b). Although the results demonstrating a reduction in COX III mRNA levels associated with increased ATP/ADP levels in ouabain-treated cells is consistent with these mechanisms of gene regulation, the observation that the estimated $t_{1/2}$ of COX III mRNA was decreased from 3.1 h in control cells to 1.6 h in ouabain-treated cells suggested that RNA degradation rather than synthesis was the primary site of control by ouabain. This result suggests that both transcriptional and posttranscriptional mechanisms are likely to be involved in the maintenance of a steady level of mtDNA-encoded COX III mRNA.

The unexpected result of this study was the observed decrease in COX III mRNA in monensin-treated cells. Monensin is a Na^+-selective ionophore that causes Na^+ influx with a corresponding efflux of H^+ or K^+ in numerous cell types including PC12 cells (Pressman and Fahim, 1982; Shier and DuBourdieu, 1992). Under our experimental conditions, we observed a 500% increase in ^{22}Na after exposure of PC12S cell cultures for 3 h to 100 nM monensin (not shown). Ionic or pharmacological interventions that increase $[Na^+]_i$ levels cause significant induction of Na/K-ATPase activity and functional Na/K-pump sites (Wolitzky and Fambrough, 1986; Lingrel and Kuntzweiler, 1994). Addition of monensin to neuronal cells enhances cellular energy metabolism and increases ATP utilization by Na/K-ATPase, presumably to restore ionic gradients to resting levels (Mata et al., 1980). Accordingly, we found that the addition of monensin to differentiated PC12S cells decreased the ATP/ADP ratio, likely due to increased ATP consumption. We anticipated that with elevated ATP consumption, there would be an up-regulation of COX III mRNA. Though there was an increase in COX III mRNA levels in the first hour after addition of monensin, the levels of COX III mRNA subsequently showed a significant decrease. We interpret these findings to suggest that the initial increase represents a mechanism of increased expression due to increased energy demand. The decrease in COX III

mRNA following chronic exposure to monensin suggests the presence of an alternate mechanism for the regulation of mitochondrial gene expression that is independent of the energetic status of the cell and that overrides the normal regulation by energy demand. This decrease in mitochondrial gene expression under conditions of increasing energy demand is not unique to this system. For example, levels of mtDNA-encoded cytochrome oxidase subunit I (COX I) mRNA decreases within hours in CA1 neurons of gerbils after transient forebrain ischemia (Abe et al., 1993). This early decrease in COX I mRNA occurs in the absence of a decrease in mtDNA, suggesting impaired mitochondrial gene expression occurring at the level of transcription and/or turnover of mitochondrial mRNA (Abe et al., 1993). In this model system, the decrease in COX I mRNA occurs when the energy demand is high on these cells not only to restore ionic gradients to resting levels but also to maintain neuronal activity (Arai et al., 1986; Abe et al., 1993). A disproportionate decrease in mtDNA-encoded COX subunit mRNA in the absence of changes in mtDNA-encoded 12S rRNA is also observed in the brains of Alzheimer's disease (AD) patients (Chandrasekaran et al., 1994,1998; Hatanpääet al., 1996).

One explanation for the observed decrease in COX III mRNA but not of 12S rRNA is the relatively short half-life of COX III mRNA. Decay of COX III mRNA, 12S rRNA, and β-actin mRNA in the presence and absence of ouabain or monensin were calculated after inhibition of de novo mitochondrial and nuclear transcription by the addition of actinomycin D to the cell culture medium. The estimated $t_{1/2}$s of COX III mRNA in control cells were 3.1 h whereas the estimated $t_{1/2}$s of 12S rRNA and of β-actin mRNA were greater than 30 h. Thus, the half-lives of mtDNA-encoded mRNAs are short. These estimated half-lives are similar to the results reported in other cell culture systems (Gelfand and Attardi, 1981; Chrzanowska-Lightowlers et al., 1994). In ouabain- and monensin-treated cells, the estimated $t_{1/2}$ decreased to 1.6 and 1 h, respectively. Thus, there is a threefold decrease in the stability of COX III mRNA in drug-treated cells. This posttranscriptional mechanism operating in both ouabain- and monensin-treated cells is likely to be responsible for the accelerated degradation of mtDNA-encoded mRNA. The precise mechanism that mediates a decrease in the stability of COX III mRNA remains unknown. RNA binding proteins that function to protect mRNA from degradation are well documented (Jackson, 1993). The presence of an abundant mitochondrial RNA-binding protein has been known (Dekkeret al., 1991). Both ouabain and monensin induce an increase in intracellular sodium ion concentration $[Na^+]_i$ in a number of cell cultures including PC12 cells (Pressman and Fahim, 1982; Boonstra et al., 1983; Shier and DuBourdieu, 1992; Blaustein and Lederer, 1999). Increased $[Na^+]_i$ causes subsequent changes in intracellular Ca^{2+}, osmolarity, pH, or a combination of the above. The mechanism by which the increased $[Na^+]_i$ and associated cellular changes influence the stability of mtDNA-encoded mRNA remains to be determined.

In summary, we suggest that there are likely to be at least two mechanisms involved in the regulation of mitochondrial gene expression. A physiological mechanism of transcriptional regulation level that allows mtDNA to synthesize the optimal level of mRNA in response to energetic demands (Enriquez et al., 1996b). The results presented here may represent a second mechanism of regulation that operates at the level of stability of mRNA that is independent of the energetic status of the cell and that may operate under pathologic conditions. This mechanism is likely to be pathological because this overrides the normal regulation by energy requirement, causes accelerated degradation of transcripts, and is counterproductive to the actual energy demand of the cell. The results provide a potential approach to determine the molecular components of this mechanism. It is also of interest to determine whether this mechanism contributes to neuronal death in acute and chronic neurodegenerative diseases. To the best of our knowledge, the present study is the first to demonstrate that mitochondrial gene expression is also regulated at the level of mRNA stability under conditions of chronic exposure to elevated intracellular sodium.

Acknowledgements

This work was supported by the grants from the US Army DAMD17-99-1-9483 to G.F., from NIH AG16966A to K.C., and from AHA 0051001U to K.C.

BEST AVAILABLE COPY

References

Abe, K., Kawagoe, J., Kogure, K., 1993. Early disturbance of a mitochondrial DNA expression in gerbil hippocampus after transient forebrain ischemia. Neurosci. Lett. 153 (2), 173–176.

Arai, H., Passonneau, J.V., Lust, W.D., 1986. Energy metabolism in delayed neuronal death of CA1 neurons of the hippocampus following transient ischemia in the gerbil. Metab. Brain Dis. 1 (4), 263–278.

Attardi, G., Schatz, G., 1988. Biogenesis of mitochondria. Annu. Rev. Cell Biol. 4, 289–333.

Blaustein, M.P., Lederer, W.J., 1999. Sodium/calcium exchange: its physiological implications. Physiol. Rev. 79 (3), 763–854.

Boonstra, J., Moolenaar, W.H., Harrison, P.H., Moed, P., van der Saag, P.T., de Laat, S.W., 1983. Ionic responses and growth stimulation induced by nerve growth factor and epidermal growth factor in rat pheochromocytoma (PC12) cells. J. Cell Biol. 97 (1), 92–98.

Chandrasekaran, K., Giordano, T., Brady, D.R., Stoll, J., Martin, L.J., Rapoport, S.I., 1994. Impairment in mitochondrial cytochrome oxidase gene expression in Alzheimer disease. Brain Res. Mol. Brain Res. 24 (1–4), 336–340.

Chandrasekaran, K., Hatanpää, K., Brady, D.R., Stoll, J., Rapoport, S.I., 1998. Downregulation of oxidative phosphorylation in Alzheimer disease: loss of cytochrome oxidase subunit mRNA in the hippocampus and entorhinal cortex. Brain Res. 796 (1–2), 13–19.

Chrzanowska-Lightowlers, Z.M., Preiss, T., Lightowlers, R.N., 1994. Inhibition of mitochondrial protein synthesis promotes increased stability of nuclear-encoded respiratory gene transcripts. J. Biol. Chem. 269 (44), 27322–27328.

Dekker, P.J., Papadopoulou, B., Grivell, L.A., 1991. Properties of an abundant RNA-binding protein in yeast mitochondria. Biochimie 73 (12), 1487–1492.

Enriquez, J.A., Perez-Martos, A., Lopez-Perez, M.J., Montoya, J., 1996a. In organello RNA synthesis system from mammalian liver and brain. Methods Enzymol. 264, 50–57.

Enriquez, J.A., Fernandez-Silva, P., Perez-Martos, A., Lopez-Perez, M.J., Montoya, J., 1996b. The synthesis of mRNA in isolated mitochondria can be maintained for several hours and is inhibited by high levels of ATP. Eur. J. Biochem. 237 (3), 601–610.

Erecinska, M., Silver, I.A., 1989. ATP and brain function. J. Cereb. Blood Flow Metab. 9 (1), 2–19.

Fukuyama, R., Chandrasekaran, K., Rapoport, S.I., 1993. Nerve growth factor-induced neuronal differentiation is accompanied by differential induction and localization of the amyloid precursor protein (APP) in PC12 cells and variant PC12S cells. Brain Res. Mol. Brain Res. 17 (1–2), 17–22.

Gaines, G., Attardi, G., 1984. Highly efficient RNA-synthesizing system that uses isolated human mitochondria: new initiation events and in vivo-like processing patterns. Mol. Cell Biol. 4 (8), 1605–1617.

Gaines, G., Rossi, C., Attardi, G., 1987. Markedly different ATP requirements for rRNA synthesis and mtDNA light strand transcription versus mRNA synthesis in isolated human mitochondria. J. Biol. Chem. 262 (4), 1907–1915.

Gelfand, R., Attardi, G., 1981. Synthesis and turnover of mitochondrial ribonucleic acid in HeLa cells: the mature ribosomal and messenger ribonucleic acid species are metabolically unstable. Mol. Cell Biol. 1 (6), 497–511.

Hatanpää, K., Brady, D.R., Stoll, J., Rapoport, S.I., Chandrasekaran, K., 1996. Neuronal activity and early neurofibrillary tangles in Alzheimer's disease. Ann. Neurol. 40 (3), 411–420.

Jackson, R.J., 1993. Cytoplasmic regulation of mRNA function: the importance of the 3′ untranslated region. Cell 74 (1), 9–14.

Kagawa, Y., Ohta, S., 1990. Regulation of mitochondrial ATP synthesis in mammalian cells by transcriptional control. Int. J. Biochem. 22 (3), 219–229.

Lingrel, J.B., Kuntzweiler, T., 1994. Na + ,K(+)-ATPase. J. Biol. Chem. 269 (31), 19659–19662.

Liu, L.I., Rapoport, S.I., Chandrasekaran, K., 1999. Regulation of mitochondrial gene expression in differentiated PC12 cells. Ann. N. Y. Acad. Sci. 893, 341–344.

Mata, M., Fink, D.J., Gainer, H., Smith, C.B., Davidsen, L., Savaki, H., Schwartz, W.J., Sokoloff, L., 1980. Activity-dependent energy metabolism in rat posterior pituitary primarily reflects sodium pump activity. J. Neurochem. 34 (1), 213–215.

Pressman, B.C., Fahim, M., 1982. Pharmacology and toxicology of the monovalent carboxylic ionophores. Annu. Rev. Pharmacol. Toxicol. 22, 465–490.

Shier, W.T., DuBourdieu, D.J., 1992. Sodium- and calcium-dependent steps in the mechanism of neonatal rat cardiac myocyte killing by ionophores. I. The sodium-carrying ionophore, monensin. Toxicol. Appl. Pharmacol. 116 (1), 38–46.

Shryock, J.C., Rubio, R., Berne, R.M., 1986. Extraction of adenine nucleotides from cultured endothelial cells. Anal. Biochem. 159 (1), 73–81.

Sokoloff, L., 1981. Localization of functional activity in the central nervous system by measurement of glucose utilization with radioactive deoxyglucose. J. Cereb. Blood Flow Metab. 1 (1), 7–36.

Wolitzky, B.A., Fambrough, D.M., 1986. Regulation of the (Na++ K +)-ATPase in cultured chick skeletal muscle. Modulation of expression by the demand for ion transport. J. Biol. Chem. 261 (21), 9990–9999.

Wong-Riley, M.T., 1989. Cytochrome oxidase: an endogenous metabolic marker for neuronal activity. Trends Neurosci. 12 (3), 94–101.

Wong-Riley, M.T., Mullen, M.A., Huang, Z., Guyer, C., 1997. Brain cytochrome oxidase subunit complementary DNAs: isolation, subcloning, sequencing, light and electron microscopic in situ hybridization of transcripts, and regulation by neuronal activity. Neuroscience 76 (4), 1035–1055.

Zhang, C., Wong-Riley, M.T., 2000a. Depolarizing stimulation upregulates GA-binding protein in neurons: a transcription factor involved in the bigenomic expression of cytochrome oxidase subunits. Eur. J. Neurosci. 12 (3), 1013–1023.

Zhang, C., Wong-Riley, M.T., 2000b. Synthesis and degradation of cytochrome oxidase subunit mRNAs in neurons: differential bigenomic regulation by neuronal activity. J. Neurosci. Res. 60 (3), 338–344.

JNC 0 1 1 5 3 B
Journal Name. Manuscript No.
Dispatch: 29.8.02 Journal: JNC
Author Received: No. of pages: 9

Journal of Neurochemistry, 2002, **83**, 1–9

Regulation of hydrogen peroxide production by brain mitochondria by calcium and Bax

Anatoly A. Starkov, Brian M. Polster and Gary Fiskum

Department of Anesthesiology, University of Maryland School of Medicine, Baltimore, Maryland, USA

Abstract

Abnormal accumulation of Ca^{2+} and exposure to pro-apoptotic proteins, such as Bax, is believed to stimulate mitochondrial generation of reactive oxygen species (ROS) and contribute to neural cell death during acute ischemic and traumatic brain injury, and in neurodegenerative diseases, e.g. Parkinson's disease. However, the mechanism by which Ca^{2+} or apoptotic proteins stimulate mitochondrial ROS production is unclear. We used a sensitive fluorescent probe to compare the effects of Ca^{2+} on H_2O_2 emission by isolated rat brain mitochondria in the presence of physiological concentrations of ATP and Mg^{2+} and different respiratory substrates. In the absence of respiratory chain inhibitors, Ca^{2+} suppressed H_2O_2 generation and reduced the membrane potential of mitochondria oxidizing succinate, or glutamate plus malate. In the presence of the respiratory chain Complex I inhibitor rotenone, accumulation of Ca^{2+} stimulated H_2O_2 production by mitochondria oxidizing succinate, and this stimulation was associated with release of mitochondrial cytochrome *c*. In the presence of glutamate plus malate, or succinate, cytochrome *c* release and H_2O_2 formation were stimulated by human recombinant full-length Bax in the presence of a BH3 cell death domain peptide. These results indicate that in the presence of ATP and Mg^{2+}, Ca^{2+} accumulation either inhibits or stimulates mitochondrial H_2O_2 production, depending on the respiratory substrate and the effect of Ca^{2+} on the mitochondrial membrane potential. Bax plus a BH3 domain peptide stimulate H_2O_2 production by brain mitochondria due to release of cytochrome *c* and this stimulation is insensitive to changes in membrane potential.

Keywords: apoptosis, BH3 domain, cytochrome *c*, membrane potential, respiration, superoxide.

J. Neurochem. (2002) **83**, 00–00.

Mitochondrial production of reactive oxygen species (ROS) is thought to contribute significantly to neuronal cell death caused by excitotoxicity and various acute and chronic neurological disorders, e.g. cerebral ischemia/reperfusion and Parkinson's disease (Benzi *et al.* 1982; Sciamanna *et al.* 1992; Dykens 1994; Fiskum *et al.* 1999; Murphy *et al.* 1999; Fiskum 2000; Nicholls and Budd 2000). Among other factors, mitochondrial accumulation of Ca^{2+} that occurs in response to these conditions has been reported to promote the generation of ROS (Dykens 1994; Kowaltowski *et al.* 1995; Kowaltowski *et al.* 1996; Kowaltowski *et al.* 1998a; Kowaltowski *et al.* 1998b; Fiskum 2000; Nicholls and Budd 2000). However, massive mitochondrial Ca^{2+} accumulation also inhibits the electron transport chain, potentially reducing the flow of electrons necessary for reduction of O_2 to superoxide anion and its metabolites, including H_2O_2 (Villalobo and Lehninger 1980). Mitochondrial Ca^{2+} sequestration also reduces the mitochondrial membrane potential ($\Delta\Psi$), which is thermodynamically linked to the redox potential of sites in the electron transport chain responsible for production of ROS. Although several reports have demonstrated that Ca^{2+} loading enhances ROS generation in brain (Dykens 1994) and liver (Kowaltowski *et al.* 1995; Kowaltowski *et al.* 1996; Kowaltowski *et al.* 1998a; Kowaltowski *et al.* 1998b) mitochondria, the mechanism responsible for this stimulation remains elusive.

Mitochondrial functions may also be perturbed during acute neural cell injury by redistribution of pro-apoptotic proteins, such as Bax and Bid, to mitochondrial membranes where permeability changes occur that result in release to the cytosol of other pro-apoptotic proteins, e.g. cytochrome *c* (Fiskum 2000). Release of cytochrome *c* has been associated with increased cellular oxidative stress (Cai and Jones 1998),

Received June 13, 2002; revised manuscript received July 25, 2002; accepted July 25, 2002.

Address correspondence and reprint requests to Dr Gary Fiskum, Department of Anesthesiology, University of Maryland School of Medicine, 685 W. Baltimore Street, MSTF-534, Baltimore, MD 21201, USA. E-mail: gfisk001@umaryland.edu

Abbreviations used: BSA, bovine serum albumin; FCCP, *p*-trifluoromethoxycarbonylcyanide phenylhydrazone, ROS, reactive oxygen species.

© 2002 International Society for Neurochemistry, *Journal of Neurochemistry*, **83**, 1–9

BEST AVAILABLE COPY

although a direct cause and effect relationship between release and stimulated mitochondrial ROS generation has not been demonstrated.

One purpose of this study was to clarify the effect of Ca^{2+} uptake on ROS production by isolated brain mitochondria. Experiments were designed to test the hypothesis that Ca^{2+} can either stimulate or inhibit mitochondrial ROS generation, depending on the source of electrons donated to the respiratory chain, and the effects of Ca^{2+} accumulation on the retention of mitochondrial cytochrome *c*. Another aim of the study was to test the hypothesis that mitochondrial ROS production is stimulated by cytochrome *c* release elicited by exposure to Bax and a peptide containing a BH3 cell death domain.

Materials and methods

Reagents

Oligomycin, antimycin A3 and rotenone (Sigma, St Louis, MO, USA) were dissolved in ethanol, and Amplex Red (10-acetyl-3,7-dihydroxyphenoxazine; Molecular Probes, Eugene OR, USA) was dissolved in dimethylsulfoxide. All other reagents were purchased from Sigma. All reagents and ethanol were tested and exhibited no interference with the H_2O_2 assay at the concentrations used in our experiments. The sources of full-length human recombinant Bax protein and of the synthetic Bax BH3 domain peptide have been described previously (Fiskum and Polster 2001; Polster *et al.* 2001).

Isolation of brain mitochondria

All animal experiments were conducted in accordance with guidelines established by the Institutional Animal Care and Use Committee of the University of Maryland, Baltimore.

Non-synaptosomal rat forebrain mitochondria were isolated by the Percoll gradient separation method as described in (Sims 1990). The quality of the mitochondrial preparation was estimated by measuring the acceptor control ratio defined as ADP-stimulated (State 3) respiration divided by resting (State 4) respiration. For these experiments, the incubation medium consisted of 125 mM KCl, 20 mM HEPES (pH 7.0), 2 mM KH_2PO_4, 1 mM $MgCl_2$, 5 mM glutamate, 5 mM malate, plus 0.8 mM ADP. Oxygen consumption was recorded at 37°C with a Clark-type oxygen electrode. State 3 respiration was initiated by the addition of 0.5 mg per ml rat brain mitochondria to the incubation medium. State 3 respiration was terminated and State 4 initiated by the addition of 1 μM carboxyatractylate, an inhibitor of the ADP/ATP transporter. Only mitochondrial preparations that exhibited an acceptor control ratio greater than 8 were used in this study.

Measurement of H_2O_2

Incubation medium contained 125 mM KCl, 20 mM HEPES (pH 7.0), 2 mM KH_2PO_4, 4 mM ATP, 5 mM $MgCl_2$, 1 μM Amplex Red, 5 U/mL HRP and 40 U/mL Cu,Zn SOD, and was maintained at 37°C, unless stated otherwise. A change in the concentration of H_2O_2 in the medium was detected by fluorescence of the oxidized Amplex Red product using excitation and emission wavelengths of 550 and 585 nm, respectively (Zhou *et al.* 1997). The response of Amplex Red to H_2O_2 was calibrated either by sequential additions of known amounts of H_2O_2 or by continuous infusion of H_2O_2 at 100–1000 pmol/min. The concentration of commercial 30% H_2O_2 solution was calculated from light absorbance at 240 nM employing $E240_{1\,M} = 43.6$; the stock solution was diluted to 100 μM with water and used for calibration immediately.

Cytochrome *c* release from mitochondria

Aliquots of mitochondrial suspensions were taken either during or at the end of experiments in which H_2O_2 generation was monitored. Mitochondria were separated from the suspending medium by centrifugation at 14 000*g* for 5 min. The supernatant was carefully removed and both the supernatant and mitochondrial pellet fractions were immediately frozen and stored at −20°C. Cytochrome *c* concentration was measured in both fractions using an ELISA kit (R & D Systems, Minneapolis, MN, USA). Before measurement, the supernatant and pellet samples were diluted 1 : 40 and 1 : 60, respectively. The release of cytochrome *c* from mitochondria was expressed as the content of cytochrome *c* in the supernatant as a percentage of the total content of cytochrome *c* present in the supernatant plus pellet.

Measurements of $\Delta\Psi$ and extramitochondrial $[Ca^{2+}]$

Qualitative changes in $\Delta\Psi$ were followed using the fluorescence of safranine O (5 μM) with excitation and emission wavelengths of 495 nm and 586 nm, respectively (Votyakova and Reynolds 2001). A semiquantitative measurement of $\Delta\Psi$ was estimated from TPP^+ ion distribution between the medium and mitochondria using a custom-made TPP^+-selective electrode (Kamo *et al.* 1979). For these experiments, incubation medium was supplemented with 1.6 μM TPP^+Cl^-. Both the TPP^+-sensitive and reference electrodes were inserted directly into the fluorimeter cuvette, and data were collected using an amplifier and a two-channel data acquisition system, with one channel acquiring the amplified TPP^+-electrode signal while another was dedicated to the Amplex Red fluorescence signal. The electrode response was calibrated by sequential addition of TPP^+Cl^- in the concentration range 0.2–1.6 μM, and the mitochondrial $\Delta\Psi$ was calculated as described by Rolfe *et al.* (1994). Alternatively, $\Delta\Psi$ values were calculated by the procedure reported by Rottenberg (1984), assuming that the matrix volume for brain mitochondria is 1.2 μL per mg protein. Both procedures yielded similar results.

Changes in the extramitochondrial medium free Ca^{2+} were followed using the fluorescence of Calcium Green 5N, with excitation and emission wavelengths of 506 nm and 532 nm, respectively.

Results

To measure relatively low rates of H_2O_2 production by brain mitochondria, we used a fluorescent dye/horseradish peroxidase detecting system employing the new peroxidase substrate Amplex Red, based on its high sensitivity and very low background fluorescence in the absence of a biological peroxide-generating system (Fig. 1a, curve 1). We also utilized an incubation medium that contained physiologically relevant concentrations of K^+, P_i, ATP and Mg^{2+}, as

BEST AVAILABLE COPY

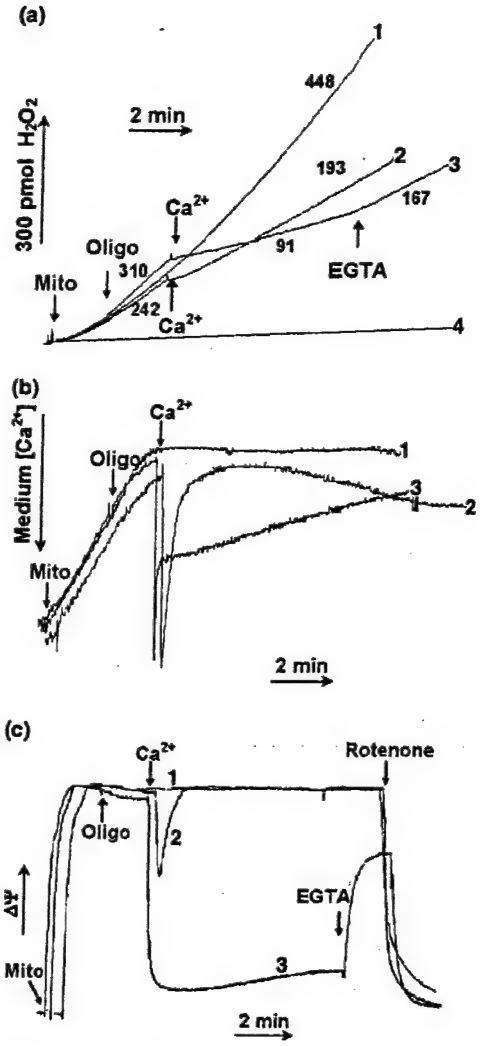

Fig. 1 Effects of Ca^{2+} uptake on ΔΨ and H_2O_2 production by brain mitochondria oxidizing glutamate and malate. Incubation medium maintained at 37°C was supplemented with 5 mM glutamate, 5 mM malate and either 1 μM Amplex Red (a), 100 nM Calcium Green 5N (b) or 5 μM safranin O (c) for measurements of H_2O_2, medium Ca^{2+} concentration or ΔΨ, respectively. Mitochondria (Mito) were added at 0.25 mg per mL ~~mitochondria~~; Ca^{2+} at 0.2 mM; EGTA at 0.5 mM, oligomycin (Oligo) at 0.5 μg/mL, and rotenone at 0.5 μM. In tracings 1, no additions were made following the addition of mitochondria. In tracings 2, Ca^{2+} was added following the addition of mitochondria. In tracings 3, oligomycin was added before the addition of Ca^{2+}. The italicized numbers in (a) represent rates of H_2O_2 production in pmoles per minute per milligram mitochondrial protein.

these components exert dramatic effects on the response of respiring mitochondria to high levels of Ca^{2+} (Murphy *et al.* 1999). Under these conditions, brain mitochondria are resistant to catastrophic bioenergetic and morphological alterations caused by the Ca^{2+}-induced inner membrane permeability transition compared with, for example, liver mitochondria, but are still susceptible to Ca^{2+}-induced alterations in membrane potential and cytochrome *c* release across the outer membrane (Andreyev and Fiskum 1999).

Figure 1a curve 1 illustrates that isolated rat brain mitochondria respiring on the NAD-linked substrates glutamate and malate produce significant amounts of H_2O_2 in the absence of added Ca^{2+} or electron transport chain inhibitors. Under these conditions the medium contaminating free Ca^{2+} (approximately 5 μM or 20 nmol per mg protein), as measured by the fluorescent indicator Calcium Green 5 N, was accumulated by the added mitochondria and a steady-state medium [Ca^{2+}] was maintained for at least 10–15 min (Fig. 1b, curve 1). Parallel safranine O fluorescent measurements of ΔΨ indicated that ΔΨ stabilized within 2 min of the mitochondrial addition and remained constant for at least 15 min thereafter, but rapidly dissipated upon addition of the respiratory Complex I inhibitor rotenone. When brain mitochondria were exposed to a single addition of Ca^{2+} (800 nmol per mg protein), H_2O_2 production was reduced by approximately 60% (193 vs. 448 pmol per mg protein) (Fig. 1a, curve 2). This amount of added Ca^{2+} was accumulated entirely by the rat brain mitochondria, followed by a slow and partial release back into the medium 5–10 min later (Fig. 1b, curve 2). The addition of Ca^{2+} resulted in a transient reduction in ΔΨ, as expected because mitochondrial Ca^{2+} uptake occurs via an electrophoretic uniporter that draws upon the ΔΨ for active Ca^{2+} sequestration. The reduction in ΔΨ stimulates respiration-dependent H^+ efflux that, in turn, drives $H_2PO_4^-$ influx via the electroneutral $H_2PO_4^-/OH^-$ antiporter. Thus, electophoretic uptake of Ca^{2+} followed by electroneutral uptake of P_i results in a transient collapse of ΔΨ without an increase in pH. Approximately 1 min after the addition of Ca^{2+}, when most of it had been accumulated, ΔΨ recovered back to its initial level and remained stable for at least 10 min.

Mitochondrial Ca^{2+} uptake can be driven by electrogenic H^+ efflux mediated by the mitochondrial F_oF_1 ATPase in addition to H^+ extrusion mediated by the electron transport chain. Experiments were therefore performed in the presence of oligomycin, a specific inhibitor of the mitochondrial ATPase, to determine the influence of ATPase activity on mitochondrial Ca^{2+} uptake, ΔΨ and H_2O_2 production. In the presence of oligomycin, the rate of H_2O_2 production before Ca^{2+} addition was slightly higher than in its absence (310 vs. 242 pmol per mg protein). However, following the addition of Ca^{2+}, the rate of H_2O_2 production was approximately 50% of that in its absence (91 vs. 193 pmol per mg protein), and only 20% of that observed in the absence of added Ca^{2+} (91 vs. 448 pmol per mg protein) (Fig. 1a, curve 3). In the presence of oligomycin, mitochondrial Ca^{2+} uptake was initially as, or more, rapid than in its absence but converted to a relatively very slow, sustained rate of net uptake within a minute after the addition of Ca^{2+} (Fig. 1b, curve 3). The presence of oligomycin also resulted in a greater decline in ΔΨ upon addition of Ca^{2+} and a sustained reduction in ΔΨ

for at least 8 min (Fig. 1c, curve 3). The Ca^{2+}-dependent reduction in $\Delta\Psi$ was partially reversed by the subsequent addition of the Ca^{2+} chelator EGTA (Fig. 1c, curve 3), as was the Ca^{2+}-dependent reduction in H_2O_2 production (Fig. 1a, curve 3). Thus, ATPase-mediated electrogenic H^+ efflux contributes to the maintenance of $\Delta\Psi$ during and following mitochondrial uptake of large Ca^{2+} loads, but is incapable of completely sustaining $\Delta\Psi$ in the absence of respiration.

Mitochondrial ROS production was much faster with Complex II-linked substrate succinate compared with Complex I-dependent substrates. Within 2 min following the addition of rat brain mitochondria to the incubation medium containing 5 mM succinate, there was a dramatic increase in H_2O_2 production (Fig. 2a), at a rate that was seven to eight

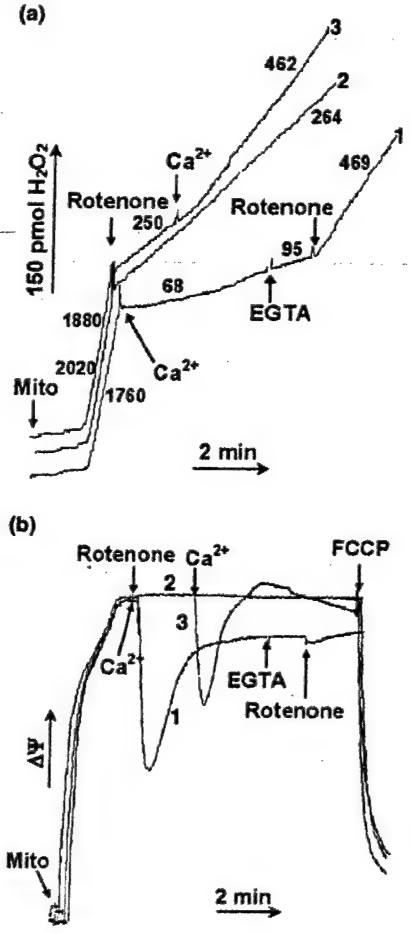

Fig. 2 Effects of Ca^{2+} uptake on $\Delta\Psi$ and H_2O_2 production by brain mitochondria oxidizing succinate. Incubation medium maintained at 37°C was supplemented with 5 mM succinate and either 1 μM Amplex Red (a) or 5 μM Safranin O (b) for measurements of H_2O_2 or $\Delta\Psi$, respectively. Mitochondria (Mito) were added at 0.125 mg per mL ~~mitochondria~~; Ca^{2+} at 0.2 mM; EGTA at 0.5 mM, rotenone at 0.5 μM, carboxyatractyloside (cAtr) at 1 μM and FCCP at 50 nM. The italicized numbers in panel (a) represent rates of H_2O_2 production in pmoles per minute per milligram mitochondrial protein.

times faster than that observed in the presence of glutamate plus malate (1700–2000 vs. 250 pmol per mg mitochondrial protein). The delayed activation of succinate-supported H_2O_2 production corresponded to the time at which the $\Delta\Psi$ reached its maximum level following addition of mitochondria to the medium (Fig. 2b) (Korshunov *et al.* 1997). Subsequent addition of 0.2 mM Ca^{2+} resulted in an immediate and almost complete inhibition of H_2O_2 production (68 vs. 1760 pmol per mg protein) (Fig. 2a, curve 1). At this level of Ca^{2+}, $\Delta\Psi$ was transiently reduced then recovered, albeit to a level that was lower than that maintained in the absence of added Ca^{2+} (Fig. 2b, curve 1). Whereas EGTA significantly reversed the effect of Ca^{2+} on ROS production and $\Delta\Psi$ in the presence of Complex I-linked substrates, it was unable to reverse the effects of Ca^{2+} in the presence of the Complex II substrate succinate (Figs 2a and b, curves 1).

The Complex I inhibitor rotenone was capable of stimulating mitochondrial H_2O_2 production in the presence of Ca^{2+} but had a negligible effect on the Ca^{2+}-induced reduction of $\Delta\Psi$ (Figs 2a and b, curves 1), as expected as rotenone inhibits NAD-linked but not succinate-supported respiration. The rate of H_2O_2 production observed following the addition of Ca^{2+} and then rotenone was still far lower than the initial rate observed in the absence of both agents (469 vs. 1760 pmol per mg protein). This finding verifies the contribution of rotenone-sensitive reversed electron flow through Complex I as a major site of ROS production supported by succinate (Hinkle *et al.* 1967; Hansford *et al.* 1997; Korshunov *et al.* 1997; Turrens 1997; Lass *et al.* 1998; Votyakova and Reynolds 2001; Liu *et al.* 2002). However, in the absence of added Ca^{2+}, the addition of rotenone resulted in a rate of H_2O_2 production that was substantially lower than that following the addition of Ca^{2+} (264 vs. 469 pmol per mg protein; Fig. 2a, curve 2). This stimulatory effect of Ca^{2+} on succinate-supported H_2O_2 production in the presence of rotenone was further verified by the addition of Ca^{2+} following rotenone, after which the rate of H_2O_2 production increased from 250 to 462 pmol per mg protein (Fig. 2a, curve 3). In contrast to the sustained reduction in $\Delta\Psi$ observed upon addition of Ca^{2+} in the absence of rotenone, mitochondrial Ca^{2+} uptake in the presence of rotenone resulted in the normal transient drop in $\Delta\Psi$ followed by a complete recovery and a subsequent steady but minor depolarization (Fig. 2b, curve 3). These results further demonstrate that when exposure of mitochondria to high levels of Ca^{2+} results in a reduction in $\Delta\Psi$, ROS production is inhibited. Under conditions in which ROS production is independent of $\Delta\Psi$, e.g. in the presence of rotenone, Ca^{2+} can actually stimulate ROS production.

Experiments were then performed to test the hypothesis that a reduction in $\Delta\Psi$ is a sufficient explanation for the inhibition of H_2O_2 production by Ca^{2+} with either succinate or the NAD-linked substrates glutamate and malate. It is known that succinate-supported H_2O_2 production is inhibited

by mitochondrial depolarization (Hansford *et al.* 1997; Korshunov *et al.* 1997). The dependence of succinate-supported ROS generation on $\Delta\Psi$ is due to the reverse electron transport from Complex II through coenzyme Q to Complex I. The potential energy of $\Delta\Psi$ is necessary to overcome the redox potential difference between Complex I and coenzyme Q that promotes Complex I oxidation and coenzyme Q reduction. Although the quantitative relationship between $\Delta\Psi$ and ROS production during succinate-dependent reversed electron transport is established (Korshunov *et al.* 1997), it has not been determined for ROS generation that occurs during electron transport driven by NAD-linked substrates. This relationship was explored by measuring mitochondrial H_2O_2 production in the presence of glutamate and malate and in the presence of several concentrations of FCCP, a protonophoric uncoupling agent. In order to demonstrate a quantitative relationship, the experimental system utilized the mitochondrial uptake of the lipophilic cation TPP^+ as a measure of $\Delta\Psi$. The system was also simplified by omitting ATP from the medium and adding the Ca^{2+} chelator EGTA to prevent possible interference from contaminating Ca^{2+} in the medium. The results shown in Fig. 3 indicated that H_2O_2 production supported by oxidation of NAD-linked substrates is indeed dependent on $\Delta\Psi$, being very sensitive to fluctuations in $\Delta\Psi$ between approximately 150 and 180 mV. These results however, also demonstrate that approximately 30% of the maximal H_2O_2 production is insensitive to $\Delta\Psi$.

The reduction in $\Delta\Psi$ caused by mitochondrial Ca^{2+} accumulation is a sufficient explanation for the inhibition by Ca^{2+} of H_2O_2 production both with succinate (in the absence of rotenone) or NAD-linked substrates. This effect cannot, however, explain the increase in succinate-supported H_2O_2 generation caused by Ca^{2+} in the presence of the Complex I inhibitor rotenone. We hypothesized that Ca^{2+}-induced cytochrome *c* release might be responsible for this phenomenon because cytochrome *c* release has been associated with increased oxidative stress in apoptotic cells (Cai and Jones 1998), and cytochrome *c* is released by brain mitochondria in response to Ca^{2+} uptake under conditions similar to those used in the current study (Andreyev *et al.* 1998; Andreyev and Fiskum 1999). A comparison between rates of H_2O_2 production and the distribution of cytochrome *c* between the mitochondria and the suspending medium at the end of the H_2O_2 measurements is provided in Figs 4 and 5 for succinate (in the presence of rotenone) and glutamate plus malate, respectively. The accumulation of Ca^{2+} resulted in a net 10% release of cytochrome *c* in the presence of succinate and 5% release in the presence of glutamate plus malate. This was accompanied by an approximately 60% increase in H_2O_2 formation with succinate and a greater than 60% reduction in H_2O_2 with glutamate and malate. Thus Ca^{2+} induces the release of mitochondrial cytochrome *c* in the presence of either malate plus glutamate or succinate but only stimulates H_2O_2 production when succinate is present as the electron donor and rotenone is present to inhibit reversed electron transport that is driven by $\Delta\Psi$.

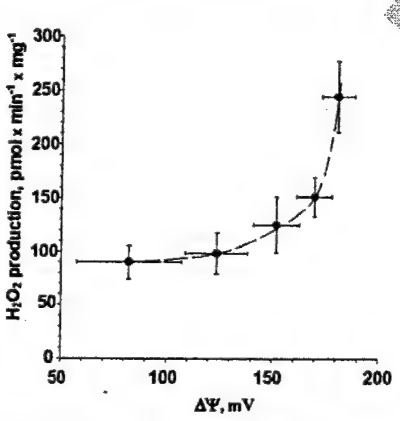

Fig. 3 Relationship between rate of H_2O_2 production and $\Delta\Psi$ for brain mitochondria oxidizing glutamate and malate. Mitochondria were added at a concentration of 0.25 mg/mL to the standard incubation medium except that ATP was omitted, $MgCl_2$ was present at 1 mM, and the medium was supplemented with 0.25 mM EGTA, 1.6 μM TPP^+Cl^-, 5 mM glutamate and 5 mM malate. A TPP^+ electrode was used to measure the medium TPP^+ concentration both in the absence of FCCP and in the presence of 22, 47, 76 and 110 pmol FCCP per mg mitochondrial protein to modulate the $\Delta\Psi$. Values for $\Delta\Psi$ were calculated as described in Materials and Methods.

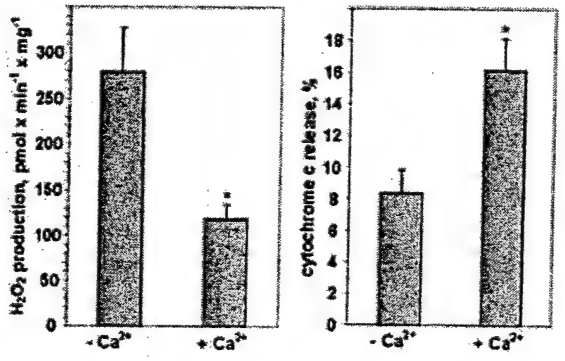

Fig. 4 Ca^{2+}-induced cytochrome *c* release and stimulation of H_2O_2 production by brain mitochondria oxidizing succinate. Mitochondria were added at a concentration of 0.25 mg/mL to the standard incubation medium maintained at 37°C and supplemented with 5 mM succinate. As in Fig. 2, approximately 3 min later, rotenone (0.2 μM) was added, followed 2 min later by either Ca^{2+} (0.2 mM) or vehicle control (H_2O). The rate of H_2O_2 production was determined by the rate of increase in Amplex Red fluorescence. At approximately 8 min following the addition of Ca^{2+}, the suspension was centrifuged and the pellet and supernatant fractions used for ELISA of cytochrome *c* content, as described in Materials and Methods. Values represent the mean ± SE of four independent experiments. $^*p < 0.05$ versus without Ca^{2+}.

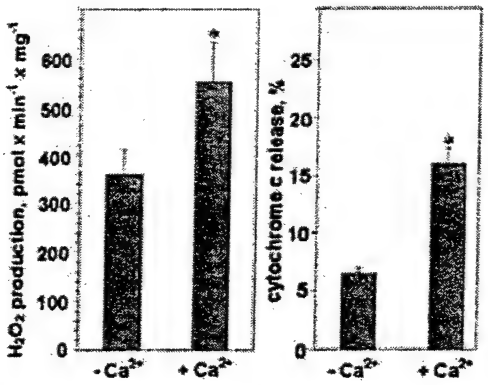

Fig. 5 Ca^{2+}-induced cytochrome *c* release and inhibition of H_2O_2 production by brain mitochondria oxidizing glutamate and malate. Mitochondria were added at a concentration of 0.25 mg/mL to the standard incubation medium maintained at 37°C and supplemented with 5 mM glutamate and 5 mM malate. As in Fig. 1, approximately 4 min later, Ca^{2+} (0.2 mM) or vehicle control (H_2O) were added and the rate of H_2O_2 production was determined by the rate of increase in Amplex Red fluorescence. At approximately 10 min following the addition of Ca^{2+}, the suspension was centrifuged and the pellet and supernatant fractions were used for ELISA of cytochrome *c* content, as described in Materials and Methods. Values represent the mean ± SE of four independent experiments. *$p < 0.05$ versus without Ca^{2+}.

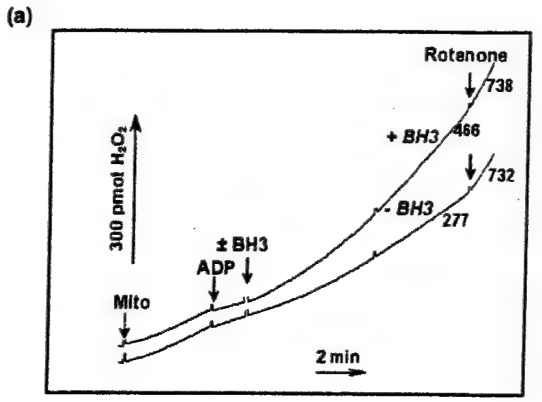

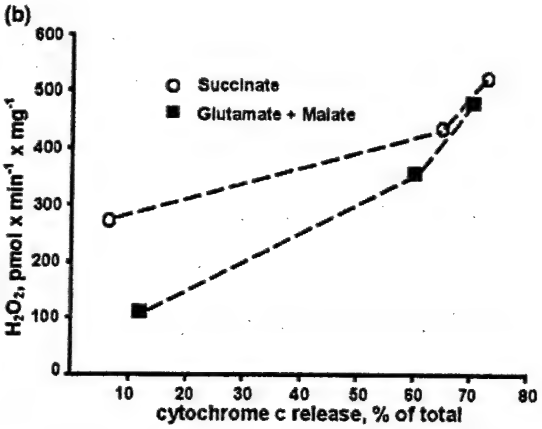

Fig. 6 Stimulation of cytochrome *c* release and H_2O_2 production by brain mitochondria by addition of Bax plus a BH3 domain peptide. Mitochondria were added at a concentration of 0.125 mg/mL to the standard incubation medium maintained at 37°C and supplemented with either 5 mM glutamate and 5 mM malate or 5 mM succinate. (a) Amplex Red measurements of H_2O_2 generation. At approximately 3 min following addition of brain mitochondria to media containing glutamate and malate and 100 nM Bax (see Materials and methods), 0.1 mM ADP was added to initiate State 3 respiration. Approximately 2 min later, 50 μM BH3 peptide or vehicle control (H_2O) was added. Rotenone (0.2 μM) was added 9 min later to elicit maximal H_2O_2 production. (b) Relationship between H_2O_2 production and release of cytochrome *c* caused by exposure of brain mitochondria to Bax plus a BH3 peptide. In experiments such as that shown in (a) aliquots of the mitochondrial suspension were removed before and two or three times after addition of the BH3 peptide or vehicle, centrifuged and used for ELISA of cytochrome *c* release from the mitochondria into the medium. The corresponding rate of H_2O_2 production refers to the rate obtained just before removal of the aliquot for cytochrome *c* measurement. Experiments were performed either in the presence of 5 mM succinate (○) or 5 mM glutamate and 5 mM malate (■).

Additional evidence for the direct role of cytochrome *c* release in stimulating mitochondrial ROS formation came from experiments in which release was mediated by exposure of brain mitochondria to the pro-apoptotic protein Bax together with a synthesized peptide that contains the BH3 death domain amino acid sequence. We previously demonstrated that this peptide triggers Bax-dependent release of cytochrome *c* by specifically increasing the permeability of the mitochondrial outer membrane without affecting inner membrane permeability or other components of the electron transport chain (Fiskum and Polster 2001). Figure 6a provides representative fluorescent measurements of H_2O_2 generation by rat brain mitochondria respiring on glutamate and malate in the presence of 100 nM human recombinant full-length Bax and in the absence or presence of 50 μM BH3 peptide. In the absence of the peptide, H_2O_2 produced in the presence of Bax was identical to that in its absence (not shown). In these experiments, ADP was added to the suspension, inducing State 3 respiration. Under these conditions, the redox state of potential sites of ROS production is relatively oxidized and therefore inhibition of electron transport by release of cytochrome *c* should cause a maximal shift toward a reduced redox state. In the absence of BH3 peptide, H_2O_2 formation increased slowly over approximately 10 min and was stimulated by over 100% upon addition of the Complex I inhibitor rotenone (732 vs. 277 pmol per min per mg protein). The rate of H_2O_2 generation observed 10 min following the addition of the BH3 peptide was 70% greater than the timed control (466 vs. 277 pmol per min per mg protein) and was further stimulated by the addition of rotenone. In the absence of added Bax, BH3 peptide had no effect on ROS production by adult rat brain mitochondria (not shown), consistent with its inability to release cytochrome *c* from these mitochondria in the absence of exogenous Bax (Fiskum and Polster 2001). Thus,

in contrast to the inhibition of H_2O_2 production by added Ca^{2+} when NAD-linked respiratory substrates were present (Fig. 1a), the presence of Bax plus a BH3 peptide substantially stimulates mitochondrial H_2O_2 formation. An approximately 70% stimulation of H_2O_2 formation by Bax plus the BH3 peptide was observed in the presence of succinate plus rotenone (not shown). Thus, cytochrome *c* release *per se* stimulates mitochondrial ROS generation in the presence of either Complex I or Complex II respiratory substrates.

As the rate of H_2O_2 production was non-linear during the course of these experiments and as Bax–BH3-mediated cytochrome *c* release takes several minutes to occur, we took aliquots of the mitochondrial suspension during the course of the H_2O_2 measurements for quantification of cytochrome *c* distribution to determine if a relationship exists between the extent of release and the rate of H_2O_2 formation. These aliquots were taken immediately before the addition of the BH3 peptide or vehicle and 5 and 8 min later. The extent of cytochrome *c* release and the corresponding rates of H_2O_2 generation measured just before sampling using glutamate and malate or succinate (in the presence of rotenone) are presented in Fig. 6b. The H_2O_2 production rate was greater for mitochondria respiring on succinate than on glutamate and malate in the absence of BH3 peptide with background release of 5–12% of the total cytochrome *c*. However, after 5 min exposure to the BH3 peptide, the extent of cytochrome *c* release was similar under these two conditions (60–65%), as were the rates of H_2O_2 formation (360–420 pmol per min per mg protein). An additional 3-min exposure to the BH3 peptide resulted in an additional approximately 10% release of cytochrome *c* and rates of H_2O_2 production that were very similar for the two sets of respiratory substrates (466–520 pmol per min per mg protein). These results indicate that the release of cytochrome *c* by Bax plus a BH3 peptide results in a dose-dependent stimulation of mitochondrial ROS formation under physiologically relevant *in vitro* conditions with either succinate or NAD-linked respiratory substrates.

Discussion

The main conclusion that can be drawn from this study is that when $\Delta\Psi$ is reduced with mitochondria respiring on either NAD-linked substrates or succinate in the absence of rotenone, ROS production is inhibited (Figs 1, 2, 3 and 5). Conversely, the release of cytochrome *c* by either mitochondrial Ca^{2+} accumulation or by exposure to Bax and a BH3 domain peptide can significantly stimulate mitochondrial ROS production apparently independently of $\Delta\Psi$ (Figs 2, 4 and 6). These observations were made *in vitro* in the absence of respiratory inhibitors and in the presence of physiologically relevant levels of ATP, Mg^{2+} and other ions that have a profound influence on mitochondrial energy coupling and on mitochondrial responses to raised levels of Ca^{2+}. We therefore believe that these observations may be highly relevant to the effects of both pathological levels of Ca^{2+} and the apoptotic redistribution of Bax and BH3 domain proteins that occurs in response to many forms of neuronal stress.

The modulation of mitochondrial ROS generation observed in the presence of NAD-linked oxidizable substrates is particularly important as these substrates constitute the primary source of fuel for oxidative cerebral energy metabolism. In the presence of ATP, the uptake of Ca^{2+} inhibited H_2O_2 generation (Figs 1 and 5). This inhibition appears to be due to more than one mechanism, as indicated by differences in Ca^{2+}-induced mitochondrial depolarization and inhibition of ROS production in the absence and presence of oligomycin (Fig. 1). When ATP turnover was blocked by oligomycin, Ca^{2+} caused a substantial collapse in $\Delta\Psi$ and ~60% inhibition of H_2O_2 generation. In the absence of oligomycin, Ca^{2+} accumulation resulted in no sustained reduction in $\Delta\Psi$ but ROS generation was still inhibited by ~80%. As independent experiments performed in the absence of Ca^{2+} and in the presence of different concentrations of the protonophore uncoupler FCCP demonstrated that > 50% of NAD-linked ROS production is sensitive to $\Delta\Psi$ (Fig. 3), we conclude that mitochondrial depolarization is one of the mechanisms by which Ca^{2+} inhibits H_2O_2 formation. Votyakova and Reynolds (2001) reported previously that the presence of an uncoupler does not stimulate NAD-linked mitochondrial ROS production; however, the rates of H_2O_2 generation they observed using the scopoletin method of detection were too low to detect any inhibitory influence of membrane depolarization. The mechanism by which loss of $\Delta\Psi$ reduces mitochondrial H_2O_2 formation probalby involves the oxidation of redox centers, e.g. coenzyme Q or iron-sulfur proteins, which probably mediate the generation of superoxide and therefore H_2O_2.

Ca^{2+}-induced mitochondrial depolarization cannot explain the inhibition of NAD-linked H_2O_2 formation observed in the absence of oligomycin as $\Delta\Psi$ was fully preserved (Fig. 1). One possible explanation for this $\Delta\Psi$-independent inhibition is that Ca^{2+} may impair the flow of electrons within the electron transport chain at a site, most likely within Complex I, that is proximal to the site of ROS generation. Evidence for selective impairment of NAD-linked respiration by Ca^{2+} was originally reported for ascites tumor cell mitochondria (Villalobo and Lehninger 1980), and more recently for neural cell mitochondria (Murphy *et al.* 1996). Although such inhibition could be caused by release of mitochondrial NAD(H) mediated by the Ca^{2+}-activated permeability transition (Maciel *et al.* 2001), it is clear from the maintenance of $\Delta\Psi$ that the permeability transition did not occur under these conditions.

Mitochondrial Ca^{2+} uptake had an even greater inhibitory effect on succinate-driven H_2O_2 production than on

NAD-linked ROS generation (Fig. 2). The explanation for the greater inhibition with succinate is that Ca^{2+}-induced loss of $\Delta\Psi$ deprives mitochondria of the energy required for reverse transport of electrons from Complex II through coenzyme Q to Complex I where sites of succinate-based ROS formation are located (Korshunov *et al.* 1997; Turrens 1997; Lass *et al.* 1998; Liu *et al.* 2002). The most novel observation made with succinate as the respiratory substrate in the presence of rotenone was that Ca^{2+} actually stimulated H_2O_2 production. Under these conditions, Ca^{2+}-induced changes in $\Delta\Psi$ were not expected to affect H_2O_2 production as reverse electron transport is inhibited by the presence of rotenone. Therefore, Ca^{2+}-induced release of cytochrome *c* was pursued as a possible mechanism for its stimulation of H_2O_2 generation.

Quantitative analysis of the extent of cytochrome *c* released by the end of experiments such as those shown in Figs 1 and 2 indicated that a small but significant percentage of cytochrome *c* was released following the addition of Ca^{2+} when either glutamate and malate, or succinate were used as respiratory substrates (Figs 4 and 5). Although cytochrome *c* was released in response to the addition of Ca^{2+} under both conditions, Ca^{2+} only stimulated the production of H_2O_2 in the presence of succinate plus rotenone. The fact that cytochrome *c* release was observed under these conditions suggested, but did not prove, that it was responsible for the stimulation of H_2O_2 generation by Ca^{2+}. Further support for this hypothesis came from experiments performed in the absence of Ca^{2+} but in the presence of Bax and a BH3 death domain peptide.

Ca^{2+}-independent stimulation of H_2O_2 production was dependent on the presence of both the human recombinant full-length Bax and the BH3 peptide as neither component alone had any effect on either ROS generation or cytochrome *c* release (Fig. 6) (Fiskum and Polster 2001; Polster *et al.* 2001). Release of cytochrome *c* was accompanied by increased H_2O_2 production in the presence of glutamate plus malate, or succinate plus rotenone. As the release of cytochrome *c* interrupts the flow of electrons at a site distal to the sites of ROS generation, their redox states shift to a more reduced level. Under these conditions, these redox centers are unaffected by $\Delta\Psi$ because electron transport is severely inhibited by the loss of cytochrome *c*. Therefore, mitochondrial H_2O_2 production is insensitive to $\Delta\Psi$ when cytochrome *c* is released by conditions, e.g. the Bax/BH3 system, in which no other electron transport activities are altered.

Although the most plausible explanation for the stimulation of ROS production by the release of cytochrome *c* relates to the effect of respiratory inhibition on the redox state of superoxide-generating sites proximal to the site of inhibition, other mechanisms may also contribute. One mechanism is the reduction of superoxide scavenging by cytochrome *c* when it is lost from the mitochondrial intermembrane space to the cytosol (Korshunov *et al.* 1999). This mode of action is supported by the findings that a substantial fraction of mitochondrial superoxide formation occurs at the outer side of the inner membrane, where cytochrome *c* is normally present in equilibrium with the unbound protein in the intermembrane space at a concentration of 100–700 μM (Hackenbrock 1966; Hackenbrock 1968). Despite its possible exacerbation of mitochondrial ROS generation, the redistribution of cytochrome *c* into the cytosol has been proposed to help scavenge superoxide or other ROS in that compartment during glutamate excitotoxicity (Atlante *et al.* 2000).

Considerable attention has been focused on the role of raised intracellular Ca^{2+} in mitochondrial dysfunction and ROS production preceding neural cell death (Fiskum 2000). Recent investigations indicate that the interaction of Bax with BH3 death domain only proteins, e.g. Bid, at the mitochondrial level also contributes significantly to cell death in animal models of acute brain injury and neurodegenerative diseases (Plesnila *et al.* 2001; Vila *et al.* 2001). One study demonstrated a relationship between these two forms of stress with Ca^{2+}-induced mitochondrial permeability transition signaling the redistribution of cytosolic Bax to the mitochondrial membrane before cytochrome *c* release during apoptosis (De Giorgi *et al.* 2002). Our observations suggest that the stimulation of mitochondrial ROS generation by Bax-mediated cytochrome *c* release may be particularly important in the pathogenesis of neural cell death. This stimulation can occur in the presence of either Complex I or Complex II respiratory substrates, physiological concentrations of ATP and inorganic ions, and in the absence of respiratory poisons. Development of inhibitors of Bax-mediated cytochrome *c* release is extremely important as they should both block caspase-mediated apoptosis and obstruct the mitochondrial generation of ROS that can promote either apoptotic or necrotic cell death.

Acknowledgements

This work was supported by USAMRMC Neurotoxin Initiative (DAMD 17-99-1-9483), NIH NS34152 and ES11838.

References

Andreyev A. and Fiskum G. (1999) Calcium induced release of mitochondrial cytochrome *c* by different mechanisms selective for brain versus liver. *Cell Death Differ.* **6**, 825–832.

Andreyev A. Y., Fahy B. and Fiskum G. (1998) Cytochrome *c* release from brain mitochondria is independent of the mitochondrial permeability transition. *FEBS Lett.* **439**, 373–376.

Atlante A., Calissano P., Bobba A., Azzariti A., Marra E. and Passarella S. (2000) Cytochrome *c* is released from mitochondria in a reactive oxygen species (ROS)-dependent fashion and can operate as a ROS scavenger and as a respiratory substrate in cerebellar neurons undergoing excitotoxic death. *J. Biol. Chem.* **275**, 37159–37166.

Benzi G., Pastoris O. and Dossena M. (1982) Relationships between gamma-aminobutyrate and succinate cycles during and after cerebral ischemia. *J. Neurosci. Res.* **7**, 193–201.

Cai J. and Jones D. P. (1998) Superoxide in apoptosis. Mitochondrial generation triggered by cytochrome *c* loss. *J. Biol. Chem.* **273**, 11401–11404.

De Giorgi F., Lartigue L., Bauer M. K., Schubert A., Grimm S., Hanson G. T., Remington S. J., Youle R. J. and Ichas F. (2002) The permeability transition pore signals apoptosis by directing Bax translocation and multimerization. *FASEB J.* **16**, 607–609.

Dykens J. A. (1994) Isolated cerebral and cerebellar mitochondria produce free radicals when exposed to elevated Ca^{2+} and Na^{+}: implications for neurodegeneration. *J. Neurochem.* **63**, 584–591.

Fiskum G. (2000) Mitochondrial participation in ischemic and traumatic neural cell death. *J. Neurotrauma* **17**, 843–855.

Fiskum G. and Polster B. (2001) BH3 cell death domain peptide-induced release of cytochrome *C* from mitochondria within cerebellar granule neurons and neural cell lines. *J. Neurochem.* **77**(Suppl. 1), 30.

Fiskum G., Murphy A. N. and Beal M. F. (1999) Mitochondria in neurodegeneration: acute ischemia and chronic neurodegenerative diseases. *J. Cereb. Blood Flow Metab.* **19**, 351–369.

Hackenbrock C. R. (1966) Ultrastructural bases for metabolically linked mechanical activity in mitochondria. I. Reversible ultrastructural changes with change in metabolic steady state in isolated liver mitochondria. *J. Cell Biol.* **30**, 269–297.

Hackenbrock C. R. (1968) Chemical and physical fixation of isolated mitochondria in low-energy and high-energy states. *Proc. Natl Acad. Sci. USA* **61**, 598–605.

Hansford R. G., Hogue B. A. and Mildaziene V. (1997) Dependence of H_2O_2 formation by rat heart mitochondria on substrate availability and donor age. *J. Bioenerg. Biomembr.* **29**, 89–95.

Hinkle P. C., Butow R. A., Racker E. and Chance B. (1967) Partial resolution of the enzymes catalyzing oxidative phosphorylation. XV. Reverse electron transfer in the flavin-cytochrome beta region of the respiratory chain of beef heart submitochondrial particles. *J. Biol. Chem.* **242**, 5169–5173.

Kamo N., Muratsugu M., Hongoh R. and Kobatake Y. (1979) Membrane potential of mitochondria measured with an electrode sensitive to tetraphenyl phosphonium and relationship between proton electrochemical potential and phosphorylation potential in steady state. *J. Membr. Biol.* **49**, 105–121.

Korshunov S. S., Skulachev V. P. and Starkov A. A. (1997) High protonic potential actuates a mechanism of production of reactive oxygen species in mitochondria. *FEBS Lett.* **416**, 15–18.

Korshunov S. S., Krasnikov B. F., Pereverzev M. O. and Skulachev V. P. (1999) The antioxidant functions of cytochrome *c*. *FEBS Lett.* **462**, 192–198.

Kowaltowski A. J., Naia-da-Silva E. S., Castilho R. F. and Vercesi A. E. (1998a) Ca^{2+}-stimulated mitochondrial reactive oxygen species generation and permeability transition are inhibited by dibucaine or Mg^{2+}. *Arch. Biochem. Biophys.* **359**, 77–81.

Kowaltowski A. J., Netto L. E. and Vercesi A. E. (1998b) The thiol-specific antioxidant enzyme prevents mitochondrial permeability transition. Evidence for the participation of reactive oxygen species in this mechanism. *J. Biol. Chem.* **273**, 12766–12769.

Kowaltowski A. J., Castilho R. F. and Vercesi A. E. (1995) Ca(2+)-induced mitochondrial membrane permeabilization: role of coenzyme Q redox state. *Am. J. Physiol.* **269**, C141–C147.

Kowaltowski A. J., Castilho R. F. and Vercesi A. E. (1996) Opening of the mitochondrial permeability transition pore by uncoupling or inorganic phosphate in the presence of Ca^{2+} is dependent on mitochondrial-generated reactive oxygen species. *FEBS Lett.* **378**, 150–152.

Lass A., Sohal B. H., Weindruch R., Forster M. J. and Sohal R. S. (1998) Caloric restriction prevents age-associated accrual of oxidative damage to mouse skeletal muscle mitochondria. *Free Radic. Biol. Med.* **25**, 1089–1097.

Liu Y., Fiskum G. and Schubert D. (2002) Generation of reactive oxygen species by the mitochondrial electron transport chain. *J. Neurochem.* **80**, 780–787.

Maciel E. N., Vercesi A. E. and Castilho R. F. (2001) Oxidative stress in Ca(2+)-induced membrane permeability transition in brain mitochondria. *J. Neurochem.* **79**, 1237–1245.

Murphy A. N., Bredesen D. E., Cortopassi G., Wang E. and Fiskum G. (1996) Bcl-2 potentiates the maximal calcium uptake capacity of neural cell mitochondria. *Proc. Natl Acad. Sci. USA* **93**, 9893–9898.

Murphy A. N., Fiskum G. and Beal M. F. (1999) Mitochondria in neurodegeneration: bioenergetic function in cell life and death. *J. Cereb. Blood Flow Metab.* **19**, 231–245.

Nicholls D. G. and Budd S. L. (2000) Mitochondria and neuronal survival. *Physiol. Rev.* **80**, 315–360.

Plesnila N., Zinkel S., Le D. A., Amin-Hanjani S., Wu Y., Qiu J., Chiarugi A., Thomas S. S., Kohane D. S., Korsmeyer S. J. and Moskowitz M. A. (2001) BID mediates neuronal cell death after oxygen/glucose deprivation and focal cerebral ischemia. *Proc. Natl Acad. Sci. USA* **98**, 15318–15323.

Polster B. M., Kinnally K. W. and Fiskum G. (2001) BH3 death domain peptide induces cell type-selective mitochondrial outer membrane permeability. *J. Biol. Chem.* **276**, 37887–37894.

Rolfe D. F., Hulbert A. J. and Brand M. D. (1994) Characteristics of mitochondrial proton leak and control of oxidative phosphorylation in the major oxygen-consuming tissues of the rat. *Biochim. Biophys. Acta* **1188**, 405–416.

Rottenberg H. (1984) Membrane potential and surface potential in mitochondria: uptake and binding of lipophilic cations. *J. Membr. Biol.* **81**, 127–138.

Sciamanna M. A., Zinkel J., Fabi A. Y. and Lee C. P. (1992) Ischemic injury to rat forebrain mitochondria and cellular calcium homeostasis. *Biochim. Biophys. Acta* **1134**, 223–232.

Sims N. R. (1990) Rapid isolation of metabolically active mitochondria from rat brain and subregions using Percoll density gradient centrifugation. *J. Neurochem.* **55**, 698–707.

Turrens J. F. (1997) Superoxide production by the mitochondrial respiratory chain. *Biosci. Rep.* **17**, 3–8.

Vila M., Jackson-Lewis V., Vukosavic S., Djaldetti R., Liberatore G., Offen D., Korsmeyer S. J. and Przedborski S. (2001) Bax ablation prevents dopaminergic neurodegeneration in the 1-methyl-4-phenyl-1,2,3,6-tetrahydropyridine mouse model of Parkinson's disease. *Proc. Natl Acad. Sci. USA* **98**, 2837–2842.

Villalobo A. and Lehninger A. L. (1980) Inhibition of oxidative phosphorylation in ascites tumor mitochondria and cells by intramitochondrial Ca^{2+}. *J. Biol. Chem.* **255**, 2457–2464.

Votyakova T. V. and Reynolds I. J. (2001) DeltaPsi(m)-dependent and -independent production of reactive oxygen species by rat brain mitochondria. *J. Neurochem.* **79**, 266–277.

Zhou M., Diwu Z., Panchuk-Voloshina N. and Haugland R. P. (1997) A stable nonfluorescent derivative of resorufin for the fluorometric determination of trace hydrogen peroxide: applications in detecting the activity of phagocyte NADPH oxidase and other oxidases. *Anal. Biochem.* **253**, 162–168.

Ovarian Steroid Modulation of Seizure Severity and Neuronal Damage after Kainic Acid Treatment

G. E. Hoffman[1], N. Moore[1], G. Fiskum[2] and A. Z.Murphy[1]

Departments of Anatomy and Neurobiology[1], and Anesthesiology[2]

University of Maryland, School of Medicine, Baltimore, MD 21201

Send all Proofs and Correspondence to:

Dr. Gloria E. Hoffman

Department of Anatomy and Neurobiology

University of Maryland

School of Medicine

Baltimore MD 21201

Phone: 410 706-2438

FAX: 410-706-2512

email: gehoffma@umaryland.edu

Status epilepticus, left unchecked, results in profound neuronal loss within the hippocampal formation. While increased estrogen (E) lowers and increased progesterone (P) raises seizure thresholds, it is unclear whether E or P at maintained levels affect seizure patterns or the ensuing neural damage from them. Additionally, it is not known whether E or P affect neuronal damage independently of their effects on seizures. To address these questions, ovariectomized female Sprague Dawley rats were implanted with 0.1 or 0.5 mg pellets of E or 1-6 silastic capsules of crystalline P to produce levels of hormone that mimic the various stages of the estrous cycle. Seven days later, the rats were administered kainic acid (8.5mg/kg, ip) and monitored for the next 6 hrs for seizure activity. Animals received a seizure composite score based on a modification of the Lothman scale. After a 4 day survival, the rats were killed and their brains processed for localization of neuron nuclear antigen (NeuN), a general neuronal marker. The hippocampus was examined throughout the rostral - caudal axis and scored for spread (number of separate regions within the hippocampal complex showing cell loss). The area occupied by NeuN immunoreactivity within the CA fields was used as an indicator of surviving neurons. P implants generated plasma levels that ranged from 8-95 ng/ml (1 implant mean P 11.00 ±.72; 2 implants, 21.54 ± 5.52; 4 implants 27.38 ± 3.72; 6 implants 48.62± 9.4); high and low E pellets generated plasma levels of 242.4 ±32.6. and 42.4±6.6, respectively.

Administration of either E or P significantly reduced mortality rates induced by KA seizures; this effect was independent of dose. Progesterone reduced seizure severity in animals that received 1-4 implants and most consistently in animals that received 2-4 implants (mean plasma P 24.7 ±3.2); surprisingly no difference in seizure severity was noted for animals with 6 P implants versus blank + KA treatment. Thus, animals that showed suppression of seizures by P

had significantly lower plasma P values (25.0 ±3.2) than animals with no seizure suppression by P (45.6 ±12.0; $p<0.05$). The reduced seizure levels in P-treated animals were accompanied by a reduction in the number of hippocampal formation areas that showed damage ($r^2=0.87$; $p<0.05$). Likewise, in P treated rats, neuron survival (determined by area of neuronal nuclear antigen immunoreactivity) was correlated with the reduction in seizure scores ($r^2=0.76$; $p<0.0001$).

E treatment at either dose had no significant effect on seizure severity ($p>0.05$) but significantly reduced both the spread of damage ($p<0.05$) and degree of neuronal loss ($p<0.05$). The neuroprotective effects of E were independent of seizure severity (spread, $r^2=0.056$, $p> 0.05$; neuron loss, $r^2=0.043$, $p>0.05$). Indeed, in the E treated rats, the presence of severe seizures produced only limited hippocampal damage; this damage was significantly lower than that observed in animals that received P treatment but had equally severe seizures ($p<0.05$). These data are consistent with the hypothesis that P produces its effects principally by reducing seizures, whereas E has little beneficial effect on seizure behavior but is capable of protecting the hippocampus from the damage seizures produce.

Complex partial seizures involve the limbic system and comprise the most common form of epilepsy. In women, the pattern of complex partial seizures is influenced by the hormonal changes that occur across the menstrual cycle (39, 41, 58, 59, 62, 71). Increased seizure incidence is observed in the menstrual phase, when both estrogen and progesterone levels are low, as well as in the follicular phase, when estrogen levels are on the rise. By contrast, decreased seizure incidence is noted during the luteal phase when progesterone levels are high relative to estrogen. In animals, estrogen administration decreases while progesterone increases seizure thresholds (13, 15-17, 21, 44); these differential steroid effects are used to explain the cycle dependent changes in seizure patterns in women. Indeed, the effects observed with progesterone form the basis for progesterone treatment of women with catemenial epilepsy (7, 14, 40, 41, 43, 58, 59, 62).

Limbic system seizures, when persistent, increase the risk of permanent damage to the hippocampal formation (48, 57, 60, 69, 76, 79). Thus, an understanding of the hormonal effects on limbic seizures and the damage they produce is critical to the design of rational treatments. In animals, the use of the toxin, kainic acid, an excitatory amino acid analog, produces limbic seizures that damage neurons in the hippocampal formation and surrounding structures, particularly CA1, CA3, hilus, and entorhinal cortex, while sparing CA2 and the dentate gyrus (12, 30, 47, 54, 64, 65, 74). Progesterone treatment reduces limbic seizures in a variety of experimental models (21, 25, 26) (77) but it is unclear if the steroid has any neuroprotective effects of its own apart from its effects on seizure activity per se.

For estrogen, a few studies suggest that despite the potential for increased seizures, estrogen may reduce neuronal death from seizures (1, 80). However, those studies only used injected steroid (which produces variable hormone levels) and doses that often exceeded the physiological range. Thus, it is unclear if the effects of estrogen are dose-dependent. To fill those gaps, the studies presented in this manuscript sought to determine if maintained physiological levels of either estrogen or progesterone affected kainic acid seizure patterns and if these hormones could alter the relationship between seizure severity and brain injury.

Methods

Animal Treatment. Adult female Sprague Dawley rats (200 - 225 gm) were maintained on 12:12 light dark cycle (lights on at 3:30 EST). After a 1 week acclimation, rats were anesthetized with Metofane and ovariectomized under sterile conditions; seven days later they were implanted with either blank silastic capsules (n=18; capsule length = 40 mm; OD=.125mm ; ID=.078mm), estrogen pellets (estradiol-17β, 0.5mg/21 day, n=6; or 0.1 mg/21 day, n=8, Innovative Research of America, Sarasota, FL) or 1 (n=3), 2 (n=9), 4 (n=6), or 6 (n=8) silastic capsules containing crystalline progesterone (Sigma, St. Louis MO); capsule length = 40 mm; OD=.125mm ; ID=.078mm designed to achieve progesterone plasma levels of 10 - 60 ng/ml.

Behavioral Testing. Seven days after implants or pellets were inserted, half the control animals and the steroid-replaced animals were administered kainic acid (KA) at a dose of 8.5 mg/kg, ip. The remaining control rats received an equal volume of saline vehicle. The behavior of the animals was monitored by an individual blind to the animal treatment for 6 hr following saline or

KA injection and assigned a score for seizure behaviors using the following scale modified from Lothman (54).

1= minor behaviors such as catatonia, wet dog shakes (WDS), scratching, sniffing and head bobbing

2= minor behaviors + chewing and salivation, rearing without loss of balance

3= minor behaviors + chewing and salivation , rearing with ataxia

4= bi-clonus seizure activity

5= death

Following the observation period the animals were returned to the vivarium.

Tissue Preparation and Neuroanatomical Analysis. Ninety six hr after injection of KA or vehicle, each animal was anesthetized with an overdose of pentobarbital (100 mg/kg, ip), a blood sample was removed directly from the heart, and the animals were perfused transcardially with saline containing 2% sodium nitrite, followed by fixation with 2.5% acrolein in 4% paraformaldehyde in 0.05M phosphate buffer pH 6.8 (42). The brains were removed, sunk in 30% sucrose and sectioned at 25 µm on a Leica freezing microtome (Bannockburn, IL). The sections were placed into antifreeze cryoprotectant solution (82) and stored at –20°C until immunocytochemical localization of NeuN (a neuron-specific marker that stains nuclei and frequently dendrites and soma (61, 84)) was initiated.

Brain sections from each animal (1:6 series) that contained the entorhinal cortex and hippocampal formation were processed for NeuN immunoreactivity using standard immunocytochemical techniques (42). Following immunocytochemical staining, the slides were

coded and examined for the number of separate regions that showed neuron loss ("spread of damage"). This parameter was chosen due to the variability in sites of hippocampal damage in less severely affected rats with respect to which particular CA subfield showed damage. Secondly, neuronal survival was assessed by measuring the area occupied by NeuN immunoreactivity within the CA subfields at the coronal level where the CA regions showed maximal length. To accomplish this, an image of the section was captured with a 4x objective on a Nikon Eclipse 800 microscope using a Sensys digital camera (Biovision Technologies, Exton PA). With IP Spectrum software (Scanalytics, Fairfax, VA) operating on a Power Computing Macintosh computer, the CA area (μm^2) occupied by NeuN immunoreactive structures was determined. Reductions in NeuN area reflected the degree of neuron loss. To control for slight variation in hippocampal orientation, the total CA length was determined for each section and the NeuN area measurements were normalized for CA length (NeuN area/μm length).

Radioimmunoassay for Estrogen and Progesterone

Atrial blood was collected at the time of perfusion to determine serum progesterone and estrogen concentrations for the various treatment paradigms. After two hours at room temperature to allow for clot formation, plasma was separated by centrifugation. Plasma samples were stored at –20°C until radioimmunoassays were initiated. For estradiol, samples were first extracted with diethyl ether. Plasma progesterone and estrogen concentrations were determined using the Diagnostics Products Corporation Coat-A-Count kit (Estradiol, TKE25; Progesterone, TKPG2; Los Angeles, CA).

Statistical Analysis. Significant differences among treatment groups were analyzed using the non-parametric Kruskall Wallis test followed by post-hoc Mann Whitney-U tests. $P<0.05$ was considered significant. Correlations between the various measures were assessed using a simple regression analysis and GB-Stat software. $P<0.05$ was considered significant.

Results

Hormone Levels The placement of 1-6 progesterone implants resulted in plasma progesterone levels averaging from 11 to 48 ng/ml (**Fig 1A**); these values are all within physiological ranges. Since the placement of 2 or 4 implants produced essentially the same progesterone levels, the data from those two groups were pooled in subsequent analyses. The 0.5 mg/21 day and 0.1 mg/21 day estrogen pellets produced plasma hormone levels of 242.4 ±32.6 pg/ml. and 42.4±6.6 pg/ml, respectively (**Fig 1B**). Only the lower dose was within the physiological range.

Mortality. One striking feature of animals replaced with estrogens or progesterone was a reduction in the mortality rate. Seven of the 24 animals (29.2%) that received blank capsules and KA died, whereas for E, only 4 of 48 animals (8.3%) died and for P, 3 of 34 animals (8.8%) died. There was no obvious relationship of mortality to dose of replaced hormone (**Table 1**).

Seizure Severity. Seizure severity was significantly reduced in progesterone-treated, but not estrogen-treated rats (**Fig. 2A**). This reduction in seizure severity by progesterone was dose-dependent. In animals with 1 or 2-4 progesterone implants, seizure scores were significantly reduced compared with ovariectomized animals treated with KA that received blank capsules (for P1, $p=0.05$; for P2-4, $p<.0.0005$). No significant difference in seizure severity was noted in

animals that received 6 implants compared to blanks ($p>0.05$). As a result, animals that had only mild seizures in the progesterone-treated group (i.e., seizure scores = 2.0) had significantly lower plasma P values (mean plasma P = 25.0 ±3.2) than animals treated with P that had severe seizures with scores > 2.0 (mean plasma P = 45.6 ±12.0; $p<0.05$; **Fig. 2B**).

Number of Areas Showing Neuronal Loss: Spread of Damage. On average, approximately 3 hippocampal areas showed neuronal loss in control animals after KA treatment (**Fig 3**). This typically included the entorhinal cortex (not shown), CA1, CA3 or the hilus (**Fig 4B** compared with controls, **4A**). CA2 and the dentate gyrus were generally spared. The spread of damage after KA administration varied significantly with the level of seizure activity (**Fig 5A**; $r^2= 0.45$; $p<0.02$).

In P treated animals, the spread of damage induced by KA administration was independent of plasma P level (**Fig 3**). Rather, in P treated animals, spread of damage was directly influenced by seizure severity. Animals displaying a high level of seizure activity (score >2.0) after KA had a greater number of areas showing neuronal loss than animals with lower seizure activity (score = 2/0) (**Figs. 4 C-E, Fig 5B,** $r^2=.665$; $p<.0001$, **Fig 6,**).

In estrogen-treated animals, fewer hippocampal regions showed signs of neuron loss after KA treatment than controls (**Fig 3**, $p<0.05$; **Fig 4 F** and **G**) despite the persistence of seizures (**Fig. 2A**). Therefore, unlike progesterone, the effect of estrogen on the spread of damage was not dose-dependent (**Fig 3;** $p> 0.05$) nor was it correlated with seizure severity (**Fig 5C;** $r^2=0.049$ $p>0.05$). Thus, even when animals displayed severe seizures following KA, estrogen

administration (at either high or low doses) limited the number of hippocampal regions that showed any neuronal damage (**Fig 6**).

Loss of Neurons in CA Subfields: Area occupied by NeuN immunoreactivity.

Compared with saline treated control animals (blank capsules), KA treated control rats with high seizure activity had significant losses of NeuN in the CA subfields ($p<.005$; **Fig. 7**). Overall, the losses in NeuN immunoreactivity in the Blank+KA group were highly correlated with seizure score (**Fig 8A**, $r^2= 0.47$; $p<0.02$).

In animals treated with P, the animals with high seizure scores also had severe reductions in NeuN compared with controls (*$p<0.005$). **Fig. 7**). The NeuN losses in P-treated animals with mild seizures after KA were significantly less than those seen in the severely affected P-treated rats (#$p<0.001$). Similar to what was noted in control animals, the losses of NeuN immunoreactivity within the CA subfields after KA treatment in P treated rats were significantly correlated with the seizure scores ($r^2=0.343$; $p<0.005$, **Fig 8B**). Thus, the higher the seizure score, the greater the degree of neuronal loss.

For estrogen treated animals, no significant losses of NeuN immunoreactivity after KA treatment were noted. This was true even in animals displaying high seizure scores. As a result, estrogen treated animals displaying severe seizures had significantly more NeuN immunoreactive neurons than was seen in the animals treated with progesterone that had equally high seizure scores (**Fig 7**; $p< 0.05$). No correlation was observed between seizure scores and NeuN immunoreactivity in the estrogen treated rats (**Fig 8C**; $r^2=0.018$; $p> 0.05$).

Discussion

The results of these studies indicate that progesterone produces its effect principally by reducing seizure behavior; by contrast, estrogen has little beneficial effect on seizure behavior but is capable of protecting the hippocampus from seizure damage. The majority of animal studies examining the effects of gonadal steroids on seizures reported that seizure susceptibility/activity was reduced by P (4, 13, 21, 63). In addition, in women with catemenial epilepsy, the luteal phase, when progesterone levels are high relative to estrogen, is associated with a lower seizure incidence than the menstrual and follicular phases where estrogen and progesterone are both low, or estrogen is elevated relative to progesterone (7, 14, 39, 41, 55, 58, 59, 62, 71, 87). Thus, it would logically follow that progesterone should reduce brain damage from seizures simply because there are fewer seizures. Indeed, in P-treated animals that exhibited reduced seizure severity, brain damage was reduced. What was surprising is that progesterone was only effective in reducing seizures at low physiological ranges. High doses of progesterone failed to reduce seizures or prevent brain damage.

Progesterone is metabolized to 3 alpha–hydroxy–5 alpha pregnan-20-one (allopregnanolone), a potent allosteric modulator of the GABAA receptor (8). Several studies have suggested allopregnanolone, acting at the GABAA receptor, is the mechanism whereby P attenuates seizure activity (13, 26, 27, 29, 58, 62). Frye (24), reported that subcutaneous administration of allopregnanolone 3 hr prior to perforant path stimulation, significantly reduced both seizure severity and the resulting hippocampal neuronal loss. What is difficult to explain is

why higher plasma levels of progesterone failed to alter seizures or the brain damage from them. Levels of allopregnanolone, and GABA receptor activity *in vitro* are positively correlated with progesterone levels (6), raising the expectation that *in vivo,* increases in plasma progesterone should result in increased seizure suppression. In the current study, however, high doses of progesterone did not reduce seizures or the damage from them. While the reason for this discrepancy is not clear, it is possible that the prolonged progesterone exposure either alters the metabolism of progesterone to alloprenanolone, or that after long-term exposure to allopregnanolone, the GABA receptor fails to respond. *In vitro*, prolonged exposure of cortical neurons to allopregnanolone abolishes the potentiation of GABAA receptors by altering the allosteric interactions of allopregnanolone with the benzodiazepine binding sites (23). *In vivo* prolonged treatment with either progesterone or allopregnalonone produces desensitization and it was proposed that alterations in GABAA receptor subunit expression was responsible (37, 83). If this phenomenon is dose dependent, such changes in the GABAA receptor composition could explain why low but not high doses of progesterone reduced seizures after KA.

In the present study, administration of E had no effect on KA seizure severity. A large number of studies *in vivo* and *in vitro* demonstrate that the steroid increases after discharge patterns and seizure thresholds (4, 15-17, 21, 36, 44, 45, 52, 56, 63, 73, 75, 78, 85, 86). Thus, one would predict that under conditions of high estrogen concentrations KA would yield the strongest stimulatory effects thereby increasing the potential for excitotoxic brain damage. Yet, despite the persistence of seizures, estrogen replacement reduced mortality from KA seizures and significantly limited the overall spread of damage and amount of neuronal loss. Earlier studies examining hormonal effects on KA induced brain damage are mixed. In intact females, injection

of KA on proestrus (when estrogen levels are maximal) still produced substantial brain damage (1). However, in that same study, animals that were ovariectomized and replaced with estrogen but not progesterone showed protection from damage, provided the steroid was administered 2 days prior to onset of seizures. Subcutaneous injections of 0.2 μg estrogen administered 48 and 24 hr prior to KA reduced hippocampal brain damage (80), as did supraphysiological doses of estrogen (150 μg/rat) administered before or along with KA (2, 3). It would appear from these studies that reduction in damage from KA seizures by estrogen administration may not be strictly dose dependent, but fluctuating hormone levels after steroid injection make that conclusion tenuous. Our data demonstrate more clearly that maintained doses of E in either the physiological range or supraphysiological range protect neurons from damage.

How E protected the hippocampus from damage is not immediately clear. Initially it was thought that KA cell death was exclusively necrotic and there would be little basis for E interfering in that process. More recent studies demonstrate that delayed cell death accompanied by DNA laddering (normally associated with apoptosis) after KA induced seizures (28, 50, 51, 53, 67, 68, 81). The pro-apoptotic molecule Bax is up-regulated following KA seizures and concomitantly the pro-survival molecule Bcl-2 is down-regulated (31). In a variety of models of neuronal injury estrogen up-regulates expression of Bcl-2 (18, 20, 38, 66, 70, 72) and, if acting similarly in our studies, this mechanism could explain E's protective effects. There are also studies suggesting that anti-oxidant effects seen with high doses of estrogen protect neurons from cell death (5, 9-11, 19, 22, 32-35, 46, 49). While our data indicate that the pellets we used generated plasma levels of estrogens high enough to produce antioxidant effects, the high

progesterone levels in our animals should also have been antioxidant (32) but did nothing to protect the animals from seizures or their damage.

In summary, our data indicate that low but not high doses of progesterone reduce seizures and in so doing reduce damage to the hippocampus. Estrogen, on the other hand, at either physiological or supraphysiological levels, reduces brain damage from seizures but has little effect on seizure severity. It will be important to determine the mechanism whereby each of the steroids produces influences seizure activity and the ensuing brain damage. These results also raise the question of whether combinations of both steroids might prove even more advantageous than treatment with only one: with P potentially suppressing seizure activity but should some seizures still persist, E would then reduce the potential for brain damage.

Supported by DAMD1799-1-9483.

Figure Legends

Figure 1. (A). Plasma Levels of Progesterone (P). Each bar represents the mean ± S.E.M. for plasma levels of P in ng/ml for animals that were ovariectomized and received either blank capsules (pooling animals that later were administered saline with animals that received KA) or 1,2,4, or 6 capsules containing P.

(B). Plasma β- estradiol (E) levels (mean ± S.E.M) in pg/ml for ovariectomized animals implanted with estradiol pellets containing either 0.5 mg/21 day release, or 0.1 mg/21 day release. Ovariectomized animals had E values below detection in the assay.

Figure 2. (A) Effects of Hormone Treatment on KA-induced Seizures. Animals fitted with 1 or 2-4 P implants showed significantly lower seizure scores (*$p=0.05$) than animals treated with KA that received no hormone treatment (B+KA). In contrast, animals that received 6 P pellets did not show suppression of KA seizures nor did animals fitted with E pellets. Values represent the mean ± S.E.M.

(B). Comparison of plasma P levels in animals which displayed either severe (score > 2.0) or mild (score = 2.0) seizures. P implanted animals with severe seizures had significantly higher plasma P levels than P treated animals that had mild seizures ($p<0.02$).

Figure 3. Effects of Hormonal Treatment on the Spread of Damage to the Hippocampal Formation after KA treatment. Values represent the number of hippocampal formation regions (mean ± S.E.M.) showing neuronal injury after KA treatment. P did not produce significant dose-dependent effects on spread of damage. Both low and high E treatment

produced a significant reduction (*p= 0.05) in the number of regions showing neuronal damage after KA treatment despite the failure of the steroid to reduce seizure severity.

Figure 4. Hippocampal Neuron Patterns. Micrographs of the Hippocampus from (A) control saline treated ovariectomized rat with blank capsules shows the CA1, CA2, CA3, hilus and dentate gyrus. (B) Blank + KA rat displaying a seizure score of 3.5 has marked neuronal losses in CA1, CA3 and the hilus (P). This same animal also possessed damage to the entorhinal cortex (not shown). (C) P + KA treated rat with a seizure score of 1.5 shows only slight neuron loss in the hilus; all other regions are normal. (D) P + KA treated rat with a seizure score of 2.5 shows clear evidence of hilar neuronal loss (P); (E) P + KA treated rat with a seizure score of 3.5 had damage to the hippocampal CA fields (P) that are quite similar to those in the blank + KA rats. (F) E-treated rat with a seizure score of 1.5 shows little or no hippocampal damage; (G) E treated rat with a seizure score of 3.5 also shows little evidence of neuronal loss.

Figure 5. Correlation of seizure score and spread of damage in KA treated ovariectomized rats with A) blank implants; B) progesterone, or C) estrogen replacement. The spread of damage was significantly correlated with seizure scores in animals with blank ($p<0.02$) and P ($p<0001$) implants but in E-treated rats this relationship was lost ($p>0.05$). Thus, despite increased seizures, damage to the hippocampus did not spread to many areas after E replacement.

Figure 6. Effects of Estrogen or Progesterone on Spread of Damage from KA in Animals Exhibiting Mild (behavioral score = 2) or Severe (behavioral score >2) Seizures. Animals treated with E that displayed severe seizures showed significantly fewer regions of neuronal damage after KA than either severely affected animals that did not receive hormone replacement(*$p<0.005$) or received P treatment(#$p<0.01$). The spread of damage in these E-treated rats was no different from that seen in animals that had only mild seizures. The spread of damage in severely affected rats that were treated with P was no different from that seen in severely affected KA treated control animals (Blank, Severe).

Figure 7. Effects of Estrogen or Progesterone on Neuron Loss in KA-treated Animals Exhibiting Mild (behavioral scores = 2) or Severe (behavioral scores >2) Seizures. Ovariectomized animals that received blank capsules and showed severe seizures after KA had significant loss of NeuN immunoreactivity compared with control rats (*$p<0.005$). Losses of NeuN immunoreactivity in P-treated rats were significantly different from control rats only when seizures where severe (*$p<0.005$). Thus P treated animals with high seizures had significant more neuron losses than P treated rats with mild seizures (#$p<0.001$). In contrast, E treated rats with either severe or mild seizures showed no significant differences in NeuN immunoreactivity (NeuN area/CA length) compared with controls.

Figure 8. Correlation of seizure severity and NeuN immunoreactivity in KA treated ovariectomized rats with A) blank implants, B) progesterone, or C) estrogen replacement. The NeuN immunoreactivity was negatively correlated with seizure scores in KA treated

animals with blank ($p<0.02$) and P ($p<.005$) implants. In E-treated rats this relationship was lost ($p>0.05$) owing to the fact that even when seizures were severe, neuron losses were reduced.

1. Azcoitia, I., Fernandez-Galaz, C., Sierra, A., and Garcia-Segura, L. M. 1999. Gonadal hormones affect neuronal vulnerability to excitotoxin-induced degeneration. *J Neurocytol* 28: 699-710.

2. Azcoitia, I., Sierra, A., and Garcia-Segura, L. M. 1998. Estradiol prevents kainic acid-induced neuronal loss in the rat dentate gyrus. *Neuroreport* 9: 3075-3079.

3. Azcoitia, I., Sierra, A., and Garcia-Segura, L. M. 1999. Neuroprotective effects of estradiol in the adult rat hippocampus: interaction with insulin-like growth factor-I signalling. *J Neurosci Res* 58: 815-822.

4. Backstrom, T., Bixo, M., and Hammarback, S. 1985. Ovarian steroid hormones. Effects on mood, behaviour and brain excitability. *Acta Obstet Gynecol Scand Suppl* 130: 19-24.

5. Bae, Y. H., Hwang, J. Y., Kim, Y. H., and Koh, J. Y. 2000. Anti-oxidative neuroprotection by estrogens in mouse cortical cultures. *J Korean Med Sci* 15: 327-336.

6. Barbaccia, M. L., Roscetti, G., Trabucchi, M., Mostallino, M. C., Concas, A., Purdy, R. H., and Biggio, G. 1996. Time-dependent changes in rat brain neuroactive steroid concentrations and GABAA receptor function after acute stress. *Neuroendocrinology* 63: 166-172.

7. Bauer, J. 2001. Interactions between hormones and epilepsy in female patients. *Epilepsia* 42: 20-22.

8. Baulieu, E. E., Schumacher, M., Koenig, H., Jung-Testas, I., and Akwa, Y. 1996. Progesterone as a neurosteroid: actions within the nervous system. *Cell Mol Neurobiol* 16: 143-154.

9. Behl, C., Moosmann, B., Manthey, D., and Heck, S. 2000. The female sex hormone oestrogen as neuroprotectant: activities at various levels. *Novartis Found Symp* 230: 221-234.

10. Behl, C., Skutella, T., Lezoualc'h, F., Post, A., Widmann, M., Newton, C. J., and Holsboer, F. 1997. Neuroprotection against oxidative stress by estrogens: structure-activity relationship. *Mol Pharmacol* 51: 535-541.

11. Behl, C., Widmann, M., Trapp, T., and Holsboer, F. 1995. 17-beta estradiol protects neurons from oxidative stress-induced cell death in vitro. *Biochem Biophys Res Commun* 216: 473-482.

12. Ben-Ari, Y., Tremblay, E., Ottersen, O. P., and Meldrum, B. S. 1980. The role of epileptic activity in hippocampal and "remote" cerebral lesions induced by kainic acid. *Brain Res* 191: 79-97.

13. Beyenburg, S., Stoffel-Wagner, B., Bauer, J., Watzka, M., Blumcke, I., Bidlingmaier, F., and Elger, C. E. 2001. Neuroactive steroids and seizure susceptibility. *Epilepsy Res* 44: 141-153.

14. Bonuccelli, U., Melis, G. B., Paoletti, A. M., Fioretti, P., Murri, L., and Muratorio, A. 1989. Unbalanced progesterone and estradiol secretion in catamenial epilepsy. *Epilepsy Res* 3: 100-106.

15. Buterbaugh, G. G. 1987. Acquisition of amygdala-kindled seizures in female rats: relationship between the effect of estradiol and intra-amygdaloid electrode location. *Pharmacol Biochem Behav* 28: 291-297.

16. Buterbaugh, G. G. 1989. Estradiol replacement facilitates the acquisition of seizures kindled from the anterior neocortex in female rats. *Epilepsy Res* 4: 207-215.

17. Buterbaugh, G. G., and Hudson, G. M. 1991. Estradiol replacement to female rats facilitates dorsal hippocampal but not ventral hippocampal kindled seizure acquisition. *Exp Neurol* 111: 55-64.

18. Choi, K. C., Kang, S. K., Tai, C. J., Auersperg, N., and Leung, P. C. 2001. Estradiol up-regulates antiapoptotic Bcl-2 messenger ribonucleic acid and protein in tumorigenic ovarian surface epithelium cells. *Endocrinology* 142: 2351-2360.

19. Culmsee, C., Vedder, H., Ravati, A., Junker, V., Otto, D., Ahlemeyer, B., Krieg, J. C., and Krieglstein, J. 1999. Neuroprotection by estrogens in a mouse model of focal cerebral ischemia and in cultured neurons: evidence for a receptor-independent antioxidative mechanism. *J Cereb Blood Flow Metab* 19: 1263-1269.

20. Dubal, D. B., Shughrue, P. J., Wilson, M. E., Merchenthaler, I., and Wise, P. M. 1999. Estradiol modulates bcl-2 in cerebral ischemia: a potential role for estrogen receptors. *J Neurosci* 19: 6385-6393.

21. Edwards, H. E., Burnham, W. M., Mendonca, A., Bowlby, D. A., and MacLusky, N. J. 1999. Steroid hormones affect limbic afterdischarge thresholds and kindling rates in adult female rats. *Brain Res* 838: 136-150.

22. Emilien, G., Beyreuther, K., Masters, C. L., and Maloteaux, J. M. 2000. Prospects for pharmacological intervention in Alzheimer disease. *Arch Neurol* 57: 454-459.

23. Friedman, L., Gibbs, T. T., and Farb, D. H. 1993. Gamma-aminobutyric acidA receptor regulation: chronic treatment with pregnanolone uncouples allosteric interactions between steroid and benzodiazepine recognition sites. *Mol Pharmacol* 44: 191-197.

24. Frye, C. A. 1995. The neurosteroid 3 alpha, 5 apha-THP has antiseizure and possible neuroprotective effects in an animal model of epilepsy. *Brain Res* 696: 113-120.

25. Frye, C. A., and Bayon, L. E. 1998. Seizure activity is increased in endocrine states characterized by decline in endogenous levels of the neurosteroid 3 alpha,5 alpha-THP. *Neuroendocrinology* 68: 272-280.

26. Frye, C. A., and Scalise, T. J. 2000. Anti-seizure effects of progesterone and 3alpha,5alpha-THP in kainic acid and perforant pathway models of epilepsy. *Psychoneuroendocrinology* 25: 407-420.

27. Frye, C. A., Scalise, T. J., and Bayon, L. E. 1998. Finasteride blocks the reduction in ictal activity produced by exogenous estrous cyclicity. *J Neuroendocrinol* 10: 291-296.

28. Fujikawa, D. G., Shinmei, S. S., and Cai, B. 2000. Seizure-induced neuronal necrosis: implications for programmed cell death mechanisms. *Epilepsia* 41: S9-13.

29. Galli, R., Luisi, M., Pizzanelli, C., Monteleone, P., Casarosa, E., Iudice, A., and Murri, L. 2001. Circulating levels of allopregnanolone, an anticonvulsant metabolite of progesterone, in women with partial epilepsy in the postcritical phase. *Epilepsia* 42: 216-219.

30. Gayoso, M. J., Primo, C., al-Majdalawi, A., Fernandez, J. M., Garrosa, M., and Iniguez, C. 1994. Brain lesions and water-maze learning deficits after systemic administration of kainic acid to adult rats. *Brain Res* 653: 92-100.

31. Gillardon, F., Wickert, H., and Zimmermann, M. 1995. Up-regulation of bax and down-regulation of bcl-2 is associated with kainate-induced apoptosis in mouse brain. *Neurosci Lett* 192: 85-88.

32. Goodman, Y., Bruce, A. J., Cheng, B., and Mattson, M. P. 1996. Estrogens attenuate and corticosterone exacerbates excitotoxicity, oxidative injury, and amyloid beta-peptide toxicity in hippocampal neurons. *J Neurochem* 66: 1836-1844.

33. Green, P. S., Gridley, K. E., and Simpkins, J. W. 1998. Nuclear estrogen receptor-independent neuroprotection by estratrienes: a novel interaction with glutathione. *Neuroscience* 84: 7-10.

34. Green, P. S., and Simpkins, J. W. 2000. Neuroprotective effects of estrogens: potential mechanisms of action. *Int J Dev Neurosci* 18: 347-358.

35. Gridley, K. E., Green, P. S., and Simpkins, J. W. 1998. A novel, synergistic interaction between 17 beta-estradiol and glutathione in the protection of neurons against beta-amyloid 25-35- induced toxicity in vitro. *Mol Pharmacol* 54: 874-880.

36. Gu, Q., and Moss, R. L. 1996. 17 beta-Estradiol potentiates kainate-induced currents via activation of the cAMP cascade. *J Neurosci* 16: 3620-3629.

37. Gulinello, M., Gong, Q. H., Li, X., and Smith, S. S. 2001. Short-term exposure to a neuroactive steroid increases alpha4 GABA(A) receptor subunit levels in association with increased anxiety in the female rat. *Brain Res* 910: 55-66.

38. Harms, C., Lautenschlager, M., Bergk, A., Katchanov, J., Freyer, D., Kapinya, K., Herwig, U., Megow, D., Dirnagl, U., Weber, J. R., and Hortnagl, H. 2001. Differential mechanisms of neuroprotection by 17 beta-estradiol in apoptotic versus necrotic neurodegeneration. *J Neurosci* 21: 2600-2609.

39. Herkes, G. K., Eadie, M. J., Sharbrough, F., and Moyer, T. 1993. Patterns of seizure occurrence in catamenial epilepsy. *Epilepsy Res* 15: 47-52.

40. Herzog, A. G. 1995. Progesterone therapy in women with complex partial and secondary generalized seizures. *Neurology* 45: 1660-1662.

41. Herzog, A. G., Klein, P., and Ransil, B. J. 1997. Three patterns of catamenial epilepsy. *Epilepsia* 38: 1082-1088.

42. Hoffman, G. E., Le, W. W., Murphy, A. Z., and Koski, C. L. 2001. Divergent effects of ovarian steroids on neuronal survival during experimental allergic encephalitis in Lewis rats. *Exp Neurol* 171:272-284.

43. Holmes, L. B., Harvey, E. A., Coull, B. A., Huntington, K. B., Khoshbin, S., Hayes, A. M., and Ryan, L. M. 2001. The teratogenicity of anticonvulsant drugs. *N Engl J Med* 344: 1132-1138.

44. Hom, A. C., and Buterbaugh, G. G. 1986. Estrogen alters the acquisition of seizures kindled by repeated amygdala stimulation or pentylenetetrazol administration in ovariectomized female rats. *Epilepsia* 27: 103-108.

45. Hom, A. C., Leppik, I. E., and Rask, C. A. 1993. Effects of estradiol and progesterone on seizure sensitivity in oophorectomized DBA/2J mice and C57/EL hybrid mice. *Neurology* 43: 198-204.

46. Inestrosa, N. C., Marzolo, M. P., and Bonnefont, A. B. 1998. Cellular and molecular basis of estrogen's neuroprotection. Potential relevance for Alzheimer's disease. *Mol Neurobiol* 17: 73-86.

47. Jarrard, L. E. 1983. Selective hippocampal lesions and behavior: effects of kainic acid lesions on performance of place and cue tasks. *Behav Neurosci* 97: 873-889.

48. Kalviainen, R., Salmenpera, T., Partanen, K., Vainio, P., Riekkinen, P., and Pitkanen, A. 1998. Recurrent seizures may cause hippocampal damage in temporal lobe epilepsy. *Neurology* 50: 1377-1382.

49. Keller, J. N., Germeyer, A., Begley, J. G., and Mattson, M. P. 1997. 17Beta-estradiol attenuates oxidative impairment of synaptic Na+/K+- ATPase activity, glucose transport,

and glutamate transport induced by amyloid beta-peptide and iron. *J Neurosci Res* 50: 522-530.

50. Kondo, T., Sharp, F. R., Honkaniemi, J., Mikawa, S., Epstein, C. J., and Chan, P. H. 1997. DNA fragmentation and Prolonged expression of c-fos, c-jun, and hsp70 in kainic acid-induced neuronal cell death in transgenic mice overexpressing human CuZn-superoxide dismutase. *J Cereb Blood Flow Metab* 17: 241-256.

51. Kondratyev, A., and Gale, K. 2001. Temporal and spatial patterns of DNA fragmentation following focally or systemically-evoked status epilepticus in rats. *Neurosci Lett* 310: 13-16.

52. Kubo, K., Gorski, R. A., and Kawakami, M. 1975. Effects of estrogen on neuronal excitability in the hippocampal-septal- hypothalamic system. *Neuroendocrinology* 18: 176-191.

53. Liu, W., Liu, R., Chun, J. T., Bi, R., Hoe, W., Schreiber, S. S., and Baudry, M. 2001. Kainate excitotoxicity in organotypic hippocampal slice cultures: evidence for multiple apoptotic pathways. *Brain Res* 916: 239-248.

54. Lothman, E. W., and Collins, R. C. 1981. Kainic acid induced limbic seizures: metabolic, behavioral, electroencephalographic, and neuropathological correlates. *Brain Research* 218: 299-318.

55. Lundberg, P. O. 1997. Catamenial epilepsy: a review. *Cephalalgia* 17 Suppl 20: 42-45.

56. Maggi, A., and Perez, J. 1985. Role of female gonadal hormones in the CNS: clinical and experimental aspects. *Life Sci* 37: 893-906.

57. Mathern, G. W., Price, G., Rosales, C., Pretorius, J. K., Lozada, A., and Mendoza, D. 1998. Anoxia during kainate status epilepticus shortens behavioral convulsions but

generates hippocampal neuron loss and supragranular mossy fiber sprouting. *Epilepsy Res* 30: 133-151.

58. Morrell, M. J. 1992. Hormones and epilepsy through the lifetime. *Epilepsia* 33: S49-61.

59. Morrell, M. J. 1999. Epilepsy in women: the science of why it is special. *Neurology* 53(4: S42-48.

60. Moshe, S. L. 1998. Brain injury with prolonged seizures in children and adults. *J Child Neurol* 13 Suppl 1: S3-6; discussion S30-32.

61. Mullen, R. J., Buck, C. R., and Smith, A. M. 1992. NeuN, a neuronal specific nuclear protein in vertebrates. *Development* 116: 201-211.

62. Murri, L., and Galli, R. 1997. Catamenial epilepsy, progesterone and its metabolites. *Cephalalgia* 17 Suppl 20: 46-47.

63. Nicoletti, F., Speciale, C., Sortino, M. A., Summa, G., Caruso, G., Patti, F., and Canonico, P. L. 1985. Comparative effects of estradiol benzoate, the antiestrogen clomiphene citrate, and the progestin medroxyprogesterone acetate on kainic acid-induced seizures in male and female rats. *Epilepsia* 26: 252-257.

64. Olney, J. W., Collins, R. C., and Sloviter, R. S. 1986. Excitotoxic mechanisms of epileptic brain damage. *Adv Neurol* 44: 857-877.

65. Olney, J. W., Fuller, T., and de Gubareff, T. 1979. Acute dendrotoxic changes in the hippocampus of kainate treated rats. *Brain Res* 176: 91-100.

66. Pike, C. J. 1999. Estrogen modulates neuronal Bcl-xL expression and beta-amyloid-induced apoptosis: relevance to Alzheimer's disease. *J Neurochem* 72: 1552-1563.

67. Pollard, H., Cantagrel, S., Charriaut-Marlangue, C., Moreau, J., and Ben Ari, Y. 1994. Apoptosis associated DNA fragmentation in epileptic brain damage. *Neuroreport* 5: 1053-1055.

68. Pollard, H., Charriaut-Marlangue, C., Cantagrel, S., Represa, A., Robain, O., Moreau, J., and Ben-Ari, Y. 1994. Kainate-induced apoptotic cell death in hippocampal neurons. *Neuroscience* 63: 7-18.

69. Salmenpera, T., Kalviainen, R., Partanen, K., and Pitkanen, A. 2001. Hippocampal and amygdaloid damage in partial epilepsy: a cross- sectional MRI study of 241 patients. *Epilepsy Res* 46: 69-82.

70. Sawada, H., Ibi, M., Kihara, T., Urushitani, M., Honda, K., Nakanishi, M., Akaike, A., and Shimohama, S. 2000. Mechanisms of antiapoptotic effects of estrogens in nigral dopaminergic neurons. *Faseb J* 14: 1202-1214.

71. Schachter, S. C. 1988. Hormonal considerations in women with seizures. *Arch Neurol* 45: 1267-1270.

72. Singer, C. A., Rogers, K. L., and Dorsa, D. M. 1998. Modulation of Bcl-2 expression: a potential component of estrogen protection in NT2 neurons. *Neuroreport* 9: 2565-2568.

73. Smith, M. D., Jones, L. S., and Wilson, M. A. 2002. Sex differences in hippocampal slice excitability: role of testosterone. *Neuroscience* 109: 517-530.

74. Sperk, G., Lassmann, H., Baran, H., Kish, S. J., Seitelberger, F., and Hornykiewicz, O. 1983. Kainic acid induced seizures: neurochemical and histopathological changes. *Neuroscience* 10: 1301-1315.

75. Stitt, S. L., and Kinnard, W. J. 1968. The effect of certain progestins and estrogens on the threshold of electrically induced seizure patterns. *Neurology* 18: 213-216.

76. Tasch, E., Cendes, F., Li, L. M., Dubeau, F., Andermann, F., and Arnold, D. L. 1999. Neuroimaging evidence of progressive neuronal loss and dysfunction in temporal lobe epilepsy. *Ann Neurol* 45: 568-576.

77. Tauboll, E., and Lindstrom, S. 1993. The effect of progesterone and its metabolite 5 alpha-pregnan-3 alpha- ol-20-one on focal epileptic seizures in the cat's visual cortex in vivo. *Epilepsy Res* 14: 17-30.

78. Teyler, T. J., Vardaris, R. M., Lewis, D., and Rawitch, A. B. 1980. Gonadal steroids: effects on excitability of hippocampal pyramidal cells. *Science* 209: 1017-1018.

79. Theodore, W. H., Bhatia, S., Hatta, J., Fazilat, S., DeCarli, C., Bookheimer, S. Y., and Gaillard, W. D. 1999. Hippocampal atrophy, epilepsy duration, and febrile seizures in patients with partial seizures. *Neurology* 52: 132-136.

80. Veliskova, J., Velisek, L., Galanopoulou, A. S., and Sperber, E. F. 2000. Neuroprotective effects of estrogens on hippocampal cells in adult female rats after status epilepticus. *Epilepsia* 41: S30-35.

81. Venero, J. L., Revuelta, M., Machado, A., and Cano, J. 1999. Delayed apoptotic pyramidal cell death in CA4 and CA1 hippocampal subfields after a single intraseptal injection of kainate. *Neuroscience* 94: 1071-1081.

82. Watson, R. E., Wiegand, S. J., Clough, R. W., and Hoffman, G. E. 1986. Use of cryoprotectant to maintain longterm peptide immunoreactivity and tissue morphology. *Peptides* 7: 155-159.

83. Wohlfarth, K. M., Bianchi, M. T., and Macdonald, R. L. 2002. Enhanced neurosteroid potentiation of ternary GABA(A) receptors containing the delta subunit. *J Neurosci* 22: 1541-1549.

84. Wolf, H. K., Buslei, R., Schmidt-Kastner, R., Schmidt-Kastner, P. K., Pietsch, T., Wiestler, O. D., and Bluhmke, I. 1996. NeuN: a useful neuronal marker for diagnostic histopathology. *J Histochem Cytochem* 44: 1167-1171.

85. Wong, M., and Moss, R. L. 1991. Electrophysiological evidence for a rapid membrane action of the gonadal steroid, 17 beta-estradiol, on CA1 pyramidal neurons of the rat hippocampus. *Brain Res* 543: 148-152.

86. Woolley, C. S. 2000. Estradiol facilitates kainic acid-induced, but not flurothyl-induced, behavioral seizure activity in adult female rats. *Epilepsia* 41: 510-515.

87. Zimmerman, A. W. 1986. Hormones and epilepsy. *Neurol Clin* 4: 853-861.

Table 1. Mortality after Kainic Acid Seizures

Treatment Group	# died	total	%
Blank + KA	7	24	**29.2**
E-.1mg/21 d + KA	2	25	**8.0**
E-.5 mg/21d + KA	2	23	**8.7**
E Combined	4	48	**8.3**
P1 + KA	0	6	**0.0**
P2-4 + KA	2	18	**11.1**
P6 + KA	1	10	**10.0**
P Combined	3	34	**8.8**

A

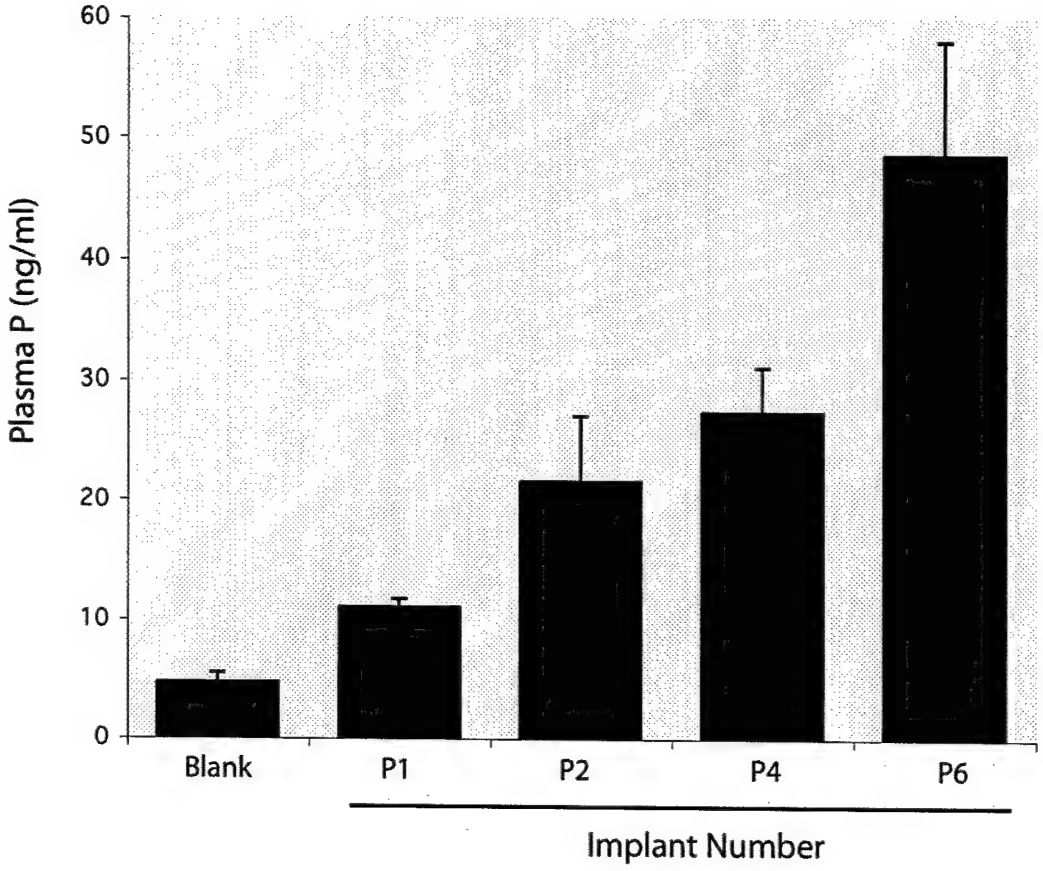
60
50
40
30
20
10
0
Plasma P (ng/ml)
Blank
P1
P2
P4
P6
Implant Number

B

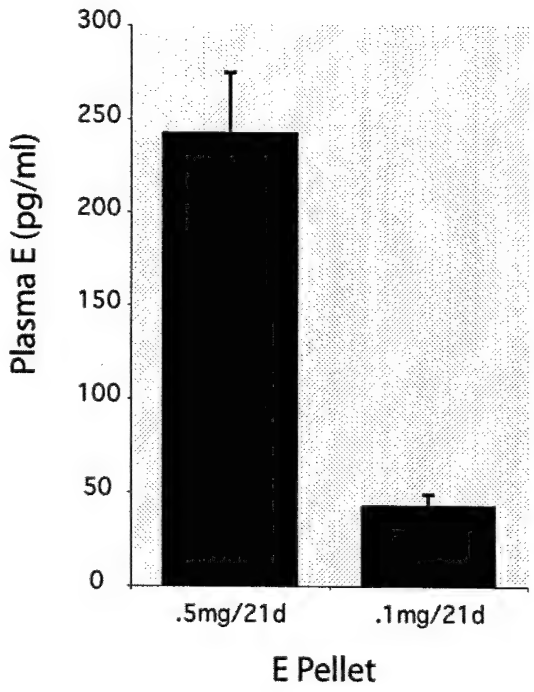
300
250
200
150
100
50
0
Plasma E (pg/ml)
.5mg/21d
.1mg/21d
E Pellet

A

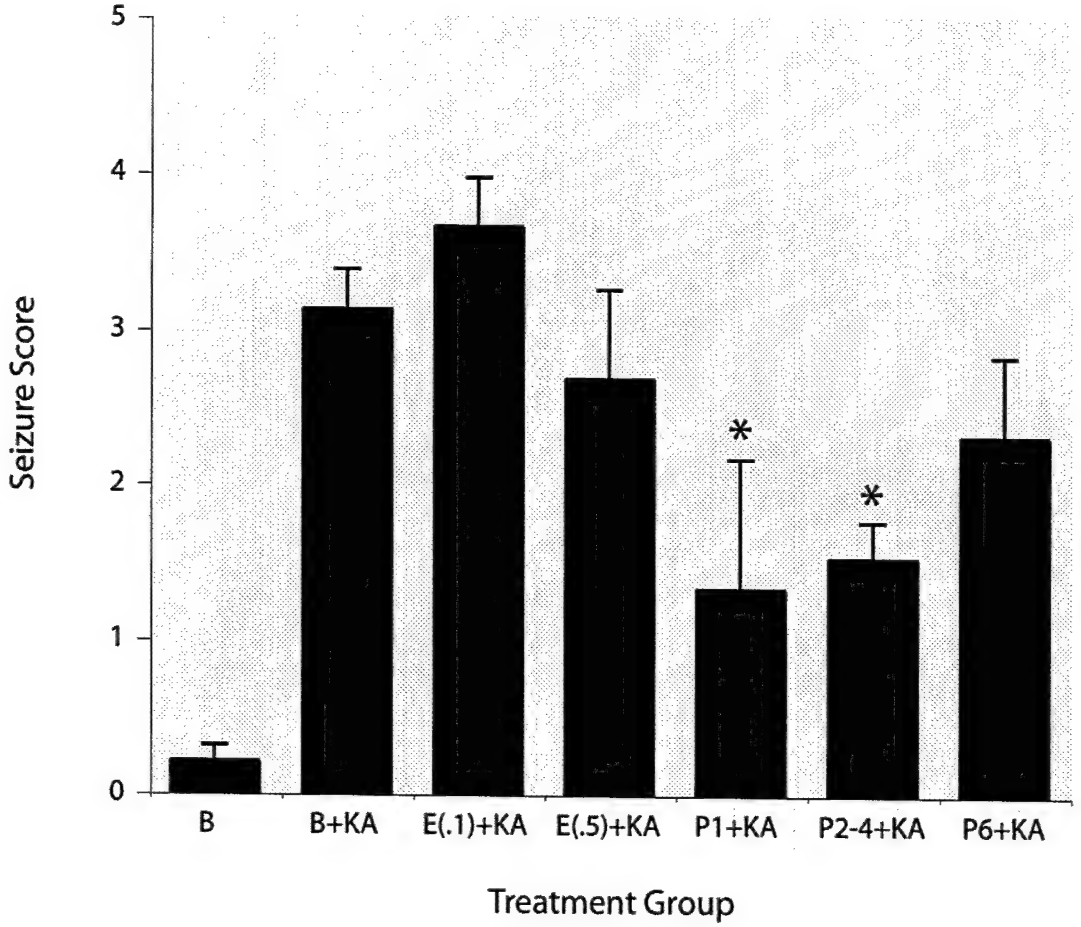
5
4
3
2
1
0
Seizure Score
*
*
B
B+KA
E(.1)+KA
E(.5)+KA
P1+KA
P2-4+KA
P6+KA
Treatment Group

B

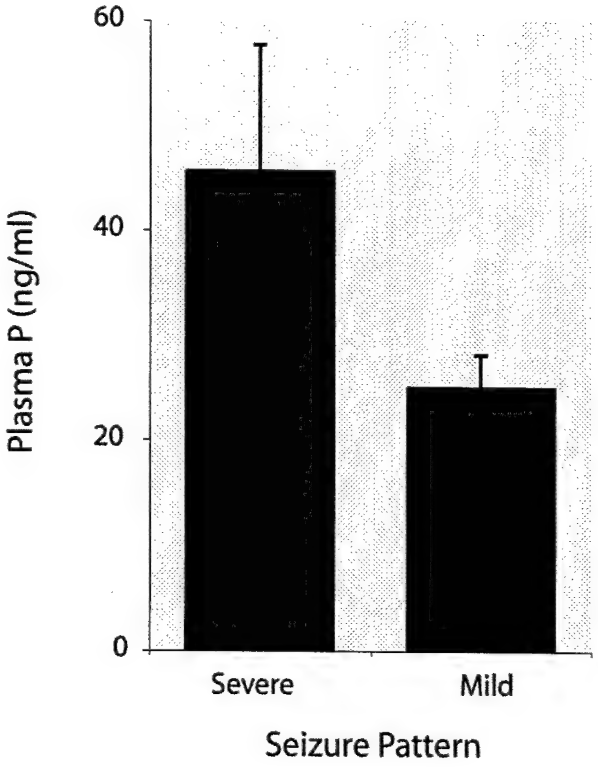
60
40
20
0
Plasma P (ng/ml)
Severe
Mild
Seizure Pattern

A.

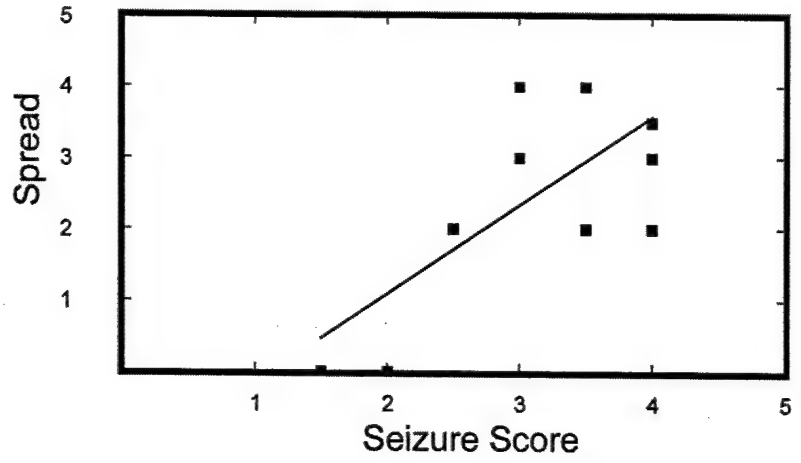
Spread
5
4
3
2
1
1
2
3
4
5
Seizure Score

B.

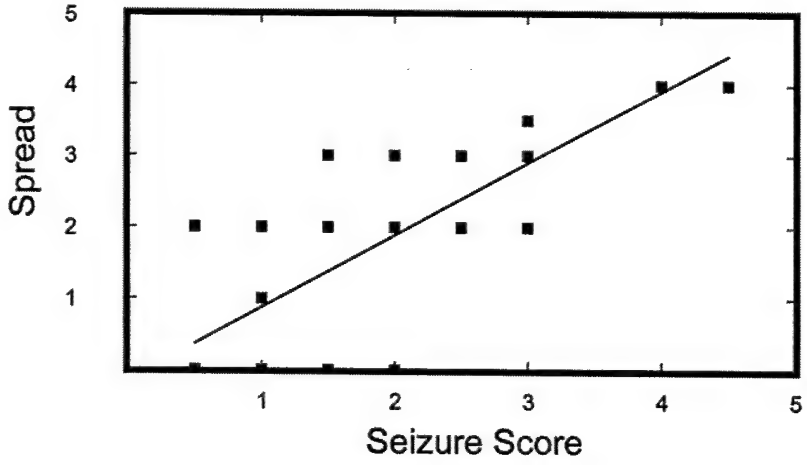
Spread
5
4
3
2
1
1
2
3
4
5
Seizure Score

C.

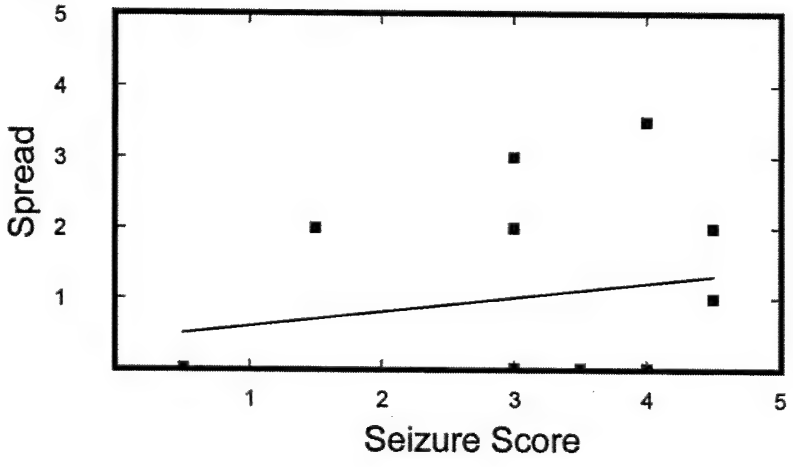
Spread
5
4
3
2
1
1
2
3
4
5
Seizure Score

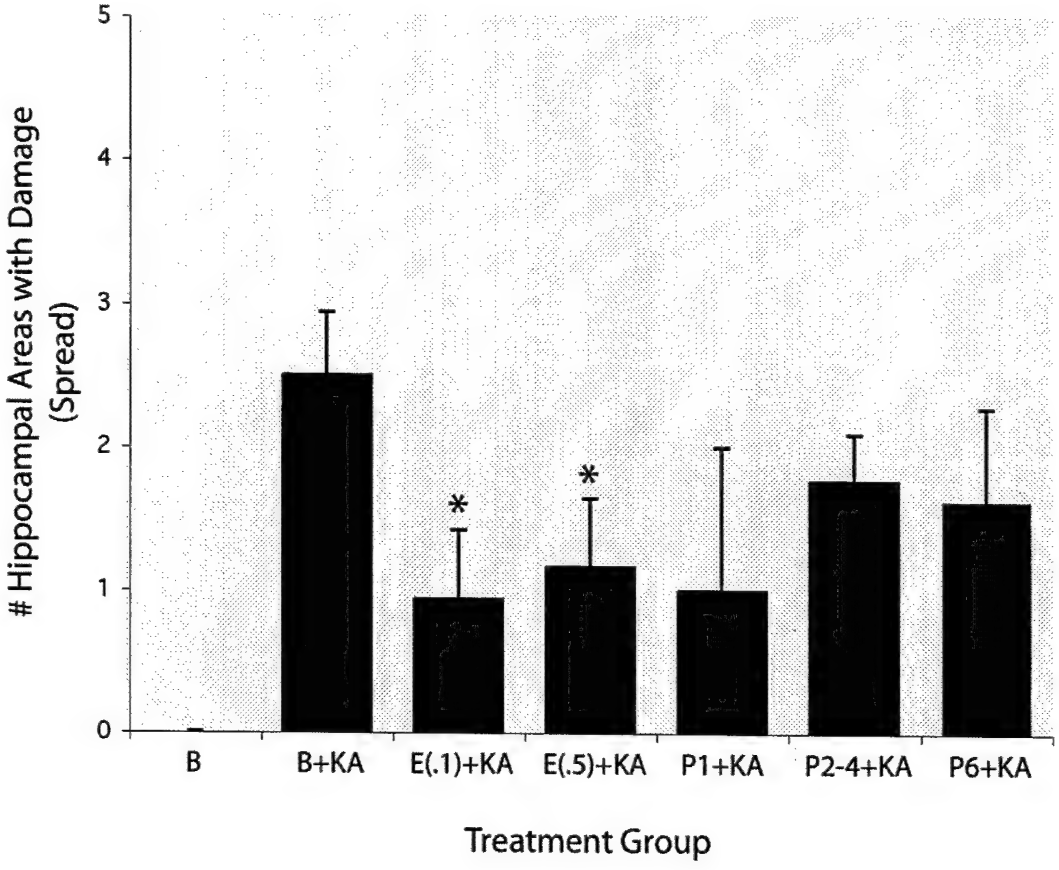
Hippocampal Areas with Damage (Spread)
5
4
3
2
1
0
*
*
B
B+KA
E(.1)+KA
E(.5)+KA
P1+KA
P2-4+KA
P6+KA
Treatment Group

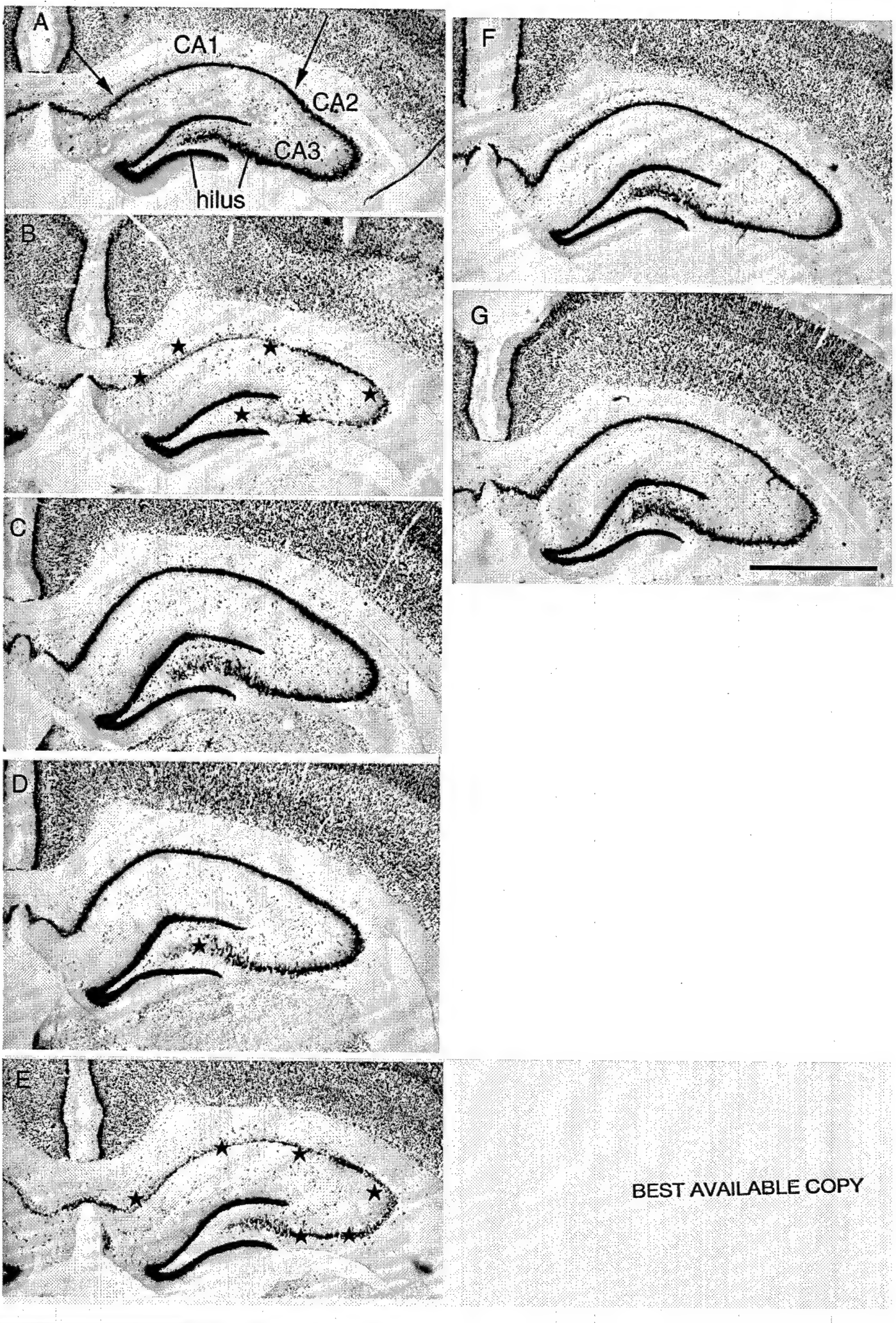

BEST AVAILABLE COPY

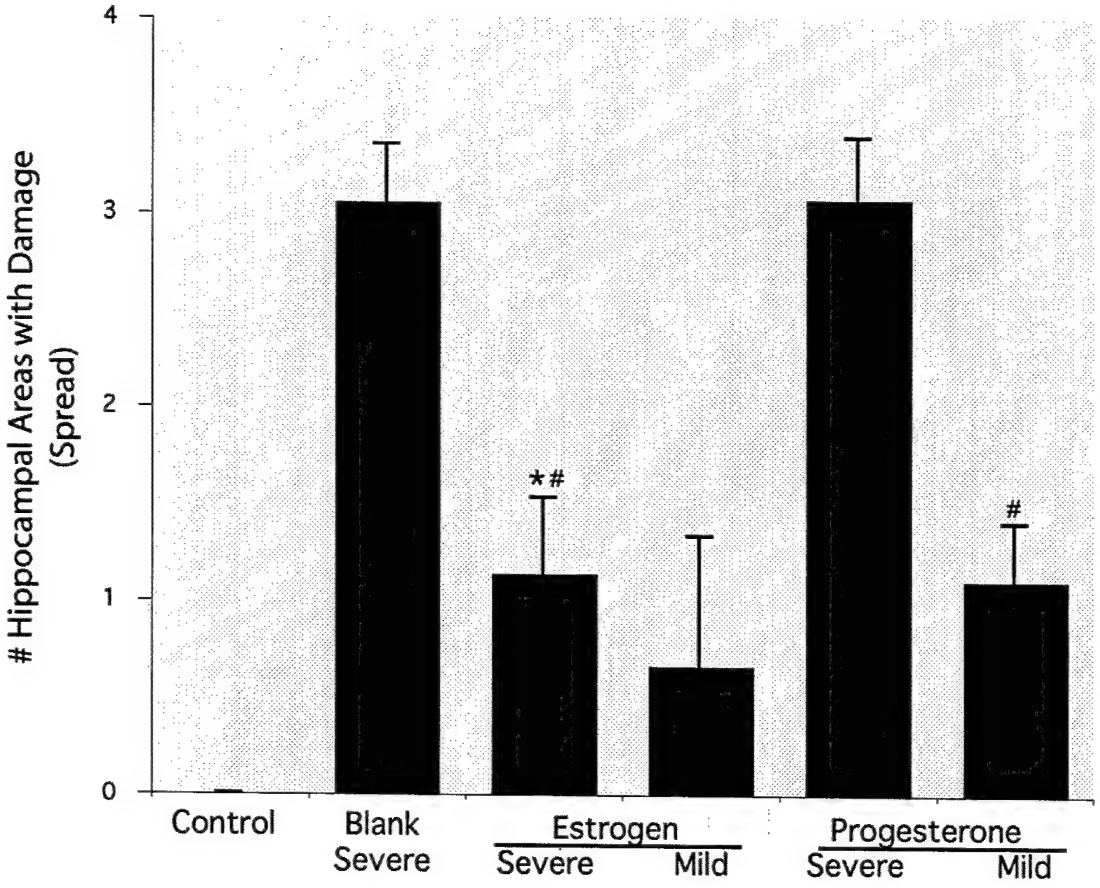
Hippocampal Areas with Damage (Spread)
4
3
2
1
0
*#
#
Control
Blank
Severe
Estrogen
Severe
Mild
Progesterone
Severe
Mild

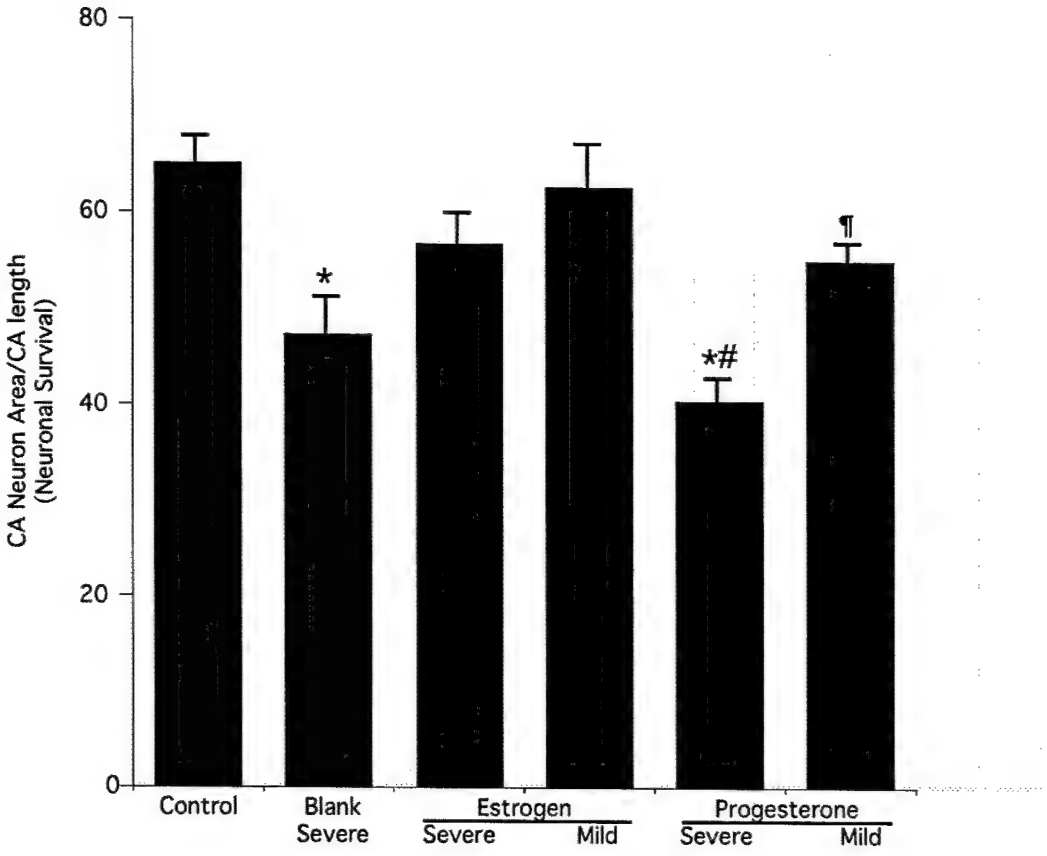
80
60
40
20
0
CA Neuron Area/CA length
(Neuronal Survival)
*
*#
¶
Control
Blank
Severe
Estrogen
Severe
Mild
Progesterone
Severe
Mild

A. Blank + KA

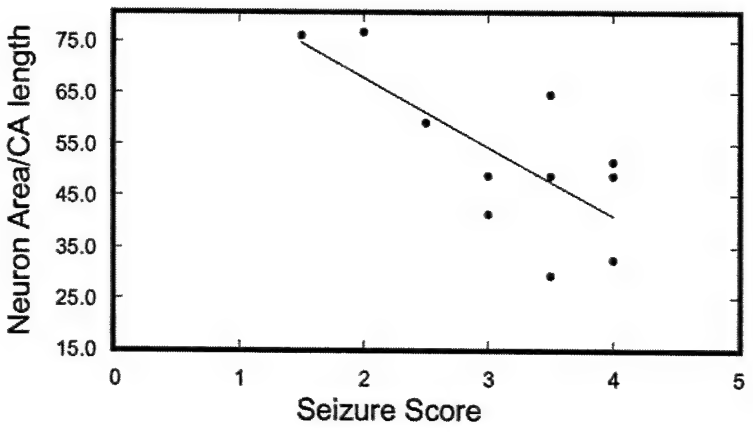

B. Progesterone + KA

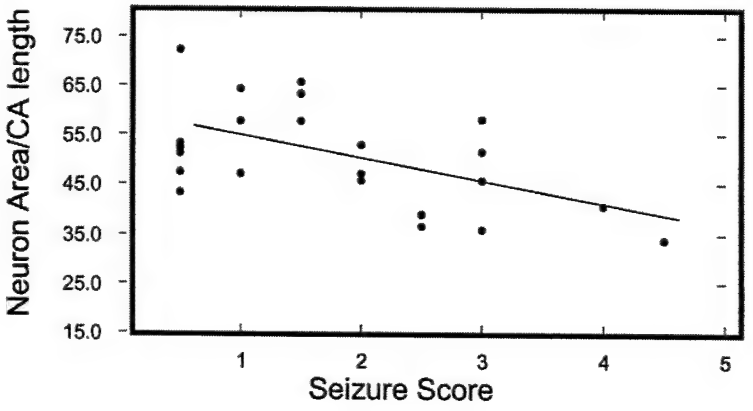

C. Estrogen + KA

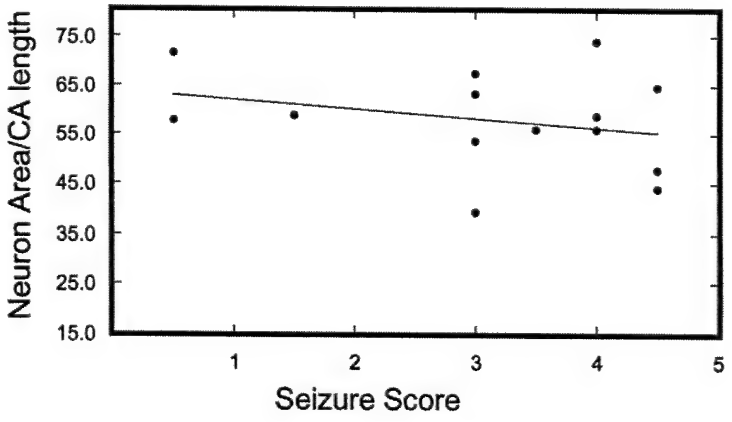

RNase-L REGULATES THE STABILITY OF MITOCHONDRIAL DNA-ENCODED mRNAs

Krish Chandrasekaran[‡¶], Zara Mehrabyan[‡], Xiao-Ling Li[§] and Bret Hassel[§]

[‡]Department of Anesthesiology, [§]Greenbaum Cancer Center, University of Maryland School of Medicine, Baltimore, MD 21201

***This work is supported by the grants from American Heart Association (0051001U to K.C.), from the US Army (DAMD-17-99-1-9483) and from NIH (AI39608 to B.H.).**

[¶]To whom correspondence should be addressed.

Department of Anesthesiology, University of Maryland School of Medicine, MSTF 5-34, 685 W. Baltimore St, Baltimore, MD 21201

Tel.: 410-706-3418; Fax: 410-706-2550;

E-mail: kchandra@anesthlab.umm.edu

ABSTRACT

To investigate the molecular basis of regulation of mitochondrial gene expression, we have been studying the role of mitochondrial RNase(s) on the stability of mitochondrial DNA (mtDNA)-encoded mRNAs (mt-mRNA). We report that in cells in devoid of interferon-regulated RNase, RNase-L, the half-life of mt-mRNAs was stabilized. In RNase-L $^{+/+}$ cells the average half-life of mt-mRNA, determined after termination of transcription with actinomycin D, was found to be 3h, whereas in RNase-L $^{-/-}$ cells the half-life of mt-mRNA were >6h. In contrast, the stability of nuclear DNA-encoded β-actin mRNA was unaffected. Steady state levels of mtDNA-encoded 12S rRNA and β-actin mRNA remained constant, whereas there was an increase in mt-mRNA levels in RNase-L $^{-/-}$ cells compared to RNase-L $^{+/+}$ cells. Induction of expression of RNase-L in mouse fibroblasts also decreased the half-life of mt-mRNA from 3h to 1.5h. We conclude that RNase-L cause (i) a decrease in the steady-state levels of mt-mRNA, and (ii) a selective decrease in the half-life of mt-mRNA. Our results demonstrate a role for RNase-L in regulating the stability of mitochondrial DNA-encoded mRNAs.

INTRODUCTION

Mitochondrial oxidative phosphorylation system (OXPHOS), responsible for the generation of ATP, consists of five multi-subunit enzyme complexes [1]. Four of these OXPHOS complexes are bipartite in nature consisting of subunits derived from both mitochondrial DNA (mtDNA) and nuclear DNA (nDNA) [1;2]. Mitochondrial DNA encodes 13 polypeptides, all of which are necessary for electron transport and oxidative phosphorylation. The large number of remaining subunits is specified by the nuclear genome. To form active enzyme complexes, both mtDNA and nDNA-encoded subunits are required [1]. Thus, although mitochondrial gene expression is a major component in the regulation of energy metabolism of the cell, the contribution of transcriptional and posttranscriptional mechanisms to the overall regulation of mitochondrial gene expression is not known [3].

Several condition that increase cellular energy demand are known to increase mitochondrial transcription [4-6]. The intracellular signals that mediate such an increase in transcription was analyzed using *in organello* method, and it was shown that high intramitochondrial ATP levels suppress transcription of mtDNA, explaining how energy demand can regulate mtDNA transcription [7-10]. Apart from transcriptional control, the primary regulation of mitochondrial gene expression is based on differences in RNA stability [11].

While attempting to study the mechanism by which energy demand regulates mitochondrial mRNA (mt-mRNA) levels in mammalian cells, we recently observed a surprising phenomena that we believed may reflect a post-transcriptional response to mitochondrial stress [12]. PC12 cells were treated with a sodium ionophore, monensin,

which increased cellular energy consumption but decreased the steady-state levels of mt-mRNA by 50% within 3-4h. Removal of the drugs restored the normal levels of COX III mRNA. Determination of half-lives of COX III mRNA, 12S rRNA and β-actin mRNA revealed a selective decrease in the half-life of COX III mRNA from 3.3h in control cells to 1h in monensin-treated cells. These results suggest the existence of a mechanism of posttranscriptional regulation of mitochondrial gene expression. However, the RNase(s) responsible for the accelerated degradation was unknown. Most recently, it was shown that an interferon-regulated RNase, called RNase L, mediate the degradation of a number of mitochondrial mRNAs in response to interferon (IFN) α treatment in human H9 cells [13]. The degradation of mt-mRNA by RNase L and associated mitochondrial dysfunction is proposed to be part of the antiproliferative effect of IFN [13;14].

To investigate the hypothesis that RNase L may regulate mitochondrial gene expression by its effect on the stability of mt-mRNA, we have measured the stability and steady state levels of mt-mRNA and control β-actin mRNA in mouse embryo fibroblasts (MEF) that contain RNase L (RNase $L^{+/+}$), in MEF cells that are devoid of RNase L (RNase $L^{-/-}$), mouse 3T3 cells that were transfected with inducible RNase L. Our results indicate that the steady state levels and the half-life of mt-mRNA were increased in RNase $L^{-/-}$ cells and the half-life of mt-mRNA were decreased in RNase L induced cells, suggesting a role for RNase L in mt-mRNA stability in mammalian cells under normal cell culture condition.

EXPERIMENTAL PROCEDURES

Cell cultures were maintained in a humidified atmosphere of 5% CO_2, 95% balanced air at 37 °C. Cells were cultured in the following growth media: RNase-L $^{+/+}$ and $^{-/-}$ mouse embryo fibroblasts ([15]; generously supplied by Robert H. Silverman, The Cleveland Clinic Foundation) were maintained in Dulbecco's modified Eagle's medium (DMEM) with 10% fetal calf serum and 1% antibiotic/antimycotic. Construction of inducible RNase L-stable transfectants into NIH 3T3 cells has been described [16]. The cells were maintained in DMEM with 10% fetal calf serum, 1% antibiotic/antimycotic, 50 μg/ml hygromycin and 500 μg/ml G418. Expression of RNase L was induced by the addition of 3M isopropyl β-d-thiogalactopyranoside (IPTG) for a period of 16h.

Cells were grown in 60x15 mm dishes. Cells were washed with Dulbecco's Phosphate Buffered Saline (DPBS) without calcium and magnesium and total RNA was isolated using Quiagen RNA isolation kit (Qiagen, USA). Total RNA was subjected to northern blot analysis as described below. The stability of mtDNA- and nDNA-encoded transcripts was determined by adding the transcriptional inhibitor actinomycin D to the cultures at a final concentration of 5 μg/ml. Total RNA was isolated at various times over a 8-hour period and processed for northern blot analysis.

Two μg of total RNA was run on a 1.2% formaldehyde agarose gel and transferred on to a GeneScreen Plus membrane as described by the manufacturer (Dupont, New England Nuclear, MA, USA). Prehybridization and hybridization were done with Hybridizol reagent (Hybridizol I and II mixed 4 to 1 ratio, Oncor, MD, USA). The blots were prehybridized at 42°C for 16 h, then [^{32}P]-labeled cytochrome oxidase subunit III (COX III) probe was added and hybridized for 48 h at 42°C [17]. The blots were

washed with increasing stringency and the final wash was performed at 65°C with 0.2 X SSC (1 X SSC = 150 mM sodium chloride and 15 mM sodium citrate) and 1% SDS (sodium dodecylsulfate. The blots were exposed to X-ray film (Bio-max MS, Kodak, NY, USA) with an intensifying screen for 45 min to 2 days at -70°C. Probe was removed from the blots by placing them in boiling DEPC-treated water for 10 min. The blots were then rehybridized with a [^{32}P] labeled control β-actin probe as described above. Finally the blots were hybridized with 12S rRNA probe. The level of RNA hybridized was quantified using an image analysis program (NIH image 1.57 program written by Wayne Rasband, NIH). To maintain measured intensities within the linear range, the blots hybridized with different probes were exposed for different periods. The level of RNA was quantified from autoradiograms of lower exposure than was used for photography. Ratios of COX III mRNA to β-actin mRNA, 12S rRNA to β-actin mRNA were calculated [17].

Blots were hybridized with probes that detect simultaneously several mt-mRNAs. The probes were created by amplification of nucleotides (nt) 3351—7570 of mtDNA (probe 1) or nt 8861-14549 of mtDNA (probe 2). Probe 1 hybridize to ND 1 and 2 and COX I and II mRNAs and Probe 2 hybridize to COX III, cyt b, ND4&4L, and ND5 mRNAs. The probe was radiolabeled by the random primer method and hybridized to the blots. The blots were then reprobed with nuclear DNA (nDNA)-encoded β-actin. Cell viability was measured by trypan blue exclusion.

The determination of the half-life of mt-mRNA was done as follows. Two μg of total RNA from cells treated with either vehicle or monensin in the presence of actinomycin D was subjected to northern blot analysis. The blots were hybridized with

mtDNA (probe 2) and β-actin probes as described and the levels of respective RNA species were quantified. Levels of mt-mRNA were calculated as the ratio of the respective species to the level of β-actin mRNA. At each experimental time, the RNA ratios are expressed as a percentage of the ratio at time zero. The half-lives were determined from the equation $t_{1/2} = 0.301/\text{slope}$ of the best fit line ($\log_{10}$ remaining RNA versus time).

The results presented are representative of at least three to five independent experiments. Where indicated, statistical analysis was carried out using a one way analysis of variance (ANOVA) followed by Tukey's test for multiple comparisons. The differences were considered significant when $P < 0.05$.

RESULTS AND DISCUSSION

Absence of RNase L Increases All Mitochondrial mRNA Levels

Recently, it has been shown that RNase L activity regulates the stability of mitochondrial mRNA (mt-mRNA) in interferon treated human H9 cells [13]. To determine whether the presence or absence of RNase L would alter the stability and thereby the steady-state levels of mt-mRNA under normal conditions, mouse embryo fibroblasts that express RNase L (RNase $L^{+/+}$) and mouse embryo fibroblasts that are devoid of RNase L (RNase $L^{-/-}$) were maintained in culture, total RNA was isolated and 2 μg aliquots were subjected to Northern blot analysis as described under "Experimental Procedures". Blots were stained with methylene blue to confirm equal loadings and transfer between lanes (data not shown). Blots of RNase $L^{+/+}$ and $^{-/-}$ cells were probed with mtDNA probes that recognize simultaneously a number of mtDNA-encoded mRNAs (probes 1 and 2), as well as control probes for β-actin, and relative levels were quantified. As illustrated in Figure 1, in RNase $L^{-/-}$ cells compared to RNase $L^{+/+}$ cells, the levels of mRNA species derived from both the light and heavy strand of mtDNA were increased, ranging from 2.8-fold (ND4&4L) to 3.6-fold (COX II). In contrast, levels of nDNA-encoded β-actin mRNA showed a 1.5-fold increase in RNase $L^{-/-}$ cells compared to RNase $L^{+/+}$ cells. Calculation of the ratio of mt-mRNA to β-actin mRNA showed 1.6-fold higher levels of steady state mt-mRNA in RNase $L^{-/-}$ cells compared to RNase $L^{+/+}$ cells.

Previous studies demonstrate that RNase-L function in the antiviral and growth inhibitory effects of interferon (IFN) and in apoptosis independent of IFN [15;18;19]. The antiviral effects of the IFN-induced RNase L system appear to be mediated through the preferential degradation of viral RNAs [20;21], whereas the antiproliferative/pro-apoptotic

effects of RNase-L are thought to occur through the degradation of cellular mRNAs. Though not all the cellular RNA substrates for RNase L have been identified, the better-characterized cellular substrates in IFN-treated cells are 18S and 28S rRNA [22]. The degradation of rRNAs contributes to the inhibition of protein synthesis that occurs in IFN-treated cells [23]. The antiproliferative effect of RNase L in IFN-treated cells was proposed to be mediated through its effect on mitochondrial function [14] and on mt-mRNA [13]. Our results extend these results to suggest RNase L may regulate the levels of mt-mRNA even under normal conditions.

Absence of RNase L Increases the Stability of Mitochondrial mRNA

We tested whether the increase in the steady state levels of mt-mRNA is due to altered stability by determining the half-life of mt-mRNA. Actinomycin D has been previously shown to inhibit cellular transcription in RNase L $^{+/+}$ and $^{-/-}$ cells by greater than 90% [24]. To estimate mRNA half-lives, actinomycin D was added to RNase L $^{+/+}$ and RNase L $^{-/-}$ cells and total RNA was isolated at time points over a 8-h-period. Cell viability was not compromised. The yield of total RNA decreased slightly after inhibition of transcription although no substantial differences was detected. The autoradiographs of RNA probed with mtDNA probe 2 and β-actin in RNase L $^{+/+}$ and $^{-/-}$ cells are shown in Figure 2A, the semi-log plot in Figure 2B, and the calculated half-lives ($t_{1/2}$) in Table 1. Clearly significantly higher levels of mt-mRNAs were present in RNase L $^{-/-}$ cells compared to RNase L $^{+/+}$ cells and the mt-mRNAs were found to be significantly stabilized in RNase L $^{-/-}$ cells. The mt-mRNA half-lives, determined after termination of transcription with actinomycin D, increased from 3h in RNase L $^{+/+}$ cells to >6h in RNase L $^{-/-}$ cells. The

estimated half-lives of mt-mRNA (~3h) are similar to the results reported in other cell culture systems [25;26]. Mitochondrial RNA species are found to be metabolically unstable, with half-lives of 2.5 to 3.5 h in HeLa cells [25] and 2-6 h in HepG2 cells [26]. However, the RNase(s) that may be responsible for the short half-life of mt-mRNA have not been identified. We suggest based on the results presented here together with the reported localization of RNase L to mitochondria [13] that RNase L may be responsible for the normal turnover of mt-mRNA.

Induction of RNase L decreases the stability of mt-mRNA

To assess the implication that RNase L may regulate the stability of mt-mRNA., an IPTG inducible RNase L gene was introduced into mouse embryo fibroblasts. Expression of RNase L was induced with IPTG (3 mM) for 16h, actinomycin D was added and total RNA was isolated at time points over a 8-h-period. The RNA samples were subjected to Northern blot analysis. The stability of mt-mRNA was determined in cells before and after induction of expression of RNase L. The northern blot results are shown in Figure 3A, the semi-log plot in Figure 3B, and the calculated half-lives ($t_{1/2}$) in Table 2. Clearly significantly higher levels of mt-mRNAs were present in non-induced cells compared to RNase L induced cells and the mt-mRNAs were significantly less stabilized in RNase L induced cells, decreasing the estimated half-life of mt-mRNA from 4h to 1.5h.

The results of the present study demonstrate that presence of RNase L compared to RNase L knock out caused a significant decrease in the steady state mtDNA-encoded mRNA level in mouse embryo fibroblasts. The levels of nDNA-encoded encoded β-actin mRNA was also decreased. But the decrease in mtDNA-encoded mRNA was

significantly higher than that of β-actin mRNA or of nDNA-encoded 28S rRNA. Estimation of mtDNA by dot blot analysis showed no significant differences between RNase L $^{+/+}$ and $^{-/-}$ cells. The observed decrease in mt-mRNA levels in RNase L $^{+/+}$ cells appears to be not due to either loss of mitochondria or a general breakdown of RNA. On the other hand, a similar reduction was observed in RNase L $^{+/+}$ cells with a number of mt-DNA-encoded mRNA. Thus, the effect of RNase L appears to be not specific for any one particular mt-mRNA. This may relate to the similarity in the stability of all mtDNA-encoded mRNAs. We have observed a similar increase in mt-mRNA levels in mouse neuroblastoma cells that were transfected with a dominant negative RNase L construct. Thus, it is likely that changes in the steady state levels of mt-mRNA are likely due to the activity of RNase L.

The result of this study showed that stability of mt-mRNA was decreased even in the absence of IFN treatment. Interferon stimulates genes (ISGs) mediate the activities of IFNs in cells [23]. Among the best characterized ISGs are the double-stranded RNA (dsRNA)-activated enzymes PKR (protein kinase RNA-activated) and 2',-5'-oligoadenylate synthetase (OAS) [27]. PKR and OAS are present at low levels in unstimulated cells, and are transcriptionally induced in response to IFN [23]. Activation of PKR phosphorylates eukaryotic initiation factor 2 α and decreases viral and cellular protein synthesis by down regulating translation. OAS catalyze the polymerization of ATP into 2',5'-linked oligoadenylates (2-5A) [28]. 2-5A, in turn, binds with high affinity to the latent endoribonuclease, RNase-L, resulting in RNase-L dimerization and activation [29]. RNase-L mediates the biologic activity of the 2-5A system by cleaving single-stranded viral, cellular and ribosomal RNAs. 2-5A pathway activity is limited through

the action of a 2'phosphodiesterase and cellular phosphatases that inactivate 2-5A, and an RNase-L inhibitor, RLI, that associates with RNase-L and antagonizes 2-5A binding [28;30]. We dot know at present how the activation of RNase L occurs in absence of IFN-treatment. Constitutive expression and mitochondrial localization of OAS, RNase L and RLI has been demonstrated [13;31]. We speculate that mitochondria being the site of ATP synthesis and also the substrate for OAS could in some way contribute to the activation of RNase L resulting in reduced stability. This may provide a link between mitochondrial bioenergetics and regulation of mitochondrial gene expression at transcriptional and post-transcriptional levels.

REFERENCES

1. Attardi, G. and Schatz, G. (1988) *Annu.Rev.Cell Biol.* **4,** 289-333

2. Grivell, L. A. (1989) *Eur.J.Biochem.* **182,** 477-493

3. Kagawa, Y. and Ohta, S. (1990) *Int.J.Biochem.* **22,** 219-229

4. Wiesner, R. J., Kurowski, T. T., and Zak, R. (1992) *Mol.Endocrinol.* **6,** 1458-1467

5. Wiesner, R. J., Hornung, T. V., Garman, J. D., Clayton, D. A., O'Gorman, E., and Wallimann, T. (1999) *J Bioenerg.Biomembr.* **31,** 559-567

6. Zhang, C. and Wong-Riley, M. T. (2000) *J.Neurosci.Res.* **60,** 338-344

7. Gaines, G. and Attardi, G. (1984) *Mol.Cell Biol.* **4,** 1605-1617

8. Enriquez, J. A., Fernandez-Silva, P., Perez-Martos, A., Lopez-Perez, M. J., and Montoya, J. (1996) *Eur.J.Biochem.* **237,** 601-610

9. Enriquez, J. A., Perez-Martos, A., Lopez-Perez, M. J., and Montoya, J. (1996) *Methods Enzymol.* **264,** 50-57

10. DasGupta, S. F., Rapoport, S. I., Gerschenson, M., Murphy, E., Fiskum, G., Russell, S. J., and Chandrasekaran, K. (2001) *Mol.Cell Biochem.* **221,** 3-10

11. Attardi, G., Chomyn, A., King, M. P., Kruse, B., Polosa, P. L., and Murdter, N. N. (1990) *Biochem.Soc.Trans.* **18,** 509-513

12. Chandrasekaran, K., Liu, L. I., Hatanpaa, K., Shetty, U, Mehrabian, Z, Murray, P. D., Fiskum, G., and Rapoport, S. I. Chronic exposure of neural cells to elevated intracellular sodium decreases mitochondrial mRNA expression. Mitochondrion 1, 141-150. 2001.
Ref Type: Journal (Full)

13. Le Roy, F., Bisbal, C., Silhol, M., Martinand, C., Lebleu, B., and Salehzada, T. (2001) *J.Biol.Chem.* **276,** 48473-48482

14. Lewis, J. A., Huq, A., and Najarro, P. (1996) *J.Biol.Chem.* **271,** 13184-13190

15. Zhou, A., Paranjape, J., Brown, T. L., Nie, H., Naik, S., Dong, B., Chang, A., Trapp, B., Fairchild, R., Colmenares, C., and Silverman, R. H. (1997) *EMBO J.* **16,** 6355-6363

16. Castelli, J. C., Hassel, B. A., Wood, K. A., Li, X. L., Amemiya, K., Dalakas, M. C., Torrence, P. F., and Youle, R. J. (1997) *J.Exp.Med.* **186,** 967-972

17. Chandrasekaran, K., Giordano, T., Brady, D. R., Stoll, J., Martin, L. J., and Rapoport, S. I. (1994) *Brain Res.Mol.Brain Res.* **24,** 336-340

18. Hassel, B. A., Zhou, A., Sotomayor, C., Maran, A., and Silverman, R. H. (1993) *EMBO J.* **12,** 3297-3304

19. Castelli, J. C., Hassel, B. A., Maran, A., Paranjape, J., Hewitt, J. A., Li, X. L., Hsu, Y. T., Silverman, R. H., and Youle, R. J. (1998) *Cell Death.Differ.* **5,** 313-320

20. Baglioni, C., De Benedetti, A., and Williams, G. J. (1984) *J.Virol.* **52,** 865-871

21. Li, X. L., Blackford, J. A., and Hassel, B. A. (1998) *J.Virol.* **72,** 2752-2759

22. Silverman, R. H., Skehel, J. J., James, T. C., Wreschner, D. H., and Kerr, I. M. (1983) *J.Virol.* **46,** 1051-1055

23. Stark, G. R., Kerr, I. M., Williams, B. R., Silverman, R. H., and Schreiber, R. D. (1998) *Annu.Rev.Biochem.* **67,** 227-264

24. Li, X. L., Blackford, J. A., Judge, C. S., Liu, M., Xiao, W., Kalvakolanu, D. V., and Hassel, B. A. (2000) *J.Biol.Chem.* **275,** 8880-8888

25. Gelfand, R. and Attardi, G. (1981) *Mol.Cell Biol.* **1,** 497-511

26. Chrzanowska-Lightowlers, Z. M., Preiss, T., and Lightowlers, R. N. (1994) *J.Biol.Chem.* **269,** 27322-27328

27. Sen, G. C. and Lengyel, P. (1992) *J.Biol.Chem.* **267,** 5017-5020

28. Silverman, R. H. (1997) 2-5A-dependent RNase-L: A regulated endoribonuclease in the interferon system. In Belasco, J. and Brawerman, G., editors. *Ribonucleases Structure and Functions,* Academic Press, New York

29. Dong, B. and Silverman, R. H. (1997) *J.Biol.Chem.* **272,** 22236-22242

30. Bisbal, C., Silhol, M., Laubenthal, H., Kaluza, T., Carnac, G., Milligan, L., Le Roy, F., and Salehzada, T. (2000) *Mol.Cell Biol.* **20,** 4959-4969

31. Besse, S., Rebouillat, D., Marie, I., Puvion-Dutilleul, F., and Hovanessian, A. G. (1998) *Exp.Cell Res.* **239,** 379-392

FIGURE LEGENDS

Figure 1. Comparison of the steady state levels of mRNAs mitochondrial proteins in RNase L $^{+/+}$ and RNase L $^{-/-}$ mouse embryo fibroblasts. Total RNA was isolated from 1 x 10^7 RNase L $^{+/+}$ and RNase L $^{-/-}$ mouse embryo fibroblasts and 2 μg aliquots were subjected to Northern blot analysis as described under "Experimental Procedures". Hybridization was quantified using image analysis of autoradiograms. The amount in RNase L $^{-/-}$ cells relative to RNase L $^{+/+}$ cells is shown.

Figure 2. Mitochondrial transcripts are stabilized in RNase L $^{-/-}$ cells. Total cytosolic RNA was isolated from RNase L $^{+/+}$ and RNase L $^{-/-}$ mouse embryo fibroblasts at indicated time points after termination of transcription by actinomycin D, and 2 μg aliquots were subjected to Northern blot analysis as described under "Experimental Procedures". Hybridization was quantified by image analysis of autoradiograms. Semi-log plots of transcript remaining *versus* time is depicted in case of β-actin mRNA.

Figure 3. Mitochondrial transcripts are de-stabilized in monensin-treated RNase L induced mouse embryo fibroblasts. Total cytosolic RNA was isolated from un-induced and RNase L-induced mouse embryo fibroblasts at indicated time points after addition of actinomycin D. Two 2 μg RNA aliquots were subjected to Northern blot analysis as described under "Experimental Procedures". Hybridization was quantified by image analysis of autoradiograms. Semi-log plots of transcript remaining *versus* time in monensin plus actinomycin D-treated cells are depicted in case of β-actin mRNA.

Table 1. Estimated half-lives for mitochondrially coded transcripts in RNase L $^{+/+}$ and RNase L $^{-/-}$ cells. Half-lives were calculated from semi-log plots as described under "Experimental Procedures". Relative increase in stability in RNase L $^{-/-}$ cells is included. Half-lives are given as the mean ± SEM, where appropriate, with the number of estimates in parentheses.

Table 2. Estimated half-lives for mitochondrially coded transcripts in non-induced and RNase L-induced. Half-lives were calculated from semi-log plots as described under "Experimental Procedures". Relative increase in stability in non-induced cells is included. Half-lives are given as the mean ± SEM, where appropriate, with the number of estimates in parentheses.

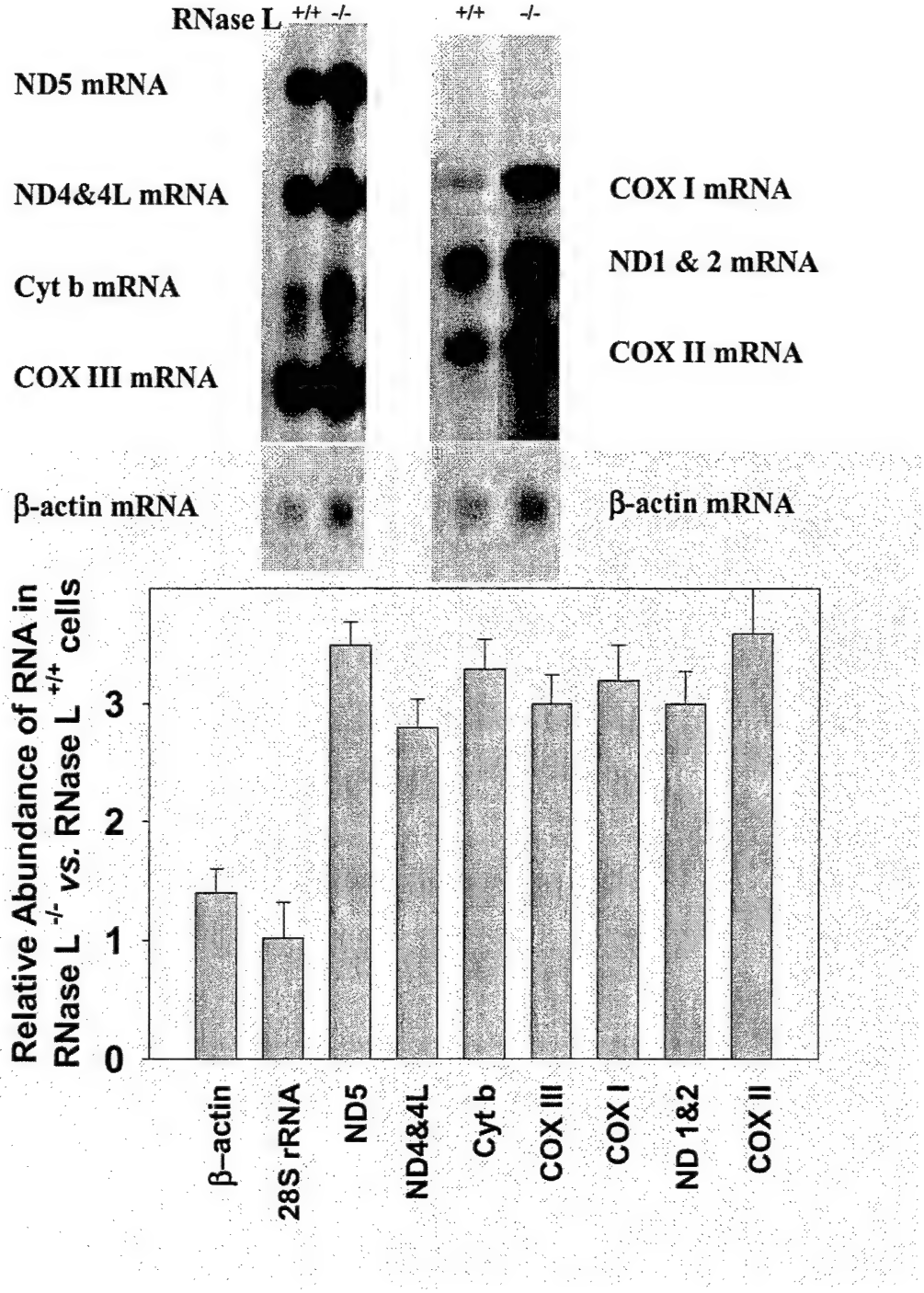
RNase L +/+ -/-
+/+ -/-
ND5 mRNA
ND4&4L mRNA
Cyt b mRNA
COX III mRNA
COX I mRNA
ND1 & 2 mRNA
COX II mRNA
β-actin mRNA
β-actin mRNA
Relative Abundance of RNA in RNase L -/- vs. RNase L +/+ cells
0
1
2
3
β–actin
28S rRNA
ND5
ND4&4L
Cyt b
COX III
COX I
ND 1&2
COX II

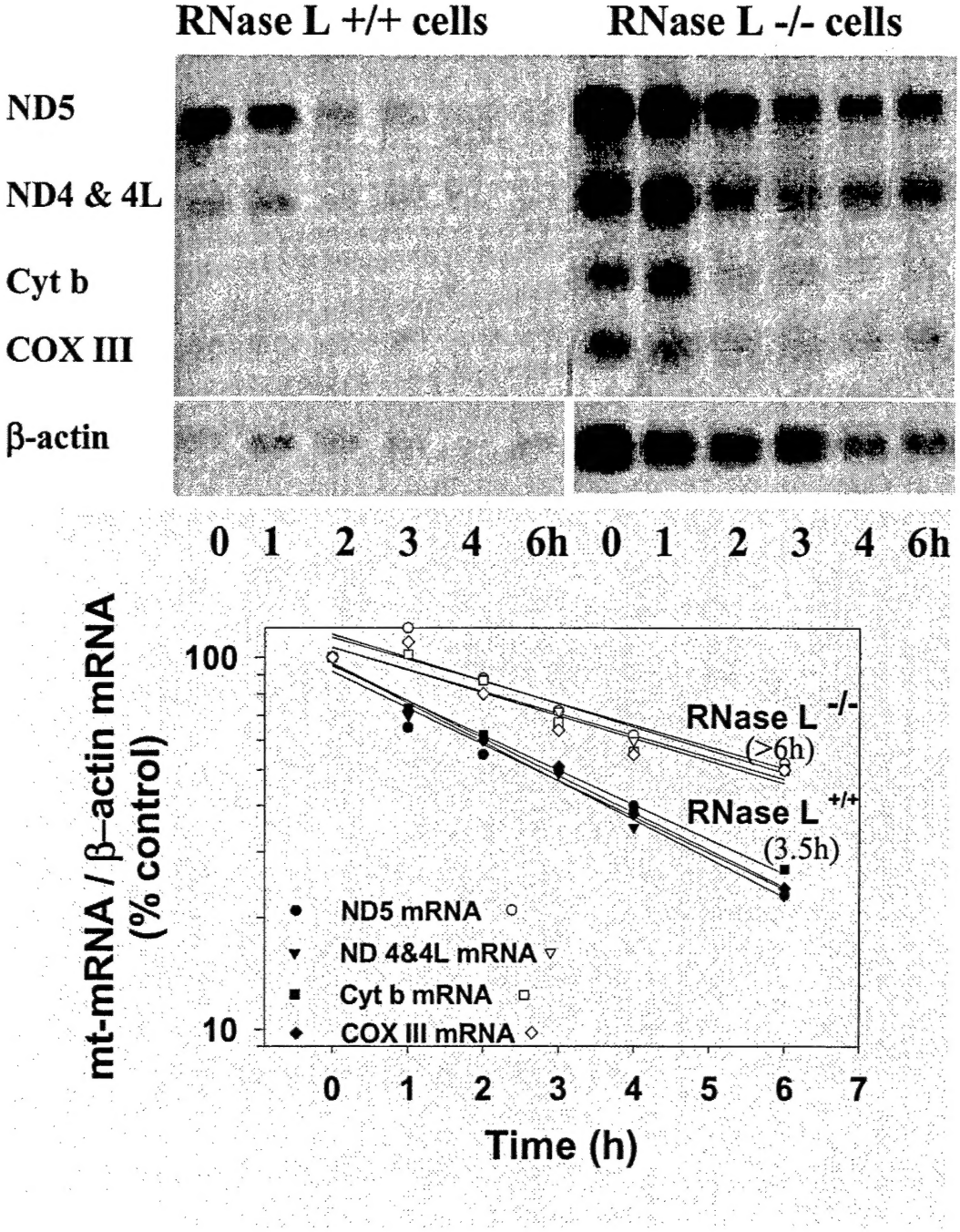
RNase L +/+ cells
RNase L -/- cells
ND5
ND4 & 4L
Cyt b
COX III
β-actin
0 1 2 3 4 6h 0 1 2 3 4 6h
mt-mRNA / β-actin mRNA (% control)
100
10
RNase L -/- (>6h)
RNase L +/+ (3.5h)
ND5 mRNA
ND 4&4L mRNA
Cyt b mRNA
COX III mRNA
0 1 2 3 4 5 6 7
Time (h)

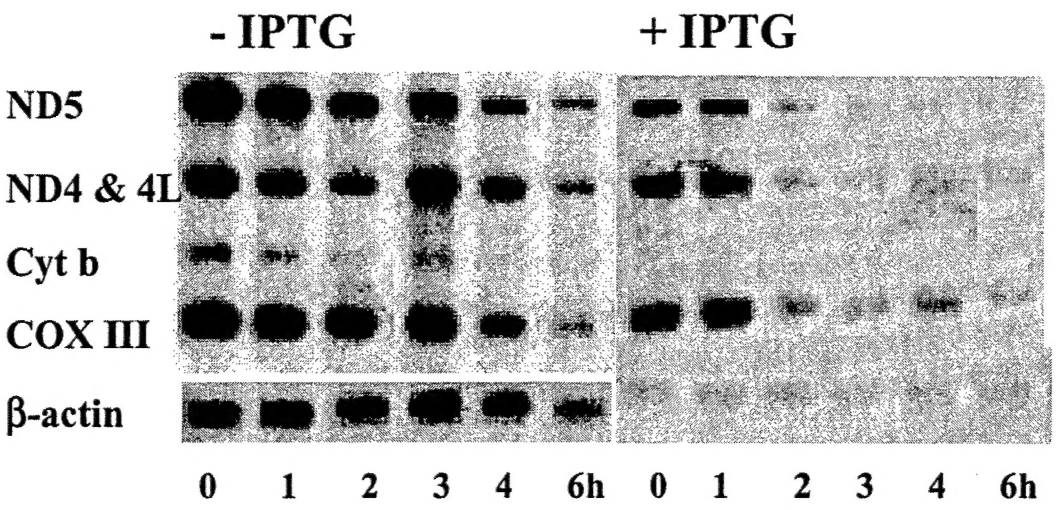
- IPTG
+ IPTG
ND5
ND4 & 4L
Cyt b
COX III
β-actin
0 1 2 3 4 6h 0 1 2 3 4 6h

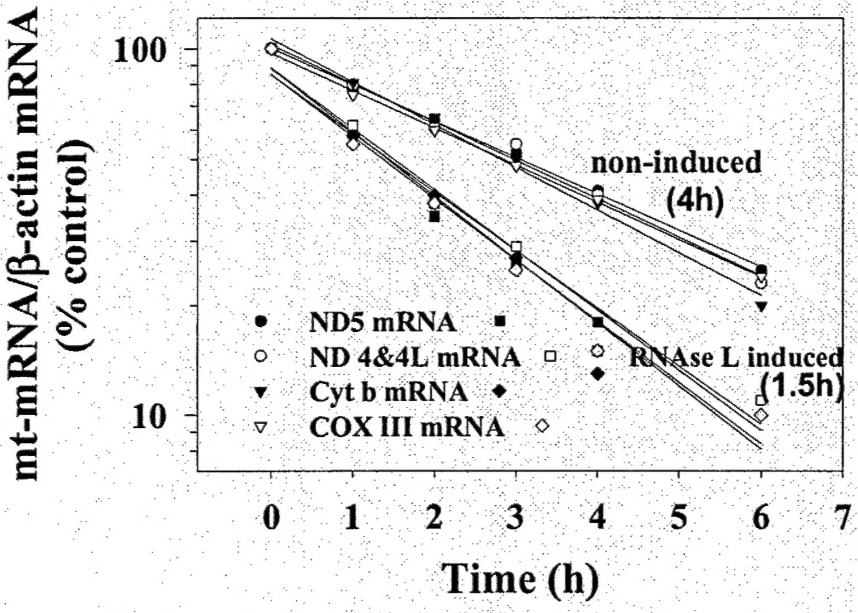
mt-mRNA/β-actin mRNA
(% control)
100
10
non-induced
(4h)
ND5 mRNA
ND 4&4L mRNA
Cyt b mRNA
COX III mRNA
RNAse L induced
(1.5h)
0 1 2 3 4 5 6 7
Time (h)

Transcript	Estimated half-life		Relative half-life
	$^{-/-}$ cells	$^{+/+}$ cells	$^{-/-}$ cells / $^{+/+}$ cells
Nuclear RNA			
β-actin	20.4 ± 5 (3)	20 ± 4 (3)	1.01
Mitochondrial RNA			
pRNA	6.2 ± 1 (5)	3.1 ± 1 (5)	2
COX III	7.5 ± .5 (5)	3.5 ± .5 (5)	2.2
ND5	6.5 ± .5 (4)	3.3 ± .5 (4)	1.97
ND4 & 4L	6.8 ± .5 (4)	3.5 ± .5 (4)	1.95
Cyt b	5 ± 1 (3)	2.5 ± .25 (3)	2

Transcript	Estimated half-life		Relative half-life
	Non-induced	induced	Non-induced/ induced
Nuclear RNA			
β-actin	21 ± 4 (3)	20 ± 4 (3)	1.04
Mitochondrial RNA			
pRNA	3.8 ± 1 (5)	1.8 ± 1 (5)	2.11
COX III	4.5 ± .5 (3)	1.5 ± .5 (3)	3
ND5	4 ± .5 (3)	1.8 ± .5 (3)	2.2
ND4 & 4L	4.5 ± .5 (3)	1.5 ± .5 (3)	3
Cyt b	2.5 ± .25 (3)	1 ± .25 (3)	2.5